

LIBRARY

Cornell University

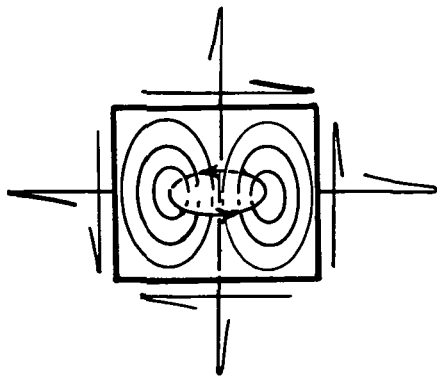


THEORETICAL AND APPLIED MECHANICS

THEORETICAL AND APPLIED MECHANICS

Theoretical and Applied Mechanics

Thurston Hall
Ithaca, New York



**U.S. DEPARTMENT OF COMMERCE
National Technical Information Service**

N78-16103

IMPACT ON MULTI LAYERED COMPOSITE PLATES

B. S. Kim, et al

**Theoretical and applied Mechanics
Cornell University
Ithaca, New York**

1. Report No. NASA CR135247	2. Government Accession No.	3. Recipient's Catalog No. N78-16103
4. Title and Subtitle Impact on Multi layered Composite Plates		5. Report Date 4/1977
7. Author(s) B.S. KIM and F.C. MOON		6. Performing Organization Code
9. Performing Organization Name and Address Department of Theoretical and Applied Mech. Cornell University Ithaca, N.Y. 14853		8. Performing Organization Report No.
12. Sponsoring Agency Name and Address National Aeronautics and Space Administration Washington, D.C., 20546		10. Work Unit No.
15. Supplementary Notes Project Manager: C.C. Chamis Materials and Structures Division NASA Lewis Research Center Cleveland, Ohio, 44135		11. Contract or Grant No. NSG-3080
16. Abstract <p>Stress wave propagation in a multilayer composite plate due to impact has been examined by means of the anisotropic elasticity theory. The plate is modelled as a number of identical anisotropic layers and the approximate plate theory of Mindlin is then applied each layer to obtain a set of difference-differential equations of motion. Dispersion relations for harmonic waves and correction factors are found. The governing equations are reduced to difference equations via integral transforms. With given impact boundary conditions these equations are solved for an arbitrary number of layers in the plate and the transient propagation of waves is calculated by means of a Fast Fourier Transform algorithm.</p> <p>The multilayered plate problem is extended to examine the effect of damping layers present between two elastic layers. A reduction of the interlaminar normal stress is significant when the thickness of the damping layer is increased but it seems that the effect is mostly due to the softness of the damping layer. Finally the problem of a composite plate with a crack on the interlaminar boundary has been formulated.</p>		13. Type of Report and Period Covered: Final Report 9/75-12/76
		14. Sponsoring Agency Code
17. Key Words (Suggested by Author(s)) Multilayered Composite Plate, Approximate Plate Theory of Mindlin, Impact, Stress Wave, Dispersion Relation, Wave surface, Damping Layer, Crack, Fast Fourier Transform.		18. Distribution Statement Unclassified, unlimited
19. Security Classif.(of this report) Unclassified	20. Security Classif. (of this page) Unclassified	21. No. of Pages
22. Price*		

REPRODUCED BY
**NATIONAL TECHNICAL
 INFORMATION SERVICE**
 U. S. DEPARTMENT OF COMMERCE
 SPRINGFIELD, VA. 22161

* For sale by the National Technical Information Service, Springfield, Virginia 22151

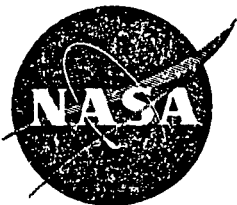
NOTICE

THIS DOCUMENT HAS BEEN REPRODUCED
FROM THE BEST COPY FURNISHED US BY
THE SPONSORING AGENCY. ALTHOUGH IT
IS RECOGNIZED THAT CERTAIN PORTIONS
ARE ILLEGIBLE, IT IS BEING RELEASED
IN THE INTEREST OF MAKING AVAILABLE
AS MUCH INFORMATION AS POSSIBLE.

IMPACT ON MULTILAYERED COMPOSITE PLATES

by

B.S. Kim and F. C. Moon



April, 1977

Final Report NASA CR 135247

Contents

	<u>Page</u>
Preface and Summary	ii
Symbols Used	iv
I Introduction	1
II Impact on Multilayer Elastic Plate	5
III Impact of a Composite Plate with an Interlaminar Damping Layer	30
IV Impact on a Plate with a Crack	37
V Conclusion and Recommended Research	43
Reference	44
Figures	47
Appendix A - Flow Chart	72
Appendix B - Sample Computer Deck	76
Appendix C - Program and Sample Output	77

SYMBOLS USED

Δ : Plate thickness (Nondimensional length unit)

b : A half of the layer thickness

N : Layer number in the plate

ρ : Density

t_0 : Impact time

$P_0(x_1, t)$: Impact stress

* $x_1(n), x_2(\xi)$: Coordinate variables

* $t(\tau)$: Time variable

T_0 : Nondimensional time unit = $a/\sqrt{c_{66}/\rho}$

* $\sigma_{ij}, \sigma(\Sigma), \tau(T), \sigma_{11}$: Stress tensor and its components

* $u_i, u(U), v(V)$: Displacement vector and its components

* $c_{ijkl}, c_{ij}(c_{ij})$: Elastic Moduli ($c_{11} = c_{11} - \frac{c_{12}}{c_{22}}$)

λ, μ : Lame's constants

$\epsilon_{ij}, \epsilon_i$: Infinitesimal strain tensor

\hat{A} : Laplace transform (in τ) and Fourier transform (in n) of A

$P_n(\xi)$: Legendre polynomial of ξ

* $k(k)$: Wave number

* $\omega(\bar{\omega})$: Frequency

θ, α, β : Phase shifts (wave number through the thickness)

C_D, C_S : Dilatational and shear wave speed

$G^*(\omega) = G'(\omega) + iG''(\omega)$: Complex modulus of elastomer

D : Thickness of viscoelastic layer

h : A half of the crack length

* Quantities in () are nondimensional quantities.

Preface and Summary

This report is the last of a series on the response of composite plates to impact forces. The motivation for these studies has been an attempt to understand the damage to aircraft jet engine fan blades by foreign object impact such as ice balls, stones, and birds. In addition, the National Aeronautics and Space Administration, sponsors of this research, have sought to develop computer codes from these analyses which will aid the fan blade designer in locating potential failure modes and positions and thus assist in optimizing fan blade fabrication to create greater impact tolerance.

The basic approach of the principal investigator in these studies has been to use wave propagation techniques to model the early response of composite plates to impact type forces. In using the wave method, the plate can be simplified in the analyses by neglecting reflections from edge boundaries far from the impact point. Thus, while the overall geometry of the plate is no longer included in the analysis, more sophisticated mathematical models near the point of impact have been used.

The basic model for the composite plate studies has been the anisotropic plate theory as extended by Mindlin [1] to account for wave phenomena. The plate equations were used as an approximation of the exact theory of elasticity because they lead to simpler computational schemes for evaluating average stresses and displacements in the plate.

Fourier and Laplace transform techniques have been used throughout these studies and inversion of the transforms has been accomplished with a fast Fourier transform algorithm. This algorithm is an effective computational tool but requires careful scaling of the impact problem in both space and time

variables. When it is properly used it can lead to calculations of thousands of stress values in a fraction of the time of conventional finite element schemes.

In summary, the use of plate models for the fan blade impact has avoided the analytical complexities of the exact theory of elasticity as well as the computational difficulties of finite element methods.

In earlier reports both central and edge impact of an anisotropic plate were studied, [2 - 4]. In those reports only wave propagation in the plane of the plate was investigated. In another report [5] a multilayer plate model was developed in order to study impact induced wave propagation in both the thickness and inplane directions. In this final report further results are presented from the multilayer model. The composite plate has been modeled with as many as eight separate layers. Each layer may itself have several plies, so that effective anisotropic constants must be used for each layer in the analysis. The mathematical model exhibits wave propagation in both the thickness and inplane directions. Impact generated waves are shown to lead to interlaminar shear stresses and interlaminar tensile stresses during and after impact.

This report also presents an analysis of an impact damping mechanism. This consists of thin damping layer introduced between composite layers in the mathematical model. The resulting response due to impact shows that considerable reduction of stress can be achieved. However it appears that this stress reduction is linked to the lower elastic moduli of the damping sublayers and not the viscous nature of the sublayer.

Fianlly an attempt was made to analyze the impact of a plate with a crack. While the problem has been formulated, no progress was made on obtaining numerical answers to the crack problem.

I. INTRODUCTION

The present research is a continuation of our previous work on the stress wave propagation in a laminated composite [2-5]. It has been motivated by the problem of the impact on jet engine fan blades caused by ingestions of foreign materials, such as birds and hailstones. The successful application of fiber-reinforced composite materials depends on the ability of these materials to withstand forces due to such impact.

The simplest approach to examine the dynamic behavior of a composite plate is based upon the work of White and Angona [6]. In their work, referred to as the effective modulus theory, the response of the composite plate to waves propagating normal to the laminate is predicted by a single constant wave speed, regardless of the internal structure of composites. Even though this theory is satisfactory for many problems, it fails in the case of some problems when the wave lengths become short. To overcome this limitation, Sun and et al. proposed a model which includes the effects of internal structure, such as the layer thickness [7]. In their work, referred to so the effective stiffness theory, displacements of both the reinforcing layer and the matrix layer are expressed as linear expansions about the midplanes of the layers and approximate equations of motion are derived for both layers. Then these approximate equations are required to satisfy the continuity conditions of displacement and stress components on every interface. Using this model the propagation of harmonic waves has been examined.

More recently a number of researchers have presented models for multilayer plates either by the discrete-continuum theory or the continuum mixture theory [8-14]. Many, however examined only the frequency-wave number dispersion relationship and stopped short of the transient

ORIGINAL PAGE IS
OF POOR QUALITY

impact problem except for a few experimental or numerical works using the finite element method which sometimes show a considerable discrepancy from the experimental results.

In this report we present a new attempt to mathematically model the multilayer plate and develop a method by which we can examine the transient propagation of an impact wave in the plate, not only along the longitudinal direction but also through the thickness direction of the plate as well, using an inexpensive Fast Fourier Transform algorithm [3,15].

The composite plate under consideration for the first part of the present report is imagined to comprise N identical elastic layers. And each layer is made of a number of unidirectional plies lying alternately at a layup angle $\pm\phi$ from the symmetry axis, as shown in Fig. 1. Then the elastic properties of the plate depend on the layup angle ϕ . A key assumption for the first step of the work is that all the layers are identical. While restricting the application, this assumption allows us to formulate the problem using difference-differential equations due to a rather simple periodic structure of the plate. This technique for periodic structures has been widely used in the study of electrical transmission lines [16] and in the vibration of multistory buildings [17]. By means of an approximate plate theory of Mindlin [18], a set of approximate equations of motion is developed for a typical layer using the inter-laminar stresses as explicit variables. The relative motion of a layer to the adjacent layers is related by phase shifts which represent the solution of the difference parts of equations. In this way the number of the layers can be increased without increasing the size of matrix in the numerical process of invert to satisfy the boundary conditions.

It is also well understood that a thin viscoelastic layer present between elastic layers can reduce the elastic impact energy significantly by dissipating the strain energy into heat [19,20]. In our previous work [5] an elastomer layer is presented between a composite half space and a protection strip on the edge on which the impact is applied. Numerical results of the work showed an appreciable reduction in the normal stress. As an extension of this research and the first part of this report we now examine the wave propagation in a composite plate made of two elastic layers and an elastomer layer. Generalization of this problem is straightforward by assuming that our new periodic composite layer is now made of an elastic sublayer and a viscoelastic sublayer lying alternately. We can now develop the approximate theory which includes both sub-layers. For the second part of the present research we will examine the simplest case of this kind, i.e., an impact on a composite plate consisting of two elastic layers and an elastomer layer between them.

Another possible extension of the multilayer composite plate which can be found in frequent practice is discussed in the last part of this report. In this chapter a crack is introduced on the interface between two elastic layers which represent the final step before a failure occurs in the composite either by spalling or by excessive shear stress. Such crack problems constitute the main part of the study of fracture mechanics. A serious mathematical difficulty arises even in the static problems because of the mixed boundary conditions along the crack direction. The difficulty becomes more serious in the case of dynamic problems due to the diffraction of waves at the crack tip [21-24]. By employing the approximate equations of motion developed in the first part, the transient wave problem has been formulated and dual integral

equations are obtained after application of the mixed boundary conditions.

But the resulting dual integral equations are not easy to solve and are under investigation at this time.

In the results presented in this report only a line impact has been examined. This has simplified the calculations and saved computer time in testing the model. The technique, however, can be extended to the two-dimensional or central impact problem. Since the impact speed is very high (~450 m/sec) and the impact time is short (< 100 μ sec), the impact can be in the range of the elastic-plastic impact or even in the range of the hydraulic impact. But the initial transmission of impact energy is propagated by elastic waves, as if in an unbounded plate, and it is useful to investigate the problem by means of the linear theory of anisotropic elasticity in an infinite composite plate.

II. IMPACT ON MULTILAYER ELASTIC PLATE

1. Formulation

Basic Theory of Linear Anisotropic Elasticity

Cauchy's equations of motion in cartesian tensor form without body forces are given by

$$\sigma_{ij,i} = \rho \ddot{u}_j \quad (II-1)$$

$$\sigma_{ij} = \sigma_{ji}$$

where the repeated index implies summation on that index. A comma represents a partial differentiation with respect to the index following the comma and a superposed dot denotes a time derivative.

tensor is related to the infinitesimal strain tensor ϵ_{ij} by

$$\sigma_{ij} = c_{ijkl} \epsilon_{kl} \text{ or } \sigma_i = c_{ij} \epsilon_j . \quad (II-2)$$

The condensed elastic moduli c_{ij} has the following form for orthotropic materials

$$c_{ij} = \begin{bmatrix} c_{11}, c_{12}, c_{13}, 0, 0, 0 \\ c_{12}, c_{22}, c_{23}, 0, 0, 0 \\ c_{13}, c_{23}, c_{33}, 0, 0, 0 \\ 0, 0, 0, c_{44}, 0, 0 \\ 0, 0, 0, 0, c_{55}, 0 \\ 0, 0, 0, 0, 0, c_{66} \end{bmatrix}$$

Analysis of a Layer

For a layer shown in Fig. 1 we employ the approximate plate theory of Mindlin [18] and the displacement field \underline{u} is expanded in terms of the Legendre polynomials as

$$\underline{u}(x_1, x_2, x_3, t) = \sum_{n=0}^{\infty} \underline{u}^{(n)}(x_1, x_3, t) \cdot P_n(\xi) \quad (\text{II-3})$$

where ξ is the local coordinate along the thickness direction, normalized by b , a half layer thick.

Instead of solving Eq. (II-1) directly we solve a new approximate equation of motion which is obtained through a variational process by integration of Eq. (II-1) over the thickness ξ (see [1], [23]). The result is

$$b \cdot \sigma_{\alpha j}^{(n)} + [P_n(\xi) \cdot \sigma_{2j}]_{\xi=-1}^1 - \sigma_{2j}^{*(n)} = \frac{2\rho b}{2n+1} \ddot{u}_j^{(n)} : \quad j = 1, 2, 3 \\ \alpha = 1, 3 \quad (\text{II-4})$$

where

$$\sigma_{\alpha j}^{(n)} = \int_{-1}^1 P_n(\xi) \cdot \sigma_{\alpha j} d\xi$$

$$\sigma_{2j}^{*(n)} = \int_{-1}^1 \frac{dP(\xi)}{d\xi} \sigma_{2j} d\xi$$

By substituting the constitutive relation (II-2) for the displacement expansion (II-3) into the above approximate equations of motion, we can find governing equations of motion in terms of $u_1^{(0)}, u_2^{(0)}, u_3^{(0)}, u_1^{(1)}, \dots$. The accuracy of this approximate theory depends on how many terms of the

displacement field we retain. Since the complexity in formulation increases rapidly with the number of terms included we keep terms only up to second order. Furthermore, we will examine harmonic waves propagating along the x_1 and x_2 directions so that we drop $u_3^{(n)}$ terms and set $\frac{\partial}{\partial x_3} \{ \} = 0$. Next to get rid of the undesired coupling with higher modes we set $\ddot{u}_1^{(2)} = \ddot{u}_2^{(2)} = 0$. Then the resulting equations are

$$2b(c_{11}u_{1,11}^{(0)} + \frac{1}{b}c_{12}u_{2,1}^{(1)}) + (\sigma_{21}^+ - \sigma_{21}^-) = 2b\rho\ddot{u}_1^{(0)}$$

$$2bc_{66}(\frac{1}{b}u_{1,1}^{(1)} + u_{2,11}^{(0)}) + (\sigma_{22}^+ - \sigma_{22}^-) = 2b\rho\ddot{u}_2^{(0)}$$

$$\frac{2b}{3}(c_{11}u_{1,11}^{(1)} + \frac{3}{b}c_{12}u_{2,1}^{(2)}) - 2c_{66}(\frac{u_1}{b} + u_{2,1}^{(0)}) + (\sigma_{21}^+ + \sigma_{21}^-) = \frac{2}{3}b\rho\ddot{u}_1^{(1)}$$

$$\frac{2b}{3}(c_{66}u_{2,11}^{(1)} + \frac{3}{b}c_{66}u_{1,1}^{(2)}) - 2(c_{12}u_{1,1}^{(0)} + \frac{1}{b}c_{22}u_2^{(1)}) + (\sigma_{22}^+ + \sigma_{22}^-) = \frac{2}{3}b\rho\ddot{u}_2^{(1)}$$

$$(\sigma_{22}^+ - \sigma_{22}^-) - 2(c_{12}u_{1,1}^{(1)} + \frac{3}{b}c_{22}u_2^{(2)}) = 0$$

(II-5)

$$(\sigma_{21}^+ - \sigma_{21}^-) - 2(c_{66}u_{2,1}^{(1)} + \frac{3}{b}c_{66}u_1^{(2)}) = 0$$

where the sign + and - represent the stress components on the top and bottom surfaces of the layer under examination, i.e., at $\xi = \pm 1$. Here we notice that the first, fourth, and last equations are written in terms of $u_i^{(n)}$, where $(n+i)$ is an odd integer and represents the thickness stretching motion (or symmetric motion). In the rest of the equations in which $(n+i)$ is an even integer the displacements represent the flexual motion (or antisymmetric motion). Hence, this process has decoupled the

stretching motion from bending motion*. To get rid of the 2nd order modes from Eq. (II-5) we solve the last two equations for $u_2^{(2)}$ and $u_1^{(2)}$, and insert them into the remaining equations. Then Eq. (II-5) can be reduced as follows:

$$2b(c_{11}u_{1,11}^{(0)} + \frac{1}{b}c_{12}u_{2,1}^{(1)}) + (\sigma_{21}^+ - \sigma_{21}^-) = 2b\rho\ddot{u}_1^{(0)}$$

$$2b c_{66}(\frac{1}{b}u_{1,1}^{(1)} + u_{2,11}^{(0)}) + (\sigma_{22}^+ - \sigma_{22}^-) = 2b\rho\ddot{u}_2^{(0)} \quad (II-6)$$

$$\frac{2b}{3}\hat{c}_{11}u_{1,1}^{(1)} - 2c_{66}(\frac{1}{b}u_{1,1}^{(1)} + u_{2,11}^{(0)}) + \frac{c_{12}b}{3c_{22}}(\sigma_{22}^+ - \sigma_{22}^-),_1 + (\sigma_{21}^+ + \sigma_{21}^-) = \frac{2}{3}b\rho\ddot{u}_1^{(1)}$$

$$-2(c_{12}u_{1,1}^{(0)} + \frac{1}{b}c_{22}u_2^{(1)}) + (\sigma_{22}^+ + \sigma_{22}^-) = \frac{2}{3}b\rho\ddot{u}_2^{(1)}$$

where $\hat{c}_{11} = c_{11} - c_{12}^2/c_{22}$.

Plate Analysis

In view of the Legendre polynomial expansion, the displacements on the both sides of a layer can be written as $u_i^\pm = u_i^{(0)} \pm u_i^{(1)}$ since the governing equations for a layer, Eq. (II-6), only include terms up to the first order of expansion, i.e., a linear expansion. Remembering that this analysis is valid for any arbitrary layer in a plate, say the nth layer, equation (II-6) can be immediately written as

* These two motions are, of course, coupled through the boundary conditions.

$$\begin{aligned}
 \rho(\ddot{u}_n + \ddot{u}_{n-1}) &= c_{11}(u_n + u_{n-1})_{,11} + \frac{c_{12}}{b}(v_n - v_{n-1})_{,1} + \frac{1}{b}(\tau_n - \tau_{n-1}) \\
 \rho(\ddot{v}_n - \ddot{v}_{n-1}) &= -\frac{3}{b}c_{12}(u_n + u_{n-1})_{,1} - \frac{3}{b^2}c_{22}(v_n - v_{n-1}) + \frac{3}{b}(\sigma_n + \sigma_{n-1}) + (\tau_n - \tau_{n-1})_{,1} \\
 \rho(\ddot{u}_n - \ddot{u}_{n-1}) &= \hat{c}_{11}(u_n - u_{n-1})_{,11} - \frac{3c_{66}}{b^2}(u_n - u_{n-1}) - \frac{3}{b}c_{66}(v_n + v_{n-1})_{,1} \\
 &\quad + \frac{c_{12}}{c_{22}}(\sigma_n - \sigma_{n-1})_{,1} + \frac{3}{b}(\tau_n + \tau_{n-1}) \\
 \rho(\ddot{v}_n + \ddot{v}_{n-1}) &= c_{66}\left\{\frac{1}{b}(u_n - u_{n-1})_{,1} + (v_n + v_{n-1})_{,11}\right\} + \frac{1}{b}(\sigma_n - \sigma_{n-1})
 \end{aligned} \tag{II-7}$$

where σ and τ are used to represent σ_{22} and σ_{12} and u and v denote u_1 and u_2 , respectively. These equations are the approximate equations of motion of a layer written in the form of a difference-differential equation. For a plate made of N layer, the above equations contain $4(N+1)$ unknowns $(u_o, v_o, \tau_o, \sigma_o, \dots, u_N, v_N, \tau_N, \sigma_N)$ and offer $4N$ equations. Since the additional four conditions are supplied by boundary conditions on the top and bottom surfaces, solutions of these equations can be found.

In Eq. (II-7) we notice some important points. The first point is that the longitudinal coordinate x_1 and the time variable are continuous variables while the thickness coordinate x_2 is now discrete. This enables us to use integral transforms in x_1 and time variables so that we can arrive at pure difference equations after integral transforms. The second point concerns the continuity conditions of stress and displacement. We note that u , v , σ_{22} , and σ_{12} have to be continuous across the layer boundary and these conditions are identically satisfied by

Eq. (II-7). But the normal stress tangential to the layer boundary is not necessarily continuous and Eq. (II-7) allows such a possibility. One can retain higher order terms in the displacement expansion given by Eq. (II-3) to give more accurate results. This can be achieved more easily by using Eq. (II-7) and increasing the number of layers in a plate under consideration. This process does not give any additional difficulties except a little more computer time.

2. Dispersion Relationships of Harmonic Waves

Harmonic Waves

Before we examine the transient propagation of stress wave due to an impact we first investigate dispersion relations of harmonic waves in a composite plate governed by approximate equations of motion (II-7). For harmonic waves propagating along the x_1 axis we assume

$$\{u_n, v_n, \sigma_n, \tau_n\} = \{U_n, V_n, \Sigma_n, T_n\} e^{i(kx_1 - \omega t)} \quad (II-8)$$

Substituting this into the approximate equations of motion (II-7) we obtain

$$(\bar{\omega}^2 - c_{11}^2)(U_n + U_{n-1}) + c_{12} i\kappa (V_n - V_{n-1}) + b(T_n - T_{n-1}) = 0$$
$$-3c_{12} i\kappa (U_n + U_{n-1}) + (\bar{\omega}^2 - 3c_{22})(V_n - V_{n-1}) + i\kappa b(T_n - T_{n-1}) + 3b(\Sigma_n + \Sigma_{n-1}) = 0$$

$$3c_{66} i\kappa (U_n - U_{n-1}) + (\bar{\omega}^2 - c_{66}^2)(V_n + V_{n-1}) + b(\Sigma_n - \Sigma_{n-1}) = 0 \quad (II-9)$$
$$(\bar{\omega}^2 - \hat{c}_{11}^2 - 3c_{66})(U_n - U_{n-1}) - 3c_{66} i\kappa (V_n + V_{n-1}) + 3b(T_n + T_{n-1}) + \frac{c_{12}}{c_{12}} i\kappa b(\Sigma_n - \Sigma_{n-1}) = 0$$

for $n = 1, 2 \dots N$. Here we set

$$\kappa = bk = k\left(\frac{\Delta}{2N}\right), \quad \Delta = 2bN$$

$$\omega^2 = \rho b^2 \omega^2 = \rho \omega^2 \left(\frac{\Delta}{2N}\right)^2$$

and Δ is the total thickness of the plate. For a plate consisting of N layers, the boundary conditions require traction free surfaces, namely, $T_o = \Sigma_o = T_N = \Sigma_N = 0$. When these conditions are applied to equation (II-9) we obtain $4N$ equations in terms of $4N$ unknowns $(U_o, V_o; U_n, V_n, T_n, \Sigma_n)$ with $n = 1, \dots, N-1$; U_N, V_N). By setting the coefficient matrix to be singular, required dispersion relationships can be obtained.

One-layer Plate

The dispersion relationship for a plate made of a single layer can be found by setting $N = 1$ in equation (II-9) with $\Sigma_o = T_o = \Sigma_1 = T_1 = 0$. The resulting equations are now written in matrix form as follows:

$$\begin{bmatrix} (\omega^2 - c_{11}\kappa^2) & c_{12}i\kappa & 0 & 0 \\ -c_{12}i\kappa & \frac{1}{3}(-3c_{22} + \omega^2) & 0 & 0 \\ 0 & 0 & c_{66}i\kappa & c_{66}\kappa^2 - \omega^2 \\ 0 & 0 & c_{11}\kappa^2 + 3c_{66} - \omega^2 & 3c_{66}i\kappa \end{bmatrix} \begin{bmatrix} U_1 + U_o \\ V_1 - V_o \\ U_1 - U_o \\ V_1 + V_o \end{bmatrix} = \begin{bmatrix} 0 \\ 0 \\ 0 \\ 0 \end{bmatrix} \quad (II-10)$$

Then by setting the determinant of the coefficient matrix to zero we obtain

$$c_{11}k^2 - \frac{1}{3}(\bar{\omega}^2 - 3c_{22})(\bar{\omega}^2 - c_{11}k^2) = 0 \quad (II-11)$$

$$c_{66}k^2 - \frac{1}{3}(\bar{\omega}^2 - c_{11}k^2 - 3c_{66})(\bar{\omega}^2 - c_{66}k^2) = 0 .$$

Here we notice that the first relationship corresponds to the state of deformation of $U_1 = U_0$ and $V_1 = -V_0$, which represents the thickness extension of the plate (or the symmetric mode), and the second describes the flexual deformation (or antisymmetric mode). The exact theory of plates gives an infinite number of dispersion relationships, but because this model only has two inertia points (namely $n = 0, 1$), each of them having two components of displacement, we only have the first four relationships.

Dispersion relationships and corresponding phase velocities for an isotropic plate with Poisson's ratio $1/4$ (namely $\lambda = \mu$) are given in Fig. 2a and 2b up to the range where the wave length becomes equal to the plate thickness. Solid lines represent the symmetric modes and dotted lines the antisymmetric modes. As predicted by Mindlin and Medick the optical branch of the symmetric mode approaches the dilatation wave [16]. The acoustic branch of the antisymmetric mode starts from the bending motion and approaches the shear wave when the wave number k becomes larger and larger*. Similar relationships for an anisotropic plate made of 55% graphite fiber-epoxy matrix with a layup angle of 45° are shown in Fig. 3a and 3b.

* See section 5 for discussion about the large wave number limit.

Two-layer Plate

In this case we obtain eight equations by putting $n = 1$ and 2 in equation (II-9). Boundary conditions require $T_0 = \Sigma_0 = T_2 = \Sigma_2 = 0$. By following the same procedure we find the dispersion relations as

$$\{(\bar{\omega}^2 - c_{11}\kappa^2)(\bar{\omega}^2 - 3c_{22}) - 3c_{12}^2\kappa^2\}(\bar{\omega}^2 - \hat{c}_{11}\kappa^2 - 3c_{66} + \frac{c_{66}c_{12}}{c_{22}}\kappa^2) \\ + 3(\bar{\omega}^2 - c_{11}\kappa^2)\{(\bar{\omega}^2 - c_{66}\kappa^2)(\bar{\omega}^2 - \hat{c}_{11}\kappa^2 - 3c_{66}) - 3c_{66}^2\kappa^2\} = 0 \quad (\text{II-12})$$

$$\{(\bar{\omega}^2 - c_{66}\kappa^2)(\bar{\omega}^2 - \hat{c}_{11}\kappa^2 - 3c_{66}) - 3c_{66}^2\kappa^2\} \\ + 3(\bar{\omega}^2 - c_{66}\kappa^2)\{(\bar{\omega}^2 - c_{11}\kappa^2)(\bar{\omega}^2 - 3c_{22}) - 3c_{12}^2\kappa^2\} = 0$$

Again the first equation represents the symmetric mode and is shown as solid lines in Fig. 4 and 5. The second equation is plotted with dotted lines representing the antisymmetric mode.

As expected we have six relationships since the this two-layer model is equivalent to a three-mass system with two degrees of freedom for each mass. When the wave number $k\Delta$ increases the following are observed: for the symmetric mode the upper optical branch approaches the dilatation wave, whereas for the antisymmetric mode the lower optical branch approaches the shear wave*.

* See section 5 for discussions about the large wave number limit.

N-Layer Plate

In general, we can obtain a $2(N+1)$ order polynomial of ω^2 by expanding a $(4N) \times (4N)$ determinant and finding $2(N+1)$ dispersion relationships. But, unfortunately, this process involves considerably complicated algebra and it may be necessary to develop a computer technique to find roots of an equation in determinant form (not in polynomial form).

A difference equation approach can be used to solve the N set of four simultaneous first order difference equations given by Eq. (II-9). This procedure is neat and can be generalized for any number of layers as discussed in the next section; but the last step of this approach, where a long polynomial is to be solved again, is not any simpler than the previous direct method.

ORIGINAL PAGE IS
OF POOR QUALITY

3. Impact on an Elastic Composite Plate

Normalization and Integral Transforms of Governing Equations

The governing equations given by (II-7) are first nondimensionalized as follows:

$$\{U_n, V_n, \eta\} = \{u_n/\Delta, U_n/\Delta, x_1/\Delta\}$$

$$\{C_{ij}, T_n, \Sigma_n\} = \{c_{ij}/c_{66}, \tau_n/c_{66}, \sigma_n/c_{66}\}$$

$$\tau = t/T_o$$

where Δ is the total thickness of the plate and T_o is the time required for the quasi-shear wave to travel the impact radius. Next we apply a Laplace transform in τ and a Fourier transform in η , i.e.,

$$\hat{g}(s) = \int_0^\infty g(\tau) e^{-s\tau} d\tau$$

$$\bar{g}(k) = \frac{1}{\sqrt{2\pi}} \int_{-\infty}^{\infty} g(\eta) e^{ik\eta} d\eta .$$

Then the resulting equations are

$$-(fs^2 + \frac{C_{11}}{2N} k^2)(\hat{U}_n + \hat{U}_{n-1}) - C_{12} ik(\hat{V}_n - \hat{V}_{n-1}) + (\hat{T}_n - \hat{T}_{n-1}) = 0$$

$$C_{12} ik(\hat{U}_n + \hat{U}_{n-1}) - (\frac{fs^2}{3} + 2NC_{22})(\hat{V}_{n-1} - \hat{V}_{n-1}) + (\hat{\Sigma}_n + \hat{\Sigma}_{n-1}) - \frac{ik}{6N} (\hat{T}_n - \hat{T}_{n-1}) = 0$$

(II-13)

$$-C_{66} ik(\hat{U}_n - \hat{U}_{n-1}) - (fs^2 + \frac{C_{66}}{2N} k^2)(\hat{V}_n + \hat{V}_{n-1}) + (\hat{\Sigma}_n - \hat{\Sigma}_{n-1}) = 0$$

$$-(\frac{fs^2}{3} + \frac{C_{11} k^2}{6N} + 2NC_{66})(\hat{U}_n - \hat{U}_{n-1}) + C_{66} ik(\hat{V}_n + \hat{V}_{n-1}) - \frac{C_{12} ik}{6NC_{22}} (\hat{\Sigma}_n - \hat{\Sigma}_{n-1}) + (\hat{T}_n - \hat{T}_{n-1}) = 0$$

where the normalization factor f is given as

$$f = \frac{1}{2N} \frac{\Delta \rho}{c_{66} T_0^2} = \frac{b \Delta \rho}{c_{66} T_0^2} .$$

Solution of Difference Equations

Since the simultaneous difference equations given are linear and all the coefficients are constants the solution [26] has to be

$$\{\hat{U}_n, \hat{V}_n, \hat{T}_n, \hat{\Sigma}_n\} = \{A, B, C, D\} e^{2i\theta n} \quad (\text{II-14})$$

where the phase shift θ is complex, in general, and propagation through the thickness direction in the plate is characterized by θ . Namely, θ is the wave number in the thickness direction. By substituting solution (II-14) into the difference equation (II-13) we obtain a set of four simultaneous homogeneous equations through which the relationships among the constants A, B, C , and D have to be determined. If we set the resulting coefficient matrix of A, B, C , and D to be singular we obtain the following equation for phase shift θ :

$$\begin{aligned} & \cos^4 \theta (fs^2 + \frac{c_{11}k^2}{2N})(fs^2 + \frac{c_{66}k^2}{2N}) \\ & + \sin^4 \theta (\frac{fs^2}{3} + 2NC_{22} - \frac{c_{12}k^2}{6N}) \cdot (\frac{fs^2}{3} + \frac{\hat{c}_{11}}{6N} k^2 + 2NC_{66} - \frac{c_{66}c_{12}}{6NC_{22}} k^2) \\ & + \cos^2 \theta \sin^2 \theta [(fs^2 + \frac{c_{11}k^2}{2N}) \{ \frac{k^2}{6N} C_{66} + \frac{fs^2}{3} + 2NC_{22} - (\frac{k}{6N})^2 \frac{2C_{66}}{C_{22}} (fs^2 + \frac{c_{66}k^2}{2N}) \}] \\ & - (c_{12} + c_{66})^2 k^2 + (fs^2 + \frac{c_{66}k^2}{2N}) (\frac{fs^2}{3} + \frac{\hat{c}_{11}}{6N} k^2 + 2NC_{66} + \frac{c_{12}^2 k^2}{6NC_{22}})] \\ & = a_1 \cos^4 \theta + a_2 \cos^2 \theta + a_3 = 0 . \end{aligned} \quad (\text{II-15})$$

This equation implies that for a given wave number k along x_1 and a frequency s (s represents the frequency for the case of harmonic waves), an infinite value of wave numbers exists for propagation through the thickness direction, but only four of them are sufficient to give all linearly independent solutions of the form of Eq. (II-14). If we denote the solution of the phase shift equation as

$$\cos^2 \beta = \frac{-a_2 + \sqrt{a_2^2 - 4a_1 a_3}}{2a_1} \quad (II-16)$$

$$\cos^2 \alpha = \frac{-a_2 - \sqrt{a_2^2 - 4a_1 a_3}}{2a_1}$$

the complete general solutions of difference equation (II-13) are

$$\begin{bmatrix} \hat{U}_n \\ \hat{V}_n \\ \hat{T}_n \\ \hat{\Sigma}_n \end{bmatrix} = \begin{bmatrix} A_1 \\ B_1 \\ C_1 \\ D_1 \end{bmatrix} e^{2i\beta n} + \begin{bmatrix} A_2 \\ B_2 \\ C_2 \\ D_2 \end{bmatrix} e^{-2i\beta n} + \begin{bmatrix} A_3 \\ B_3 \\ C_3 \\ D_3 \end{bmatrix} e^{2i\alpha n} + \begin{bmatrix} A_4 \\ B_4 \\ C_4 \\ D_4 \end{bmatrix} e^{-2i\alpha n} \quad (II-17)$$

Next, by substituting the above solutions into the original difference equations (II-13) we find the relationships among A_i , B_i , C_i , and D_i . The results are

$$\begin{bmatrix} \hat{\bar{U}}_n \\ \hat{\bar{V}}_n \\ \hat{\bar{T}}_n \\ \hat{\bar{\Sigma}}_N \end{bmatrix} = \begin{bmatrix} X_1(\beta) & E_1 \\ X_2(\beta) & E_2 \\ X_3(\beta) & E_3 \\ E_1 \end{bmatrix} \cdot \cos 2n\beta + i \begin{bmatrix} X_1(\beta) & E_2 \\ X_2(\beta) & E_1 \\ X_3(\beta) & E_1 \\ E_2 \end{bmatrix} \cdot \sin 2n\beta$$

(II-18)

$$+ \begin{bmatrix} Y_1(\alpha) & E_4 \\ Y_2(\alpha) & E_3 \\ E_3 \\ Y_3(\alpha) & E_4 \end{bmatrix} \cdot \cos 2n\alpha + i \begin{bmatrix} Y_1(\alpha) & E_3 \\ Y_2(\alpha) & E_4 \\ E_4 \\ Y_3(\alpha) & E_3 \end{bmatrix} \cdot \sin 2n\alpha$$

where $E_1 = D_1 + D_2$, $E_2 = D_1 - D_2$, $E_3 = C_3 + C_4$, $E_4 = C_3 - C_4$ and

$$X_i(\beta) = - \frac{\Delta_i(\beta)}{\Delta(\beta)}$$

$$\Delta(\beta) = (fs^2 + \frac{C_{11}k^2}{2n})(fs^2 + \frac{C_{66}k^2}{2n})\cos^3\beta$$

$$+ \{(fs^2 + \frac{C_{66}k^2}{2n})(\frac{fs^2}{3} + \frac{\hat{C}_{11}k^2}{6n} + 2nC_{66}) - C_{66}C_{12}k^2 - C_{66}^2k^2\}\sin^2\beta \cdot \cos\beta$$

$$\Delta_1(\beta) = ik \sin^2\beta \cos\beta \{ \frac{C_{12}}{6nC_{22}}(fs^2 + \frac{C_{66}k^2}{2n}) - (C_{12} + C_{66}) \} \quad (II-19)$$

$$\Delta_2(\beta) = i \sin^3\beta \{ \frac{C_{66}C_{12}k^2}{6nC_{22}} - (\frac{fs^2}{3} + \frac{\hat{C}_{11}k^2}{6n} + 2nC_{66}) \} - \cos^2\beta \sin\beta (fs^2 + \frac{C_{11}k^2}{2n})$$

$$\begin{aligned}
 \Delta_3(\beta) &= k \sin^3\beta \{ (\frac{fs^2}{3} + \frac{\hat{C}_{11}k^2}{6n} + 2nC_{66})C_{12} - \frac{C_{12}^2k^2}{6nC_{22}}C_{66} \} \\
 &\quad + k \sin\beta \cos^2\beta \{ \frac{C_{12}}{6nC_{22}}(fs^2 + \frac{C_{11}k^2}{2n}) \cdot (fs^2 + \frac{C_{66}k^2}{2n}) - (fs^2 + \frac{C_{11}k^2}{2n})C_{66} \}
 \end{aligned}$$

and

$$Y_i(\alpha) = - \frac{\bar{\Delta}_i(\alpha)}{\bar{\Delta}(\alpha)}$$

$$\bar{\Delta}(\alpha) = i \cos^2 \alpha \cdot \sin \alpha \{ C_{66} k^2 (C_{12} + C_{66}) - (fs^2 + \frac{C_{66} k^2}{2n}) \cdot (\frac{fs^2}{3} + \frac{\hat{C}_{11} k^2}{6n}$$

$$+ 2nC_{66} + \frac{12k^2}{6nC_{22}}) \} + i \sin^3 \alpha (\frac{fs^2}{3} + 2nC_{22})$$

$$x (\frac{C_{66} C_{12} k^2}{6nC_{22}} - \frac{fs^2}{3} - \frac{C_{11} k^2}{6n} - 2nC_{66})$$

$$\bar{\Delta}_1(\alpha) = \cos^3 \alpha (fs^2 + \frac{C_{66} k^2}{2n})$$

$$+ \sin^2 \alpha \cdot \cos \alpha \{ -(\frac{k}{6n})^2 \frac{C_{12}}{C_{22}} (fs^2 + \frac{C_{66} k^2}{2n}) + \frac{k^2}{6n} C_{66} + (\frac{fs^2}{3} + 2nC_{22}) \}$$

$$\bar{\Delta}_2(\alpha) = k \cdot \cos^2 \alpha \sin \alpha (C_{12} + C_{66}) \quad (II-20)$$

$$+ k \sin^3 \alpha \{ \frac{1}{6n} (\frac{fs^2}{3} + \frac{\hat{C}_{11} k^2}{6n} + 2nC_{66}) - (\frac{k}{6n})^2 \frac{C_{12} C_{66}}{C_{22}} \}$$

$$\bar{\Delta}_3(\alpha) = ik \sin^2 \alpha \cos \alpha \{ \frac{C^2}{6n} k^2 - \frac{1}{6n} (\frac{fs^2}{3} + \frac{\hat{C}_{11} k^2}{6n} + 2nC_{66}) (fs^2 + \frac{C_{66} k^2}{2n})$$

$$+ C_{66} k (\frac{fs^2}{3} + 2nC_{22}) \} + ik \cos^3 \alpha \{ -C_{12} (fs^2 + \frac{C_{66} k^2}{2n}) \} .$$

Equations (II-18) with (II-19,20) and the phase shifts α and β given by (II-16) constitute the final form of the general solutions of the difference equations (II-13).

In Eqs. (II-19,20) we notice that when $k \rightarrow 0$ we have $X_1(\beta) = X_3(\beta) = Y_2(\alpha) = Y_3(\alpha) = 0$. Namely the propagation of the normal stress (with phase shift β) and the propagation of the shear stress (with phase shift α) are completely decoupled. This occurs when the waves are propagating only through the thickness direction [27].

Impact Boundary Condition

Boundary conditions for an impact can be described by any two conditions among u_o , v_o , σ_o , and τ_o and another two conditions from u_N , v_N , σ_N , and τ_N . For our present problem we have chosen a line impact by a normal stress along the x_3 axis (Figure 1), i. e.,

$$\begin{aligned}\sigma_o &= -\frac{P_o}{4} (1-\cos \frac{2\pi t}{t_o}) (1+\cos \frac{\pi x}{a}) : |x| \leq a \text{ and } 0 \leq t \leq t_o \\ &= 0 : |x| > a \text{ or } t > 0 \text{ or } t > t_o \\ \tau_o &= \sigma_N = \tau_N = 0 .\end{aligned}\tag{II-21}$$

Hence, the boundary conditions for the present impact problem lead to the following equation

$$\begin{bmatrix} 0 & , & X_3(\beta) & , & 1 & , & 0 \\ 1 & , & 0 & , & 0 & , & Y_3(\alpha) \\ iX_3(\beta)\sin 2\beta N & , & X_3(\beta)\cos 2\beta N & , & \cos 2\alpha N & , & i\sin 2\alpha N \\ \cos 2\beta N & , & i\sin 2\beta N & , & iY_3(\alpha)\sin 2\alpha N & , & Y_3(\alpha)\cos 2\alpha N \end{bmatrix} \cdot \begin{bmatrix} E_1 \\ E_3 \\ E_3 \\ E_4 \end{bmatrix} = \begin{bmatrix} 0 \\ q \\ 0 \\ 0 \end{bmatrix}$$

(II-22)

where q is the integral transform of the impact function (II-21)*.

Solving the above equations for E_i 's we can have

$$E_i = \frac{D_i}{D} q$$

$$D = \{1+X_3^2(\beta)Y_3^2(\alpha)\}\sin 2\alpha N \cdot \sin 2\beta N + 2X_3(\beta)Y_3(\alpha)(\cos 2\alpha N \cdot \cos 2\beta N - 1)$$

$$D_1 = X_3(\beta)Y_3(\alpha)(\cos 2\alpha N \cdot \cos 2\beta N - 1) + \sin 2\alpha N \cdot \sin 2\beta N$$

$$D_2 = i\{\cos 2\beta N \cdot \sin 2\alpha N - X_3(\beta)Y_3(\alpha)\cos 2\alpha N \cdot \sin 2\alpha N\} \quad (\text{II-23})$$

$$D_3 = iX_3(\beta)\{X_3(\beta)Y_3(\alpha)\sin 2\beta N \cdot \cos 2\alpha N - \cos 2\beta N \cdot \sin 2\alpha N\}$$

$$D_4 = X_3(\beta)\{X_3(\beta)Y_3(\alpha)\sin 2\alpha N \cdot \sin 2\beta N + \cos 2\beta N \cdot \cos 2\alpha N - 1\} .$$

Substituting the E_i 's into the general solution (II-18) we can find the complete solutions which satisfy the impact boundary conditions given by (II-21). In other words, for given values of k and s we first find the phase shift α and β from (II-15,16) and with these we can find solutions in integral transform from equations (II-18,23) which are the final solutions under impact. After \hat{U}_n , \hat{V}_n , \hat{T}_n and $\hat{\bar{T}}_n$ are calculated

* Allowing the determinant of the coefficient matrix to vanish leads to dispersion relations of an N -layer plate, namely $D(\alpha, \beta) = 0$. Then, α and β are obtained from (II-15,16) which gives the complete dispersion relationships.

with a given impact function q , they can be inverted easily by means of the fast Fourier transform routine [3,20] to give the complete displacement and the stress fields after impact.

Tangential Normal Stress

As discussed following Eq. (II-7), the tangential normal stress does not appear explicitly in the approximate equations of motion. Therefore, this component of the stress has to be calculated from the constitutive equation. Namely,

$$\sigma_{11_o} = c_{11} u_{o,1} + \frac{c_{12}}{2b} (v_1 - v_o)$$

$$\sigma_{11_n} = c_{11} u_{n,1} + \frac{c_{12}}{2b} (v_n - v_{n-1}) \quad 1 \leq n \leq N$$

or after normalization and integral transform they are

$$\hat{\sigma}_{11_o} = -ikC_{11}\hat{U}_o + N \cdot C_{12}(\hat{V}_1 - \hat{V}_o) \quad (\text{II-24})$$

$$\hat{\sigma}_{11_n} = -ikC_{11}\hat{U}_n + N \cdot C_{12}(\hat{V}_n - \hat{V}_{n-1}) \quad 1 \leq n \leq N .$$

Then once the displacement field is computed the tangential normal stress can be obtained from the above equation and inverted.

4. Some Numerical Results

The analysis discussed in the previous section includes the transient propagation in all directions but suitable choices of impact time, impact radius, sizes of time and distance steps are essential to make good use of the fast Fourier transform. For example, if we take a large time increment with a relatively thin plate propagation through the thickness will not be seen. For this matter we have examined several different cases.

Case 1: Longitudinal propagation

Propagation of impact generated waves along the longitudinal direction is examined for an isotropic plate (steel plate: $\lambda = \mu = 1.2 \times 10^7$ psi) employing a two-layer model. For these calculations we used an impact time $t_0 = 10 \mu\text{sec}$, plate thickness $\Delta = 1 \text{ cm}$, and impact radius $a = 4 \text{ cm}$. Some of the results at a few different time sequences are shown in Fig. 6 a-f.

In these figures we can see two distinct states of propagation and corresponding wave fronts: one for horizontal displacements (u) and longitudinal normal stresses (σ_{11}), and another for vertical displacements (v) and shear stresses (τ). In other words, the initial signals of the horizontal displacements and longitudinal normal stresses propagate through the plate with longitudinal wave speed at amplitudes that are relatively small. But the major parts of their signals are due to a bending wave propagating with shear stresses and vertical displacements with a lower velocity. When the group velocities of these waves are calculated from the numerical results, they are about $5 \text{ mm}/\mu\text{sec}$ and $3 \text{ mm}/\mu\text{sec}$, respectively, while the phase velocities of the unbounded

medium of this material are $C_d = \sqrt{(\lambda+2\mu)/\rho} = 5.61 \text{ mm}/\mu\text{sec}$ and $C_s = \sqrt{\mu/\rho} = 3.25 \text{ mm}/\mu\text{sec}$.

Case 2: Propagation Through Thickness

To examine the propagation through the thickness it is necessary to have a sufficient number of layers in a plate. It is also essential to make the time step relatively small compared to the layer thickness. To do this we increase the thickness of the plate and the number of layers and reduce the impact time.

In Figs. 7 and 8 propagation of the transverse normal stress in the same plate ($\Delta = 4 \text{ cm}$, $t_0 = 2\mu\text{sec}$, $a = 40 \text{ cm}$; 4-layer model) is shown at different time sequences. As seen in Fig. 7, the transverse normal stress is initially compressive due to the impact and a compression wave propagates through the thickness. But later it becomes a tension wave after reflection from the free surface and the tension wave propagates back to the impact surface. In Fig. 8 we see the change of the transverse normal stress and the interlaminar shear stress with time for the same impact conditions as in Fig. 7.

Similar results are also shown for the case of an anisotropic plate in Fig. 9 (55% graphite fibers-epoxy matrix, layup angle = 15° ; $\Delta = 1 \text{ cm}$, $t_0 = 2\mu\text{sec}$, $a = 2 \text{ cm}$; 8-layer model). Here we again notice a clear delay in time for waves to travel from one layer to the next one. Another important point is that the shape of the impact stress is relatively well preserved during the initial stage of propagation but changes immediately afterwards. The distortion of the shape becomes more serious with further propagation due to reflection, thus, showing the highly dispersive nature of the harmonic waves in the approximate plate theory.

When the group velocities are calculated from these results, we find 6.32 mm/ μ sec for the dilatation wave and 3.33 mm/ μ sec for the shear wave in the case of the isotropic plate and 2.5 mm/ μ sec for the quasi-dilatation wave of the anisotropic plate. Their expected values are, respectively, 5.61, 3.25, and 2.36 mm/ μ sec. In other words, waves going through the thickness are traveling faster than expected.

Case 3. Wave Surfaces

In the previous two cases we examined the transient waves propagating dominantly along either the x_1 axis or through the thickness direction by suitable choices of the plate geometry and impact condition. now examine the combined effect, simultaneous propagation in both directions. This effect is shown in Fig. 10 (isotropic plate; $\Delta = 4$ cm, $t_o = 4\mu$ sec, $a = 4$ cm; 4-layer model) where the transverse normal stress generated from the line source due to impact not only spreads out in all directions but also reflects from the free surface.

When the plate is anisotropic, the situation is more complex in the sense that waves are neither dilatation nor shear but they are coupled together (now called quasi-dilational or quasi-shear waves). Due to the coupling, phase velocities of the anisotropic wave vary from one direction to another, resulting in complicated shapes for the velocity surfaces and wave fronts [2]. For an anisotropic plate (made of 55% graphite fiber-epoxy matrix with layup angle 45°) the velocity surfaces and the wave surfaces are shown in Fig. 11. The stress state at 10 μ sec after the impact on the same plate ($\Delta = 4$ cm, $t_o = 4\mu$ sec, $a = 2$ cm; 8-layer model) with the corresponding wave fronts are shown in Fig. 12a. In the

propagation of the quasi-longitudinal wave we notice that the longitudinal propagation is well bounded by the quasi-dilatational wave surface but the transverse propagation is not. The shear wave is not bounded by the quasi-shear wave front in either direction.

This interesting phenomenon of higher propagation speeds through the thickness is related to the dispersion relationship at short wave length limits; it is discussed in the next section.

5. Correction Factor and Conclusion

Correction Factor

According to the present model of a multilayer plate, one of the antisymmetric modes of the dispersion relationships approaches the shear speed when the wave length becomes shorter and shorter, as mentioned in Section 2. It is well understood that such a limit is incorrect, i.e., in the limit of short wave length there should be a Rayleigh wave instead of a shear wave. Such a discrepancy can be eliminated by introduction of proper correction factors, as shown by Mindlin and Medick [18]. Correction factors can be found by examining either the large wave number limit or the cut-off frequencies of both the exact theory and the present approximate theory. Since these two ways lead us to the same results we will find the factors by matching the cut-off frequencies of the two theories.

The cut-off frequencies of the exact theory for an isotropic plate can be obtained from the well-known Rayleigh-Lam's equation. The lowest cut-off frequencies are $\frac{\pi}{\Delta} \sqrt{(\lambda+2\mu)/\rho}$ for the symmetric mode and $\frac{\pi}{\Delta} \sqrt{\mu/\rho}$ for the antisymmetric mode. The corresponding cut-off frequencies of our approximate theory are $\frac{2}{\Delta} \sqrt{3c_{22}/\rho}$ and $\frac{2}{\Delta} \sqrt{3c_{66}/\rho}$ *. Hence, we notice that replacing c_{22} by $c_{22}\pi^2/12$ and c_{66} by $c_{66}\pi^2/12$ makes the two theories have the same two lowest cut-off frequencies. Furthermore the shear wave observed in the short wave length limit of the present approximation becomes a wave with a speed of $\frac{\pi}{\sqrt{12}} \sqrt{\mu/\rho}$, i.e., the Rayleigh wave.

Another important consequence of the correction factor is to reduce propagation speeds through the thickness, which are related to $\sqrt{c_{22}/\rho}$

* The lowest two cut-off frequencies are found from Eq. (II-11) and they are independent of the layer number in the plate under investigation.

and $\sqrt{c_{66}/\rho}$, with a factor of $\pi/\sqrt{12}$. Propagation of the maximum value of the interlaminar normal stress through the thickness is examined with and without correction factors and the results are shown in Fig. 13. Without the correction factor the propagation speed in a composite plate is roughly about 2.60 mm/ μ sec obtained from the numerical results used in Fig. 12. When the same plate is subjected to identical impact conditions this reduces to about 2.41 mm/ μ sec with the correction factor. Comparing this with the group velocity in an unbounded composite space (= 2.36 mm/ μ sec) the agreement of the present approximate theory is remarkable. Similar results are also observed in the case of shear and quasi-shear waves. When these correction factors are introduced in the previous cases, shown in Figs. 8, 9, and 12, all the signals propagating through the thickness are now well bounded within the corresponding wave fronts, as shown in Fig. 12b and from this we can notice the importance of the correction factors.

Discussion and Computation Time

It is interesting to compare the computation time of this model with some other methods, such as the finite element method or the finite difference method. In the case of an 8-layer anisotropic plate model, from which Figs. 9 and 12 are produced, we have

9 steps along the thickness: 8-layer model;

32 step along the x_1 direction: 64 points are used in practice but only half of them are useful because of the symmetry of the problem,

32 steps in time;

2 displacement components at each point.

Therefore the total number of the unknowns, which are the basic unknowns either in case of the finite difference or finite element methods, is

18,432. After these primary variables are calculated, 27,648 secondary variables (three stress components at each points) have to be calculated again. According to our present model all these processes require only 200 K of computer space without using magnetic tapes or any kind of additional storage space and only 1 minute 6 seconds for CPU time in the IBM 370-168 model including compiling, linkage editing, I/O and execution.

Conclusion

The present theory is a generalization of Mindlin's approximate plate theory applied to a multilayer plate under an impact. By combined use of the finite difference technique in the thickness direction and the fast Fourier transform in the plane of plate and time, this model can be very useful for the study of wave propagation in a composite plate under impact forces. However, reasonable attention in usage of the fast Fourier transform is required to avoid spurious data. From the limited numerical data obtained from this model it appears that the anisotropy in the plate will lead to a considerable interlaminar shear which might lead to ply bonding failures. The model also shows that for short enough impact times, an interlaminar tension can develop as one would expect, which might also account for interlaminar ply failure.

III. IMPACT OF A COMPOSITE PLATE WITH AN INTERLAMINAR DAMPING LAYER

1. Description of Problem

Geometry of Plate

As an extension of the multilayer plate discussed in Chapter II we now examine the impact and the consequent stress wave propagation in a composite plate with viscoelastic damping layers.

Possible models for damping mechanisms in plates are shown in Fig. 14. We will formulate a model made of an alternating number of elastic and viscoelastic layers, as shown in Fig. 14-c.

As long as the layer structure of the plate is periodic, the main part of the analysis in Chapter II for an elastic plate is valid with additional equations for viscoelastic layers.

Viscoelastic Property of Elastomer

The mechanical properties of an elastomer are usually expressed in terms of a complex modulus depending on the frequency, i.e.,

$$G^*(\omega) = G'(\omega) + iG''(\omega) . \quad (\text{III-1})$$

With this the constitutive equation is written as

$$\bar{\sigma}_{ij}(\omega) = G^*(\omega) \bar{\epsilon}_{ij}(\omega) \quad (\text{III-2})$$

in the frequency space where $\bar{\sigma}_{ij}(\omega)$ and $\bar{\epsilon}_{ij}(\omega)$ are respectively the Fourier transforms of σ_{ij} and ϵ_{ij} in time* [29].

* For (III-2) the Fourier transform is defined as

$$\bar{f}(\omega) = \frac{1}{\sqrt{2\pi}} \int_{-\infty}^{\infty} f(t) e^{-i\omega t} dt .$$

ORIGINAL PAGE IS
OF POOR QUALITY

The constitutive relation (III-2) with the complex modulus (III-1) implies the following constitutive equation in a time space:

$$\underline{\sigma}(x,t) = \int_{-\infty}^t G(t-\tau) \underline{\epsilon}(x,\tau) d\tau \quad (\text{III-3})$$

where the relaxation function $G(t)$ is related with the complex modulus $G^*(\omega)$ as

$$G^*(\omega) = \frac{1}{i\omega} \int_0^\infty G(t) e^{-i\omega t} dt . \quad (\text{III-4})$$

Therefore, when the complex modulus $G^*(\omega)$ is obtained by experiments, usually by means of harmonic excitation of strain, the relaxation function $G(t)$ can be found by inversion of equation (III-4).

The viscoelastic property of the elastomer under consideration has been extensively investigated (e.g. [19]) and its complex modulus is given in Fig. 15. This complex modulus can be reasonably well described by a three parameter equation as

$$G'(\omega) = a - \frac{6}{\omega^2 + c} . \quad (\text{III-5})$$

These three parameters are obtained from another set of parameters: the maximum values of $G'(\omega)$ when $\omega \rightarrow \infty$, the maximum value of $G''(\omega)/G'(\omega)$ and the ω_0 at which $G''(\omega)/G'(\omega)$ becomes the maximum. Therefore, if we characterize the complex modulus by proper choice of $G'(\omega)$, ω_0 and the maximum of $G''(\omega_0)/G'(\omega_0)$, the relaxation functions are completely described.

2. Formulation

Elastic Layer

In Fig. 16 a typical viscoelastic layer (n^{th}) is shown between two adjacent elastic layers (n^{th} and $(n+1)^{\text{th}}$) with appropriate discretization. The approximate equations of motion for the n^{th} elastic layer given by Eq. (II-7) are still valid. But remembering the new discretizing notation in Fig. 16 we now have to replace $(\cdot)_n$ and $(\cdot)_{n-1}$ by $(\cdot)_n^-$ and $(\cdot)_{n-1}^+$, respectively. The results are

$$\begin{aligned}\rho(\ddot{u}_n^- + \dot{u}_{n-1}^+) &= c_{11}(u_n^- + u_{n-1}^+),_{11} + \frac{c_{12}}{b}(v_n^- - v_{n-1}^+),_1 + \frac{1}{b}(\tau_n^- - \tau_{n-1}^+) \\ \rho(\ddot{v}_n^- - \dot{v}_n^+) &= -\frac{3c_{12}}{b}(u_n^- + u_{n-1}^+),_1 - \frac{3c_{22}}{b^2}(v_n^- - v_{n-1}^+),_1 + \frac{3}{b}(\sigma_n^- + \sigma_{n-1}^+) + (\tau_n^- - \tau_{n-1}^+),_1 \\ \rho(\ddot{u}_n^- - u_{n-1}^+) &= \hat{c}_{11}(u_n^- - u_{n-1}^+),_{11} - \frac{3c_{66}}{b^2}(u_n^- - u_{n-1}^+),_1 - \frac{3c_{66}}{b}(v_n^- + v_{n-1}^+),_1 \quad (\text{III-6}) \\ &\quad + \frac{c_{12}}{b^2}(\sigma_n^- - \sigma_{n-1}^+),_1 + \frac{3}{b}(\tau_n^- + \tau_{n-1}^+) \\ \rho(\ddot{v}_n^- + v_{n-1}^+) &= c_{66}\left\{\frac{1}{b}(u_n^- - u_{n-1}^+),_1 + (v_n^- + v_{n-1}^+),_{11}\right\} + \frac{1}{b}(\sigma_n^- - \sigma_{n-1}^+)\end{aligned}$$

Viscoelastic Layer

Since the thickness of the elastomer is thin compared with the elastic layer, we can assume that the stress field is uniform through the thickness of the elastomer. In other words, we have $\sigma_n^- = \sigma_n^+ = \sigma_n$ and $\tau_n^- = \tau_n^+ = \tau_n$ for (III-6). Therefore, the following compatibility conditions for the

elastomer can be obtained immediately:

$$\varepsilon_{12(n)} = \frac{1}{4} \frac{\partial}{\partial x_1} (v_n^+ + v_n^-) + \frac{1}{2D} (u_n^+ - u_n^-)$$

(III-7)

$$\varepsilon_{22(n)} = \frac{1}{D} (v_n^+ - v_n^-)$$

where D is the thickness of the elastomer.

We further assume that the dissipation is mostly due to shear motion, i.e., that the normal component of the continuous traction vector is transmitted through the viscoelastic layer purely elastically. Therefore, by combining (III-7) with (III-3) we find

$$\sigma_n = \frac{E}{D} (v_n^+ - v_n^-)$$

(III-8)

$$\tau_n = \int_{-\infty}^t G(t-\tau) \left\{ \frac{1}{2} \frac{\partial}{\partial x_1} (\dot{v}_n^+ + \dot{v}_n^-) + \frac{1}{D} (\dot{u}_n^+ - \dot{u}_n^-) \right\} d\tau .$$

These two equations and four more from Eq. (III-6) are the complete equations needed to solve the impact on a composite plate with elastomer. For a plate made of N elastic layers and $(N-1)$ viscoelastic layers Eq. (III-6) provides $4N$ equations and (III-8) gives $2(N-1)$ equations. Since the total number of the unknowns are now $6N+2$ ($u_o, v_o, \sigma_o, \tau_o; u_1^-, v_1^-, u_1^+, v_1^+, \sigma_1, \tau_1; \dots; u_{N-1}^-, v_{N-1}^-, u_{N-1}^+, v_{N-1}^+, \sigma_{N-1}, \tau_{N-1}; u_N, v_N, \sigma_N, \tau_N$) we can solve this system of equations with four additional conditions supplied by the suitable boundary conditions.

Here we notice that the governing equations are now a set of six difference-integro-partial differential equations. These equations can be

reduced to difference equations after appropriate integral transforms and the resulting difference equations can be handled rather simply, as in the previous chapter.

3. Numerical Results and Discussion

Impact on Plate

For the report we examine the impact on a plate consisting of two elastic layers and a viscoelastic layer, as shown in Fig. 17, with an impact function

$$\begin{aligned}\sigma_0 &= P_0 \left\{ 1 - \left(\frac{x_1}{a} \right)^2 \right\} \sin \frac{\pi t}{t_0} ; \quad |x_1| < a \text{ and } 0 < t < t_0 \\ &= 0 \quad ; \quad |x_1| > a \text{ or } t > t_0, \text{ or } t < 0\end{aligned}\tag{III-9}$$

with all other stress components vanishing on both surfaces of the plate.

Now by putting $n = 1$ and 2 into Eq. (III-6) we have eight equations and two more equations are obtained from Eq. (III-8). We again normalize these equations and take the integral transform, as in Chapter II. The resulting equations are:

$$\begin{aligned}
 & -(fs^2 + \frac{c_{11}}{\Delta} bk^2)(\hat{U}_1^- + \hat{U}_o^-) - c_{12} ik(\hat{V}_1^- - \hat{V}_o^-) + \hat{T}_1 = 0 \\
 & 3c_{12} ik(\hat{U}_1^- + \hat{U}_o^-) - (fs^2 + \frac{3c_{22}\Delta}{b})(\hat{V}_1^- - \hat{V}_o^-) + 3\hat{\Sigma}_1 - ik\frac{b\hat{\Sigma}}{\Delta} = -3\hat{\Sigma}_o \\
 & -(fs^2 + \frac{b}{\Delta} c_{66} k^2)(\hat{V}_1^- + \hat{V}_o^-) - c_{66} ik(\hat{U}_1^- - \hat{U}_o^-) + \hat{\Sigma}_1 = \hat{\Sigma}_o \\
 & -(fs^2 + \frac{b}{\Delta} c_{11} k^2 + \frac{\Delta}{b} 3c_{66})(\hat{U}_1^- - \hat{U}_o^-) + 3c_{66} ik(\hat{V}_1^- + \hat{V}_o^-) - \frac{c_{12}}{c_{22}} \frac{b}{\Delta} ik\hat{\Sigma}_1 + 3\hat{T}_1 = -\frac{c_{12}}{c_{22}} \frac{b}{\Delta} ik\hat{\Sigma}_o \\
 & -(fs^2 + \frac{c_{11}}{\Delta} bk^2)(\hat{U}_2^- + \hat{U}_1^+) - c_{12} ik(\hat{V}_2^- - \hat{V}_1^+) - \hat{T}_1 = 0
 \end{aligned}
 \tag{III-10}$$

$$\begin{aligned}
 & 3c_{12} ik(\hat{U}_2^- + \hat{U}_1^+) - (fs^2 + \frac{3c_{22}\Delta}{b})(\hat{V}_2^- - \hat{V}_1^+) + 3\hat{\Sigma}_1 + \frac{b}{\Delta} ik\hat{T}_1 = 0 \\
 & -(fs^2 + \frac{b}{\Delta} c_{66} k^2)(\hat{V}_2^- + \hat{V}_1^+) - c_{66} ik(\hat{U}_2^- - \hat{U}_1^+) - \hat{\Sigma}_1 = 0 \\
 & -(fs^2 + \frac{b}{\Delta} c_{11} k^2 + \frac{\Delta}{b} 3c_{66})(\hat{U}_2^- - \hat{U}_1^+) + 3c_{66} ik(\hat{V}_2^- + \hat{V}_1^+) + \frac{c_{12}}{c_{22}} \frac{b}{\Delta} ik\hat{\Sigma}_1 + 3\hat{T}_1 = 0
 \end{aligned}$$

$$\hat{\Sigma}_1 = E \frac{\Delta}{D} (\hat{V}_1^+ - \hat{V}_1^-)$$

$$\hat{T}_1 = \bar{G}(s) \left\{ \frac{\Delta}{D} (\hat{U}_1^+ - \hat{U}_1^-) - \frac{ik}{2} (\hat{V}_1^+ + \hat{V}_1^-) \right\}$$

where $\bar{G}(s)$ is the Laplace transform of the relaxation function $G(t)$

with respect to $\tau = t/T_o$ and we have used the boundary conditions

$\tau_o = \tau_2 = \sigma_2 = 0$. From the above 10 equations we can find 10 unknowns $(\hat{U}_o^-, \hat{V}_o^-, \hat{U}_1^-, \hat{V}_1^-, \hat{U}_1^+, \hat{V}_1^+, \hat{\Sigma}_1, \hat{T}_1; \hat{U}_2^-, \hat{V}_2^+)$ with given impact function $\hat{\Sigma}_o$ and once these are calculated the displacement and the stress fields can be computed by inversions of the integral transforms by means of the FFT algorithm.

Numerical Results

For the present computation we have used the Young's modulus $E = .7 \times 10^4$ psi and the shear modulus $G'(\omega) = .817 \times 10^4 - \frac{2.41 \times 10^{12}}{3 \times 10^4 + \omega^2}$ for the elastomer where ω is given in hertz. The $G'(\omega)$ in this case implies that $G'(\infty) = .817 \times 10^4$ psi and $\max(G''(\omega)/G'(\omega)) = 3.3$ at $\omega_0 = 800$ Hz.

The propagation of stress wave in this case is quite similar to that of the composite plate without an elastomer layer except the peak values of the interlaminar stress. Values of the peak stress with different thickness of the elastomer layer are plotted with those of the purely elastic plate in Fig. 18. As we can see in this figure the interlaminar shear stress has increased by a small amount while a reduction of the normal stress is considerable when the elastomer layer becomes thicker and thicker. From this result it is obvious that the reduction of the normal component of stress can be achieved by introducing such a soft and energy-dissipating elastomer layer.

Discussion

In addition to the simple reduction of the normal stress it is also observed that the amount of reduction increases with the value of $G''(\omega)/G'(\omega)$ and the location of ω_0 at which $G''(\omega)/G'(\omega)$ becomes the maximum value. In other words, we can make the dissipation effect more serious by choosing an elastomer whose $G''(\omega)/G'(\omega)$ becomes maximum at ω_0 around which the most of the impact energy is carried out.

It is also believed that a further dissipation effect will be possible if we make the transmission of the normal stress viscoelastic across the elastomer layer, which we have assumed is elastic for this report.

IV. IMPACT ON A PLATE WITH A CRACK

1. Introduction

When the impact stress is low, the impact is elastic and the stresses in the plate can be described by elastic wave propagation. When the stress is increased beyond a certain limit then the impact damage occurs. Elastic-plastic impact is complicated for two reasons, namely, unloading and loading must be treated differently, and the strain rate effect [30] must be included. If the impact stress is increased further to a certain level where the induced stress is higher than the strength of a target material then penetration begins to occur. In this limit the target material sometimes behaves as a fluid and such a state of impact is known as a hydraulic impact [31]. Another failure mode is the occurrence of interlaminar cracks.

Investigation of the stress state in solids with cracks falls in the category of so-called fracture mechanics and has been under an extensive scrutiny since the famous enunciation by Griffith [32]. Presence of cracks inside a material usually leads us to a mixed boundary value problem and only a limited class of problems can be solved [33,34]. In the case of dynamic loading the problem becomes more difficult due to the scattering of the stress wave by the crack [21-24]. In this report we will formulate the problem of a plate with a crack which is subject to a dynamic loading.

Our original goal was to study the effect of interlaminar cracks in composite plates in response to impact loads. Debugging problems in other parts of this report, however, used valuable time originally set aside for this problem. The following section is an attempt to illustrate the

use of the Mindlin plate theory for the study of interlaminar cracks and to point out the mathematical difficulties that must be overcome in solving the problem.

2. Formulation

Description of Problem

The plate under consideration has a crack on the midplane running from $x_1 = -h$ to $+h$ as shown in Fig. 19. Stress can be applied either on the surface of the plate or on the crack surface. In the former case the crack surfaces can be in contact and the boundary conditions become more complex due to the partial continuity of stresses and displacements during the contact. For the present report to illustrate the mathematical difficulties we assume that the crack surface is subject to a known compressive impact.

Governing Equation and Boundary Conditions

We can formulate this crack problem by assuming that the lower and the upper half plates are made of a number of layers but for simplicity we consider the plate to consist of two identical layers and the crack to be present on the interface of these two layers. Following the notation shown in Fig. 19 we have the governing equations identical to Eq. (III-6) with $n = 1$ and 2. The boundary condition requires that both plate surfaces remain traction free. The crack surface is subject to a prescribed impact condition while the displacement and stress are continuous along the layer boundary outside the crack. Namely, we have

$$\begin{aligned} \sigma_0 &= \tau_0 = \sigma_2 = \tau_2 = 0 \\ \sigma_1^+ &= \sigma_1^- = -P_o(x_1, t) \\ \tau_1^+ &= \tau_1^- = 0 \end{aligned} \quad \left. \begin{array}{l} \\ \\ \end{array} \right\} |x| < h \quad (IV-1)$$
$$\begin{aligned} u_1^+ &= u_1^- , \quad v_1^+ = v_1^- \\ \sigma_1^+ &= \sigma_1^- , \quad \tau_1^+ = \tau_1^- \end{aligned} \quad \left. \begin{array}{l} \\ \\ \end{array} \right\} |x| > h .$$

Due to the twofold symmetry of the problem we now have $u_o = u_2$, $v_o = -v_2$, $\tau_1^+ = \tau_1^- = 0$ and we can set $u_1^+ = u_1^- = u_1$, $-v_1^+ = v_1^- = v_1$.

Thus, the eight equations obtained from Eq. (III-6) are now reduced to

$$\begin{aligned} \rho(\ddot{u}_1 + \ddot{u}_o) &= c_{11}(u_1 + u_o)_{,11} + \frac{c_{12}}{b}(v_1 - v_o)_{,1} \\ \rho(\ddot{v}_1 - \ddot{v}_o) &= -\frac{3c_{12}}{b}(u_1 + u_o)_{,1} - \frac{3c_{22}}{b^2}(v_1 - v_o) + \frac{3\sigma}{b} \\ \rho(\ddot{u}_1 - \ddot{u}_o) &= \hat{c}_{11}(u_1 - u_o)_{,11} - \frac{3c_{66}}{b^2}(u_1 - u_o) - \frac{3c_{66}}{b}(v_1 + v_o)_{,1} + \frac{c_{12}\sigma}{c_{22}},_1 \\ \rho(\ddot{v}_1 + \ddot{v}_o) &= c_{66}\left\{\frac{1}{b}(u_1 - u_o)_{,1} + (v_1 + v_o)_{,11}\right\} + \frac{\sigma}{b} \end{aligned} \quad (\text{IV-2})$$

and the boundary condition is now

$$\left. \begin{array}{l} \sigma = -P_o(x_1, t) \\ v_1 = 0 \end{array} \right\} \begin{array}{l} |x_1| < h \\ |x_1| > h \end{array} \quad \text{along } x_2 = 0 \quad (\text{IV-3})$$

Dual Integral Equation

We now normalize the governing equation (IV-2) and take the integral transform. Then we have

$$\begin{bmatrix} (fs^2 + \frac{b}{\Delta}C_{11}k^2), & C_{12}ik, & 0, & 0 \\ -3C_{12}ik, & (fs^2 + \frac{3\Delta}{b}C_{22}), & 0, & 0 \\ 0, & 0, & C_{66}ik, & (fs^2 + \frac{b}{\Delta}C_{66}k^2) \\ 0, & 0, & (fs^2 + \frac{b}{\Delta}\hat{C}_{11}k^2 + \frac{3\Delta}{b}C_{66}), & -3C_{66}ik \end{bmatrix} \begin{bmatrix} \hat{\bar{u}}_1 + \hat{\bar{u}}_o \\ \hat{\bar{v}}_1 - \hat{\bar{v}}_o \\ \hat{\bar{u}}_1 - \hat{\bar{u}}_o \\ \hat{\bar{v}}_1 + \hat{\bar{v}}_o \end{bmatrix} = \begin{bmatrix} 0 \\ 3\hat{\Sigma} \\ \hat{\Sigma} \\ -\frac{C_{12}}{C_{22}} \frac{b}{\Delta} ik \hat{\Sigma} \end{bmatrix} \quad (\text{IV-4})$$

and these can be solved for \hat{U}_o , \hat{U}_1 , \hat{V}_o , and \hat{V}_1 in terms of $\hat{\Sigma}$. Since the mixed boundary conditions are given by σ and v_1 we solve \hat{V}_1 as

$$\hat{V}_1 = K(s, k) \hat{\Sigma} \quad (\text{IV-5})$$

with

$$K(s, k) = \frac{1}{2} \left[\frac{3}{A} (fs^2 + \frac{b}{\Delta} C_{11} k^2) + \frac{1}{B} \left(\frac{C_{12}}{C_{22}} \frac{b}{\Delta} C_{66} k^2 - (fs^2 + \frac{b}{\Delta} C_{11} k^2 + \frac{3b}{\Delta} C_{66}) \right) \right]$$

$$A = \text{Det} \begin{vmatrix} (fs^2 + \frac{b}{\Delta} C_{11} k^2), C_{12} ik \\ -3C_{12} ik, (fs^2 + \frac{3\Delta}{b} C_{22}) \end{vmatrix} \quad (\text{IV-6})$$

$$B = \text{Det} \begin{vmatrix} C_{66} ik, (fs^2 + \frac{b}{\Delta} C_{66} k^2) \\ (fs^2 + \frac{b}{\Delta} C_{11} k^2 + \frac{3\Delta}{b} C_{66}), -3C_{66} ik \end{vmatrix} .$$

Next we take the inverse transform of $\hat{\Sigma}$ and \hat{V}_1 , and apply the mixed boundary condition given in Eq. (IV-3). Since the boundary conditions are for all times $t > 0$ we only take the inverse Fourier transform to apply the boundary conditions, i.e.,

$$\hat{\Sigma}(n, s) = \frac{1}{\sqrt{2\pi}} \int_{-\infty}^{\infty} \hat{\Sigma} e^{-ikn} dk \quad (\text{IV-7})$$

$$\hat{V}_1(n, s) = \frac{1}{\sqrt{2\pi}} \int_{-\infty}^{\infty} K(s, k) \hat{\Sigma} e^{-ikn} dk .$$

Application of the boundary condition given by Eq. (IV-3) results in the following integral equation:

$$-\hat{P}_o(n, s) = \frac{1}{\sqrt{2\pi}} \int_{-\infty}^{\infty} \hat{\Sigma} e^{-ikn} dk : |n| < h/\Delta \quad (IV-8)$$

$$0 = \frac{1}{\sqrt{2\pi}} \int_{-\infty}^{\infty} K(s, k) \hat{\Sigma} e^{-ikn} dk : |n| > h/\Delta$$

for an unknown function $\hat{\Sigma}$.

3. Discussion

The integral equations of the type given in Eq. (IV-8) are known as dual integral equations, each of which has its own region of application and occur in mixed boundary value problems [35]. There are a number of ways to solve this type of integral equations, such as by reduction to a single Fredholm integral equation or by using the Wiener-Hopf technique [36]. Finding the solution depends on the kernel and in general it is rather difficult to do except for some special cases such as for Bessel kernels or trigonometric kernels.

Once the unknown function $\hat{\Sigma}$ is determined the other variables $(\hat{U}_o, \hat{U}_1, \hat{V}_o, \hat{V}_1)$ can be computed by solving the algebraic equation (IV-4) and the complete displacement can be found by inversions of the integral transform.

The problem formulated in this chapter is the simplest impact problem in that the contact of the crack surface does not occur and that it has a twofold symmetry. But it is expected that the critical response of the plate, particularly the stress field near the crack, can be a guideline for a more complex problem.

V. CONCLUSION AND RECOMMENDED RESEARCH

The present theory is a generalization of Mindlin's approximate theory of plate applied to a multilayer plate under impact. By combined use of the finite difference technique in the thickness direction and integral transforms this model has been shown to be very effective for wave propagation analyses.

This model is extended to examine the effects of an elastomer layer between elastic layers of the plate. The reduction of interlaminar normal stress is significant due to the damping layer but further investigation seems necessary to determine the nature of the reduction.

The presence of a crack in the plate has been formulated. The resulting equations are given by dual integral equations which, as in many cases, are rather difficult to solve.

The basic idea of the periodic structure of the multilayer plate, where the governing equations are derived for each layer and given by a set of difference-differential equations, may be useful to handle different types of problems, such as heat conduction and thermoelastic problems in composite plates.

References

- [1] Mindlin, R.D., - "High Frequency Vibrations of Crystal Plates", Quart. Appl. Math., Vol. 19, p. 51-61 (1961).
- [2] Moon, F.C., - "Wave Surfaces Due to Impact on Anisotropic Plates", J. Composite Materials, Vol. 6, p. 62 (1972).
- [3] Moon, F.C. and Kang, C.K., - "Analysis of Edge Impact Stresses in Composite Plates", TR to NASA Lewis Research Center, Princeton University (1974).
- [4] Moon, F.C., - "One Dimensional Transient Waves in Anisotropic Plate", J. Appl. Mech., Trans. ASME, p. 485 (1973).
- [5] Moon, F.C., Kim, B.S. and Fang - Landau, S.R., - "Impact of Composite Plates: Analysis of Stresses and Forces", TR to NASA Lewis Research Center, Princeton University (1976).
- [6] White, J.E. and Angona, F.A., - "Elastic Wave Velocities in Laminated Media", J. Acoust. Soc. Am., Vol. 27, p. 310 (1955).
- [7] Sun, C.T., Achenbach, J.D. and Herrmann, G., - "Continuum Theory for a Laminated Media", J. Appl. Mech., Trans. ASME, p. 467 (1968).
- [8] Nayfeh, A.H. and Gurtman, G.A., - "A Continuum Approach to the Propagation of Shear Waves in Laminated Wave Guides", J. Appl. Mech., Trans. ASME, p. 106 (1974).
- [9] Hegemier, G.A., Gurtman, G.A. and Nayfeh, A.M., - "A Continuum Mixture Theory of Wave Propagation in Laminated and Fiber Reinforced Composites", Int. J. Solids Struc., Vol. 9, p. 395 (1973).
- [10] Chao, T. and Lee, P.C.Y., - "Discrete Continuum Theory for Periodically Layered Composite Materials", J. Acoust. Soc. Am., Vol. 57, p. 78 (1975).
- [11] Lee, P.Y.C. and Nikodem, Z., - "An Approximate Theory for High Frequency Vibrations of Elastic Plates", Int. J. Solids Struc., Vol. 8, p. 581 (1972).
- [12] Dong, S.B. and Nelson, R.B., - "On Natural Vibrations and Waves in Laminated Orthotropic Plates", J. Appl. Mech., Trans. ASME, p. 739 (1972).
- [13] Hegemier, G.A. and Nayfeh, A.H., - "A Continuum Theory for Wave Propagation in Laminated Composites, Case 1: Propagation Normal to the Laminates", J. Appl. Mech., Trans. ASME, p. 503 (1973).
- [14] Hegemier, G.A. and Nayfeh, A.H., - "A Continuum Theory for Wave Propagation in Laminated Composites, Case 2: Propagation Parallel to the Laminates" J. Elasticity, Vol. 3, p. 125-140 (1973).

- [15] Cooley, J.W., Lewis, P.A.W. and Welch, P.D., - "The Fast Fourier Transform Algorithm: Programming Considerations in the Calculation of sine, cosine and Laplace Transforms", J. Sound Vib., Vol. 12, p. 315-337 (1970).
- [16] Brillouin, L. - Wave Propagation in Periodic Structures, Dover, N.Y. (1946).
- [17] Thomson, W.T., - Vibration Theory and Application, Prentice Hall, N.J. (1965).
- [18] Mindlin, R.D. and Medick, M.A., - "Extensional Vibrations of Elastic Plates", J. Appl. Mech., Trans. ASME, p. 561 (1959).
- [19] Yan, M.J. and Dowell, E.H., - "High Damping Measurements and Preliminary Evaluation of an Equation for Constrained Layer Damping", AIAA Journal, Vol. 11, p. 388 (1973).
- [20] Nakra, B.C. and Grootenhuis, P., - "Structural Damping Using a Four Layer Sandwich", J. Eng. Ind., Trans. ASME, p. 81 (1972).
- [21] Achenback, J.D., - "Crack Propagation Generated By a Horizontally Polarized Shear Wave", J. Mech. Phys. Solids, Vol. 18, p. 245 (1970).
- [22] Achenback, J.D. and Nuismer, R., - "Fracture Generated by a Dilatational Wave", Int. J. Frac. Mech., Vol. 7, p. 77 (1971).
- [23] Nuismer, R.J. and Achenback, J.D., - "Dynamically Induced Fracture", J. Mech. Phys. Solids, Vol. 20, p. 203 (1972).
- [24] Keer, L.M. and Luong, W.C., - "Diffraction of Waves and Stress Intensity Factors in a Cracked Layered Composite", J. Acoust. Soc. Am., Vol. 56, p. 1681 (1974).
- [25] Levy, H. and Lessman, F., - Finite Difference Equations, MacMillan Co. (1961).
- [26] Kim, B.S. and Moon, F., - "Impact on a Laminated Half Space", to be published.
- [27] Premont, E.J. and Stubenrauch, K.R., - "Impact Resistance of Composite Fan Blades", Tech. Rep. to NASA Lewis Research Center, NASA CR-134515, Pratt and Whitney Aircraft (1973).
- [28] Novak, R.C., - "Multi-Fiber Composites", Tech. Rep. to NASA Lewis Research Center, NASA OR-135062, United Technology (1976).
- [29] Christensen, R.M., - Theory of Viscoelasticity, Academic Press, N.Y. (1971).
- [30] Christescu, N., - Dynamic Plasticity, North-Holland, New York (1967).
- [31] Birkhoff, A. et al, - "Explosives with Lined Cavities", J. Appl. Phys. Vol. 19, p. 563 (1948).

- [32] Griffith, A., - "Phenomenon of Rupture and Flaw in the Solids",
Phil. Trans. Roy. Soc. (London), Vol. A221, p. 163 (1921).
- [33] Liebowitz, H., (Ed.) - Fracture, Vol. 2, Academic Press, N.Y. (1968).
- [34] Sneddon, I.N. and Lowengrub, M. - Crack Problems in the Classical Theory of Elasticity, John Wiley and Sons, New York (1969).
- [35] Sneddon, I.N., - Mixed Boundary Value Problems in Potential Theory, North-Holland, Amsterdam (1966).
- [36] Noble, B., - Method Based On the Wiener-Hopf Technique, Pergamon Press, New York (1958).

Figures

1. Composite Plate and Layer
- 2 a,b. Dispersion Relationship and Phase Velocity for Isotropic Plate: One-layer Model ($\lambda = \mu$).
- 3 a,b. Dispersion Relationship and Phase Velocity for Composite Plate: One-layer Model (55% Graphite Fiber-Epoxy Matrix, Layup Angle 45°).
- 4 a,b. Dispersion Relationship and Phase Velocity for Isotropic Plate: Two-layer Model ($\lambda = \mu$).
- 5 a,b. Dispersion Relationship and Phase Velocity for Composite Plate: Two-layer Model (55% Graphite Fiber-Epoxy Matrix, Layup Angle 45°).
- 6 a-f. Longitudinal Propagation Impact Stress in Isotropic Plate: Two-layer Model ($\lambda = \mu = 1.2 \times 10^7$ psi; $\Delta = 1$ cm, $t_0 = 10$ μ sec, $a = 4$ cm).
7. Transverse Propagation of Normal Stress in Isotropic Plate: 4-layer Model ($\lambda = \mu = 1.2 \times 10^7$ psi; $\Delta = 4$ cm, $t_0 = 2$ μ sec, $a = 40$ cm).
8. Transverse Propagation of Normal and Shear Stress in Isotropic Plate: (Same as in Fig. 7).
9. Transverse Propagation of Normal Stress in Composite Plate: 8-layer Model (55% Graphite Epoxy-Fiber Matrix, Layup Angle 15° ; $\Delta = 1$ cm, $t_0 = 2$ μ sec, $a = 2$ cm).
10. Two Dimensional Propagation of Normal Stress in Isotropic Plate: 4-layer Model ($\lambda = \mu = 1.2 \times 10^7$ psi; $\Delta = 4$ cm, $t_0 = 4$ μ sec, $a = 4$ cm).
11. Velocity Surface and Wave Surface of Composite Plate (55% Graphite Fiber-Epoxy Matrix, Layup Angle 45°).
- 12a,b. Comparison of Theoretical Wave Front and Numerical Wave Front of Composite Plate 10 μ sec after Impact: 55% Graphite Fiber-Epoxy Matrix (For Numerical Results; 8-layer Model, $\Delta = 4$ cm, $t_0 = 4$ μ sec, $a = 2$ cm). Without and with Correction Factors.
13. Effect of Correction Factor or Transverse Propagation of Peak Value of Normal Stress: 8-layer Model (55% Graphite Fiber-Epoxy Matrix, Layup Angle 45° ; $\Delta = 4$ cm, $t_0 = 4$ μ sec, $a = 2$ cm).
14. Viscoelastic Impact Energy Absorbing Models.
- 15a,b. Complex Modulus of Elastomer.
16. Plate with Viscoelastic Layers.
17. Impact of Plate Made of 2 Elastic Layers and a Viscoelastic Layer.

18. Peak Value of Interlaminar Stress Vs Elastomer thickness (Two Elastic Layers and a Viscoelastic Layer: ($\Delta = 1 \text{ cm}$, $t_o = 10 \mu\text{sec}$, $a = 4 \text{ cm}$).
19. Composite Plate with Crack.

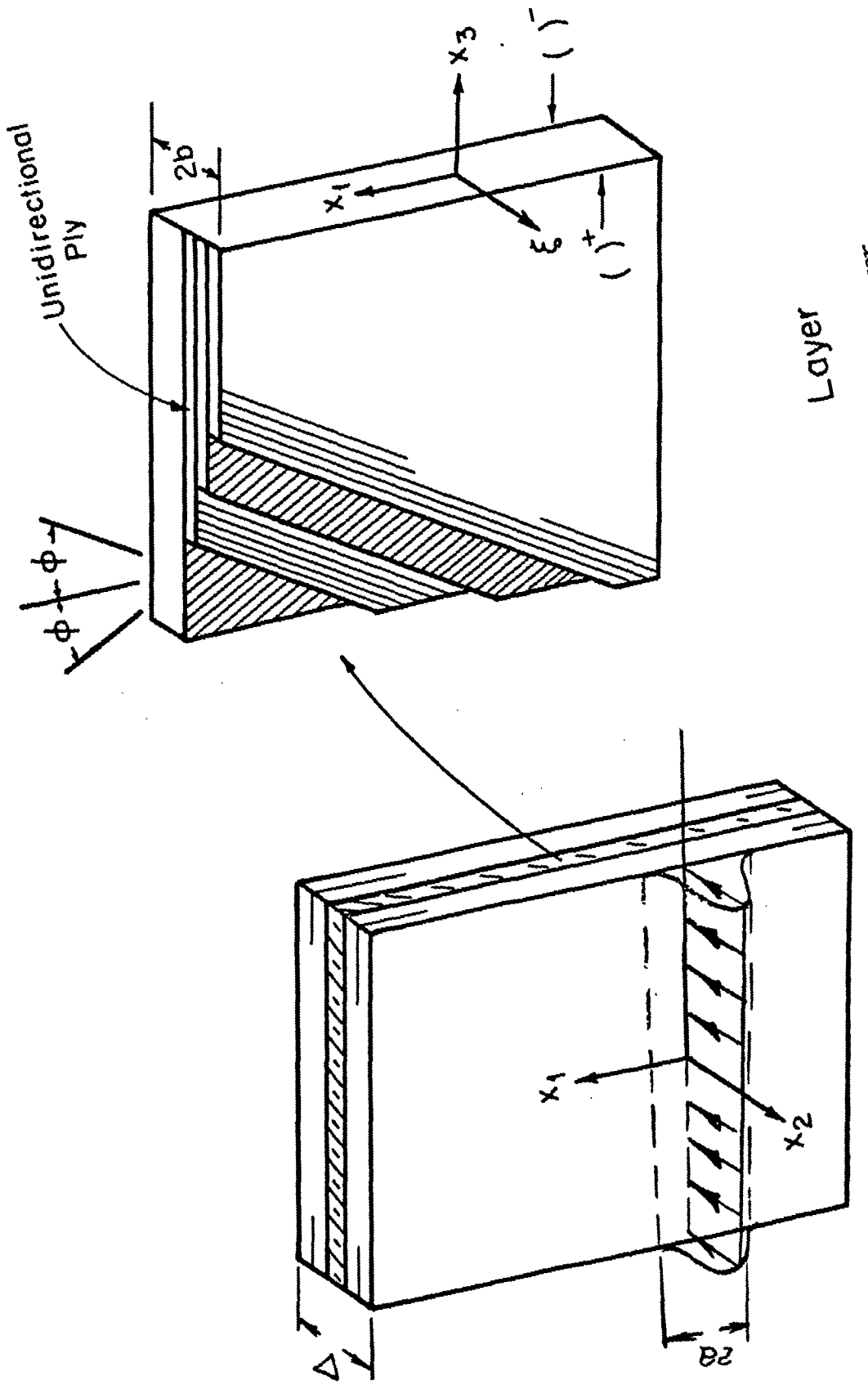


Figure 1.
Plate
Layer

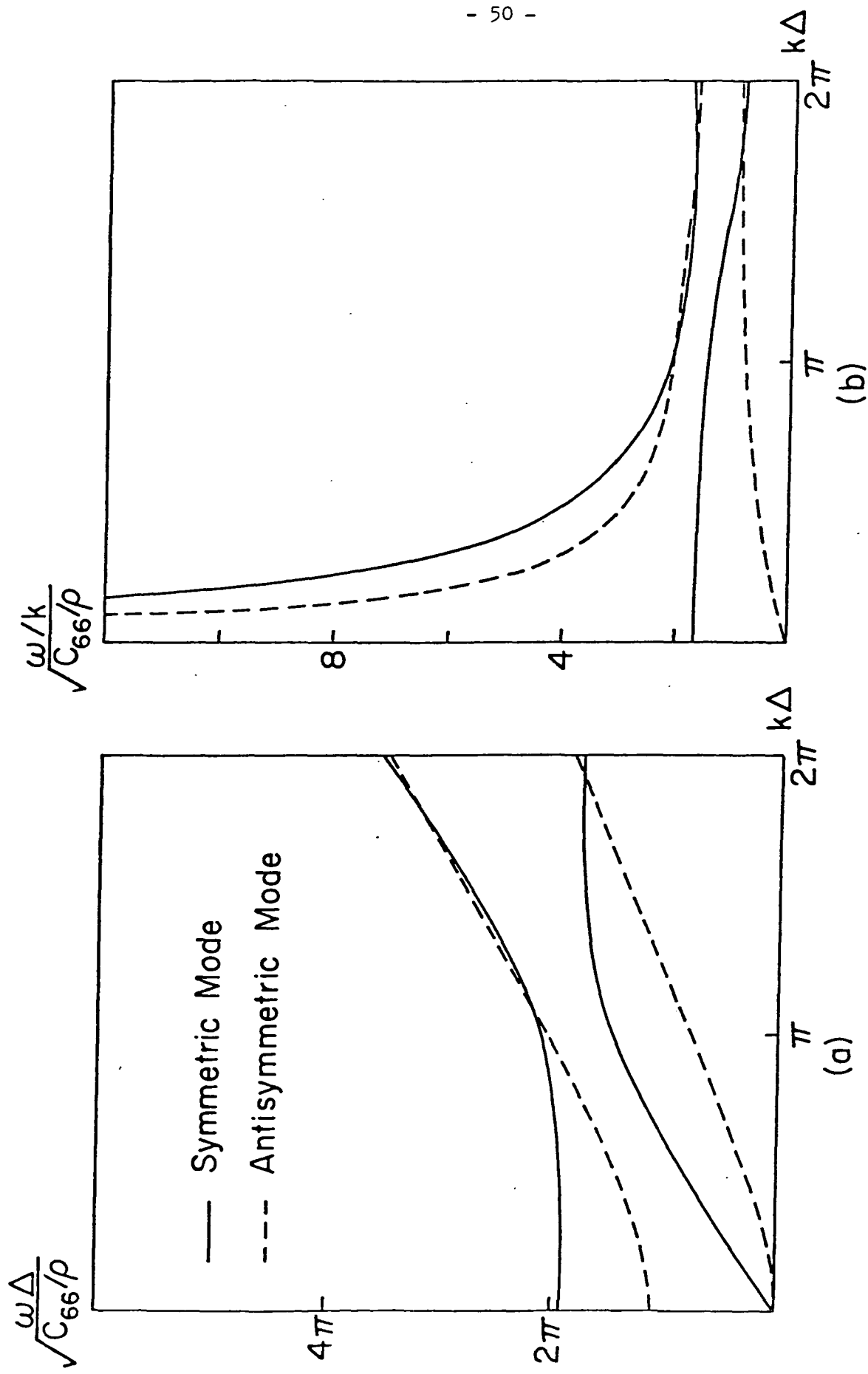


Figure 2. Dispersion Relationship and Phase Velocity of Isotropic Plate:
One-Layer Model ($\lambda = \mu$, Poisson's Ratio = $1/4$)

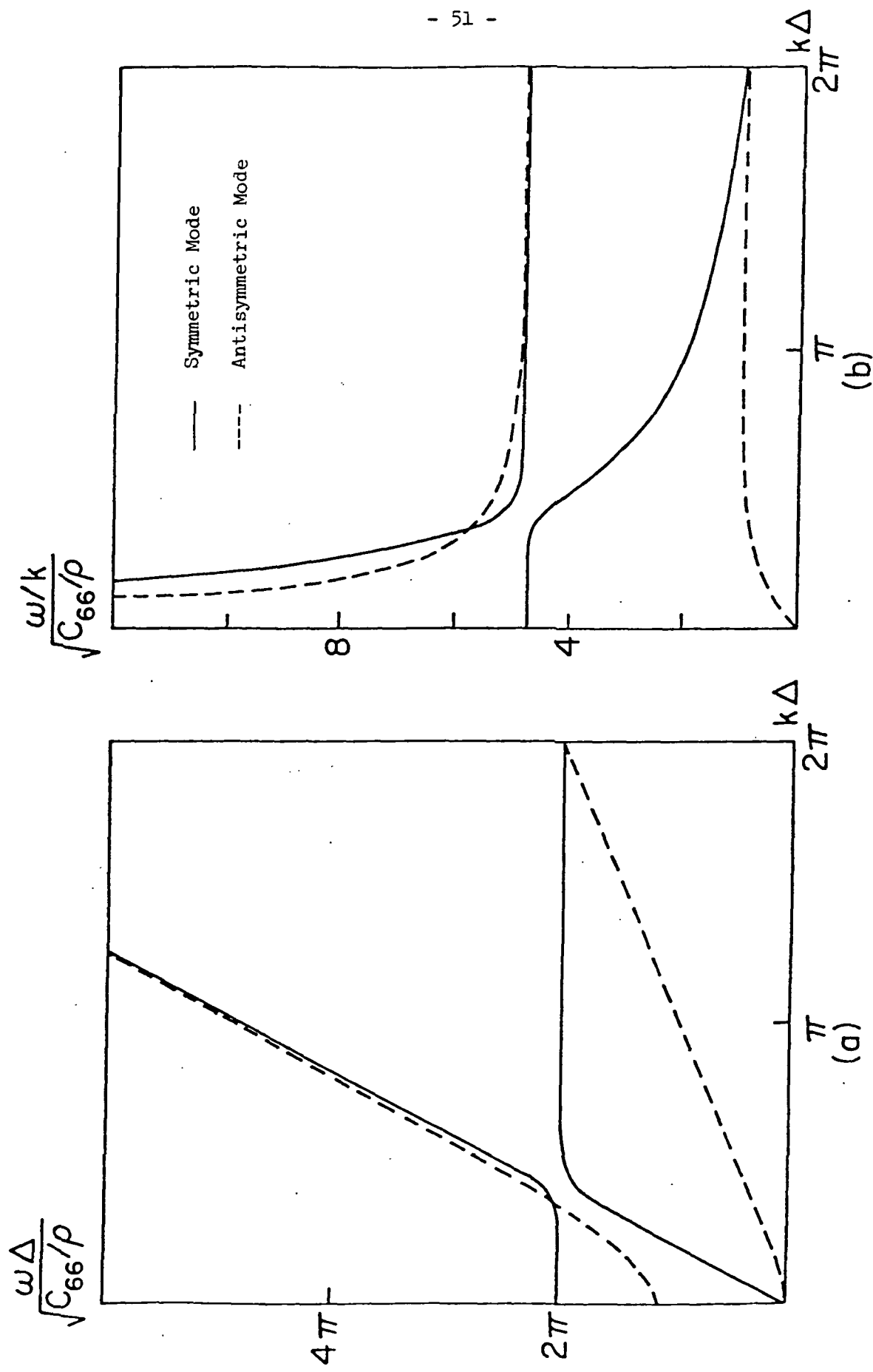


Figure 3. Dispersion Relationship and Phase Velocity of Composite Plate:
One-Layer Model (55% Graphite Fiber - Epoxy Matrix; Layup Angle = 45°)

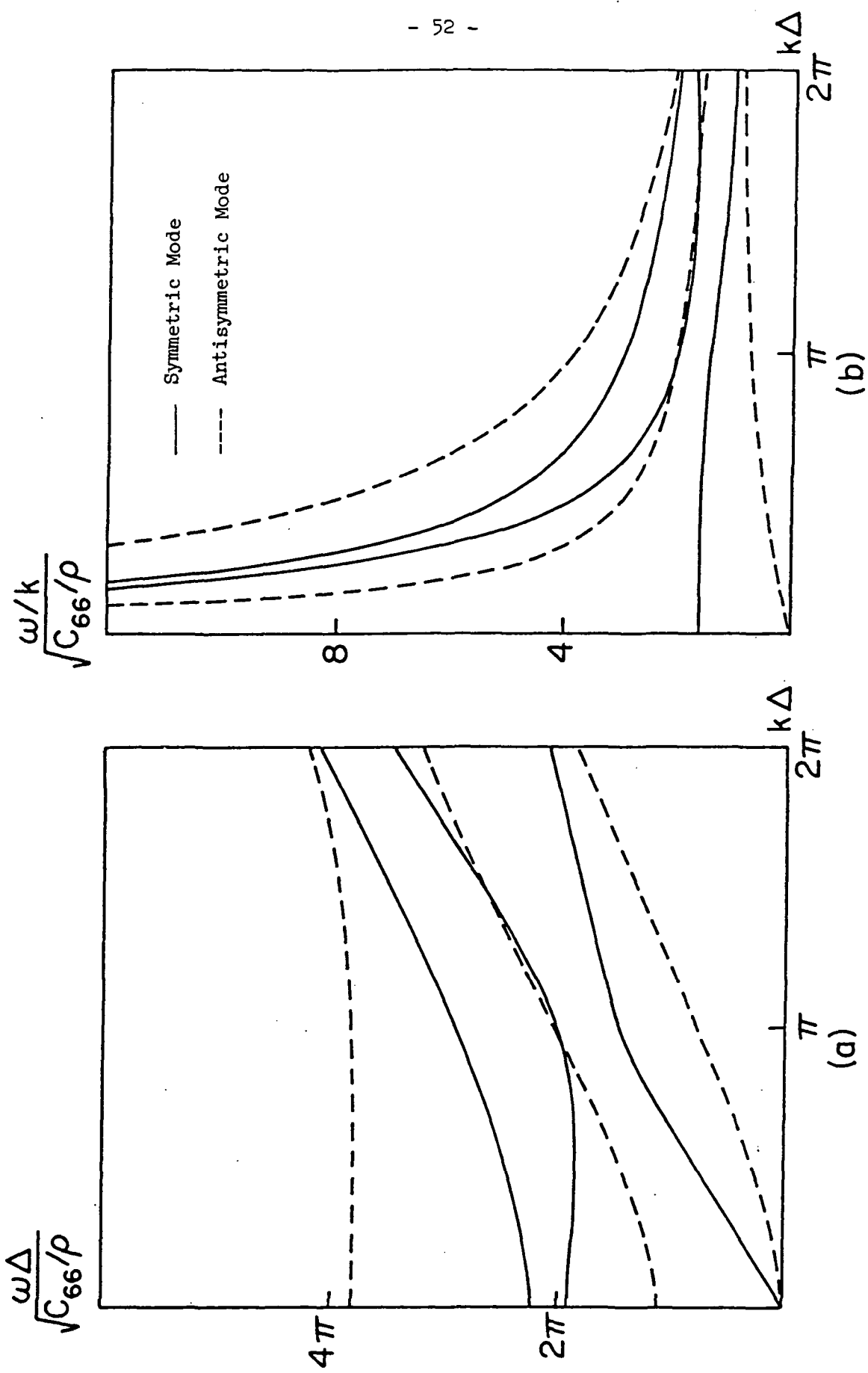


Figure 4. Dispersion Relationship and Phase Velocity of Isotropic Plate:
Two-layer Model ($\lambda = \mu$, Poisson's Ratio = $1/4$)

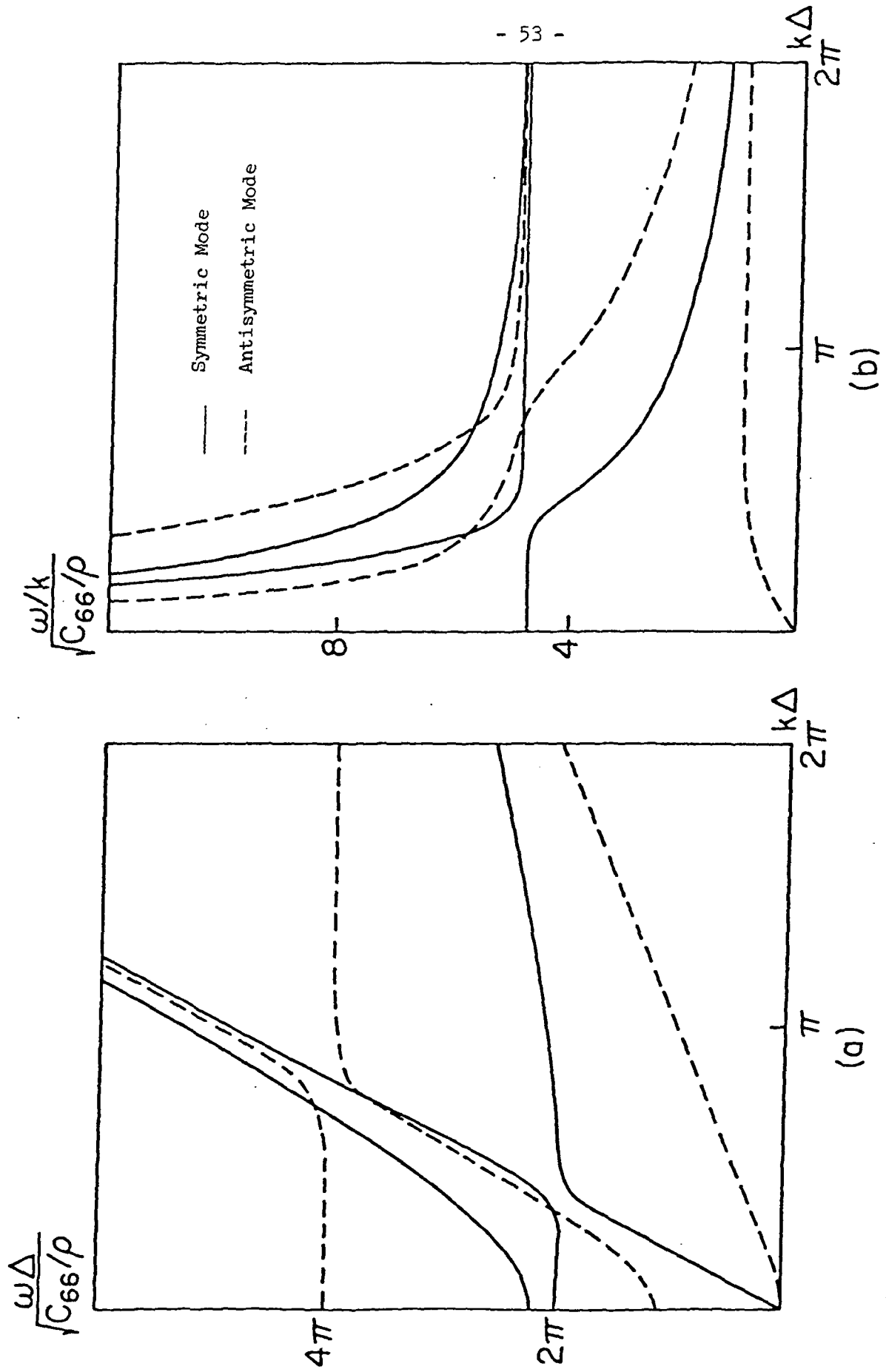


Figure 5. Dispersion Relationship and Phase Velocity of Composite Plate:
Two-Layer Model (55% Graphite Fiber - Epoxy Matrix, Layup Angle = 45°)

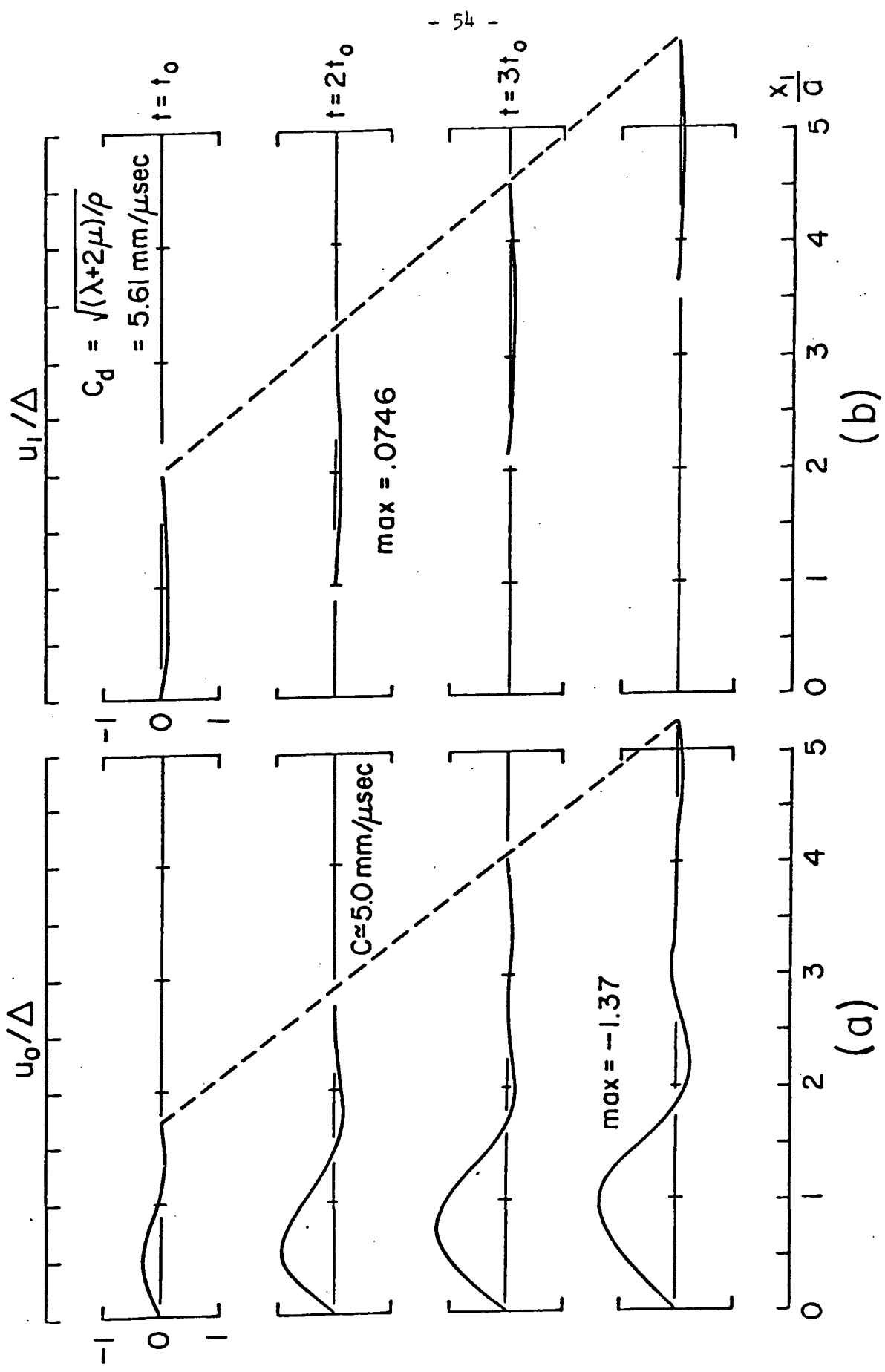


Figure 6 Longitudinal Propagation in Isotropic Plate; 2-layer Model
 $(\lambda = \mu = 1.2 \times 10^7 \text{ psi}; \Delta = 1 \text{ cm}, t_0 = 10 \mu\text{sec}, a = 4 \text{ cm})$

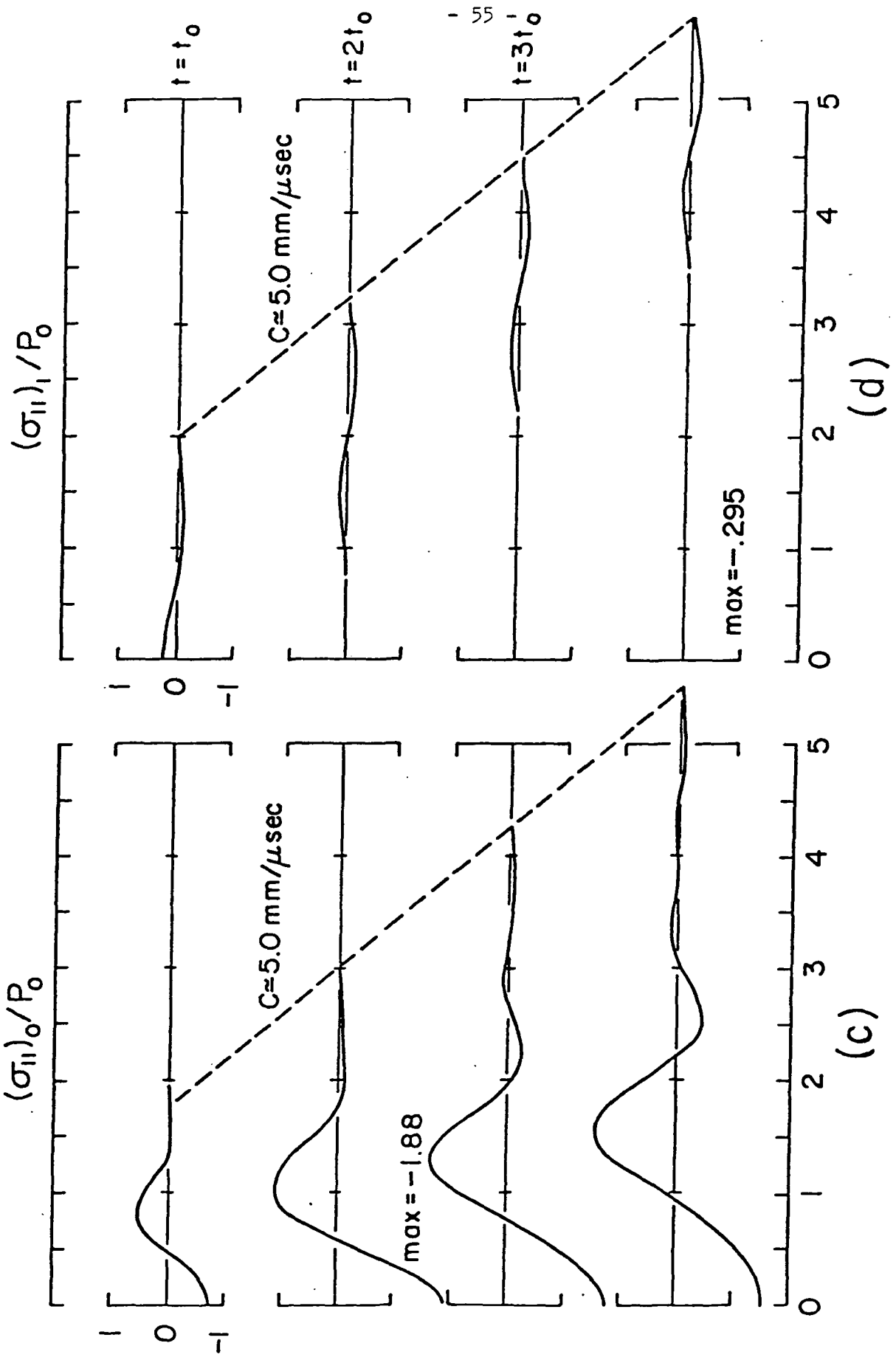


Figure 6 Continued

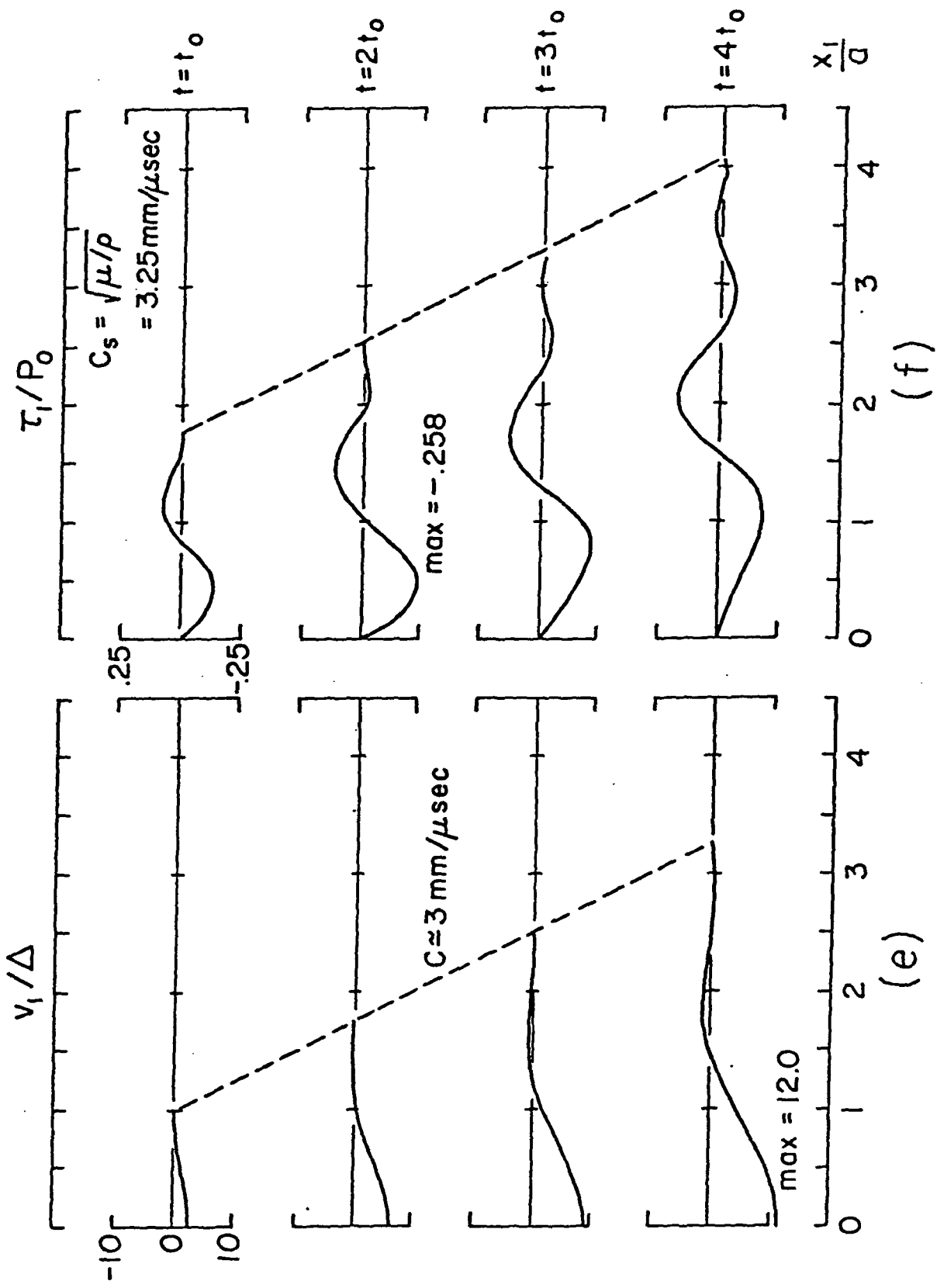


Figure 6 Continued

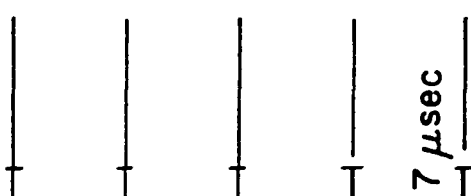
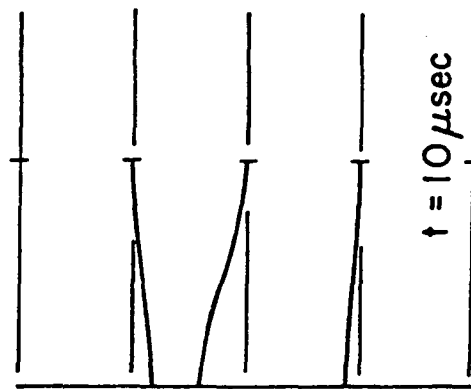
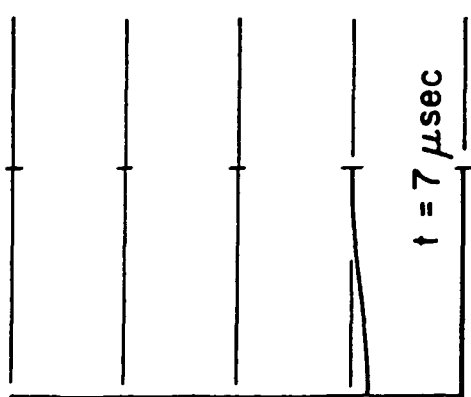
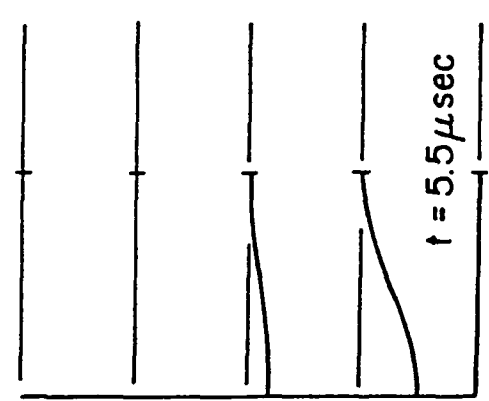
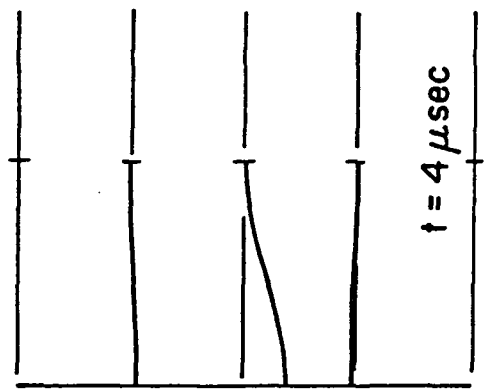
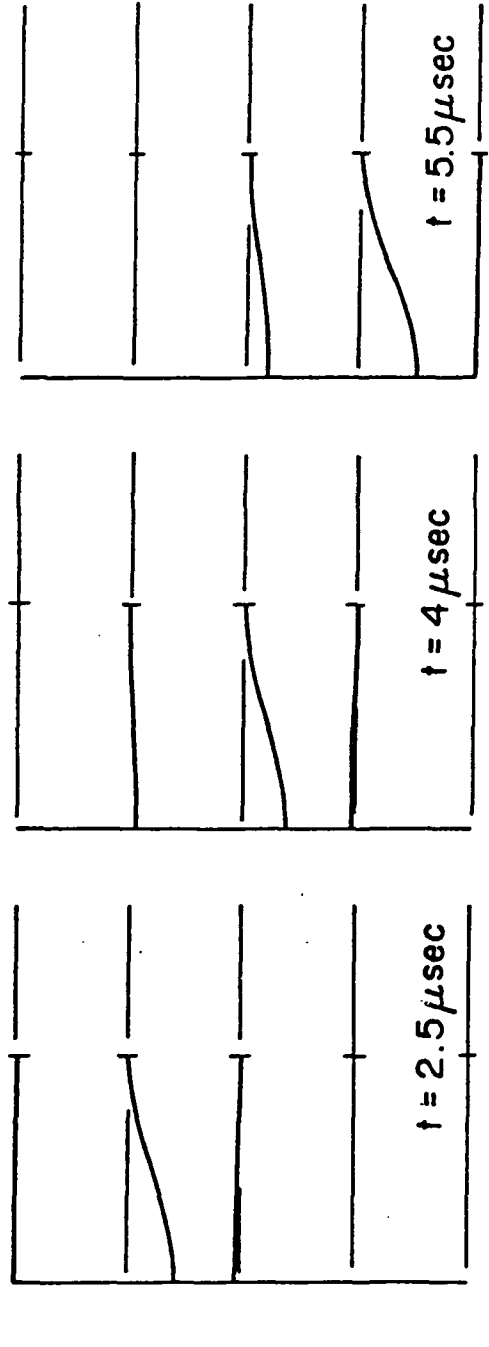
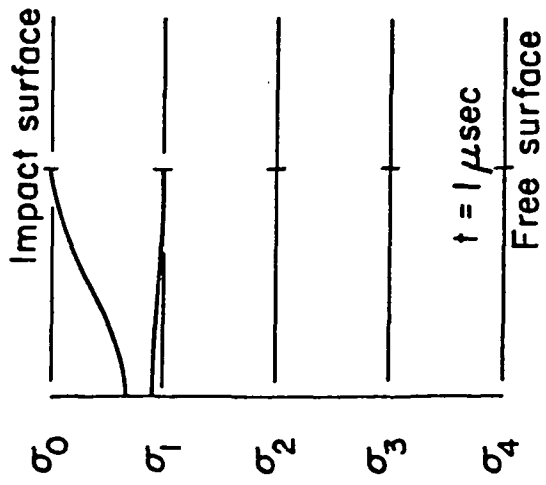


Figure 7. Transverse Propagation of Normal Stress in Isotropic Plate: 4-layer Model ($\lambda' = \frac{\nu}{1 - 2\nu} = 1.2 \times 10^7$ psi;
 $\Delta = 4$ cm, $t_0 = 2$ μsec , $a = 40$ cm)

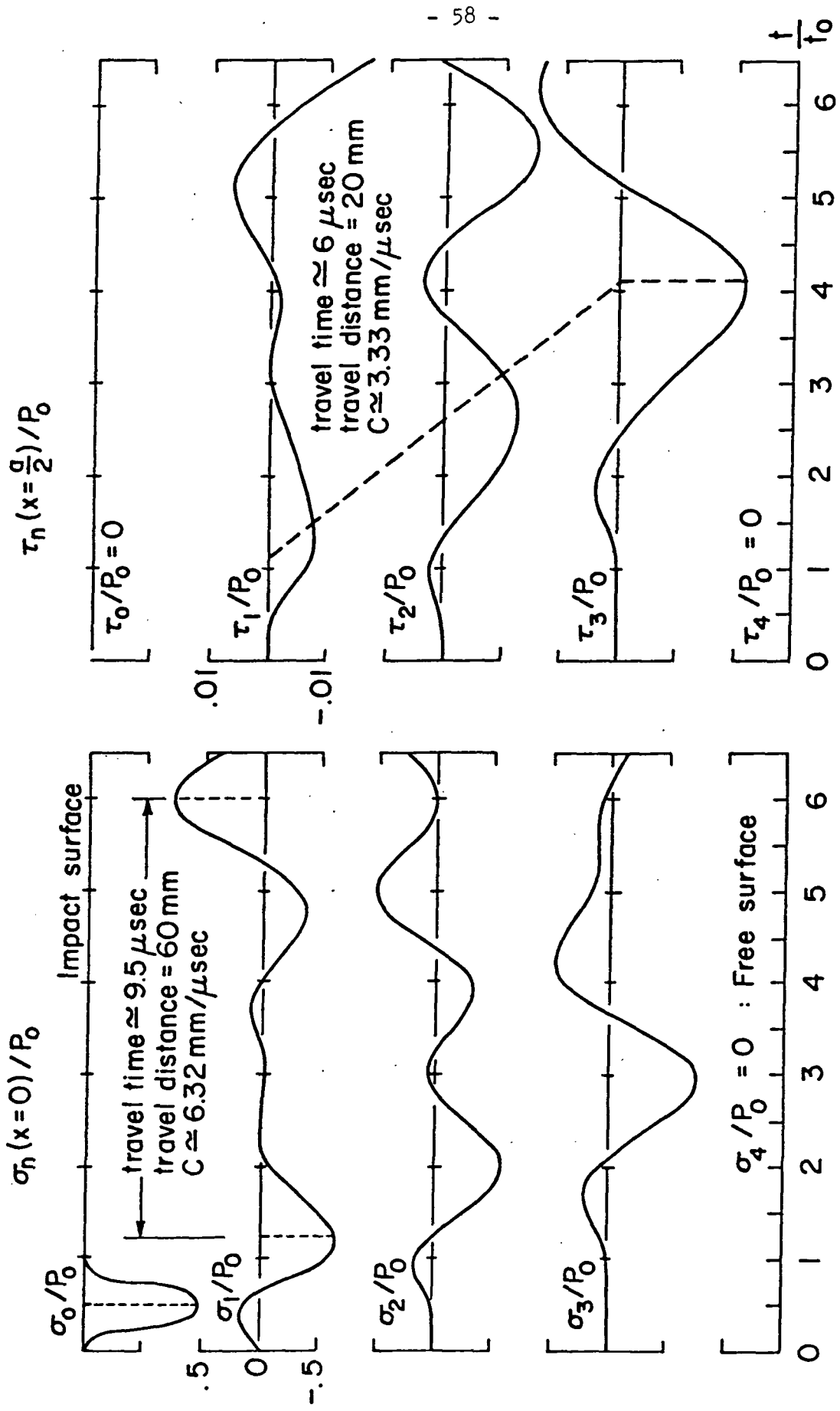


Figure 8. Transverse Propagation of Normal and Shear Stress
(Same as in Figure 7)

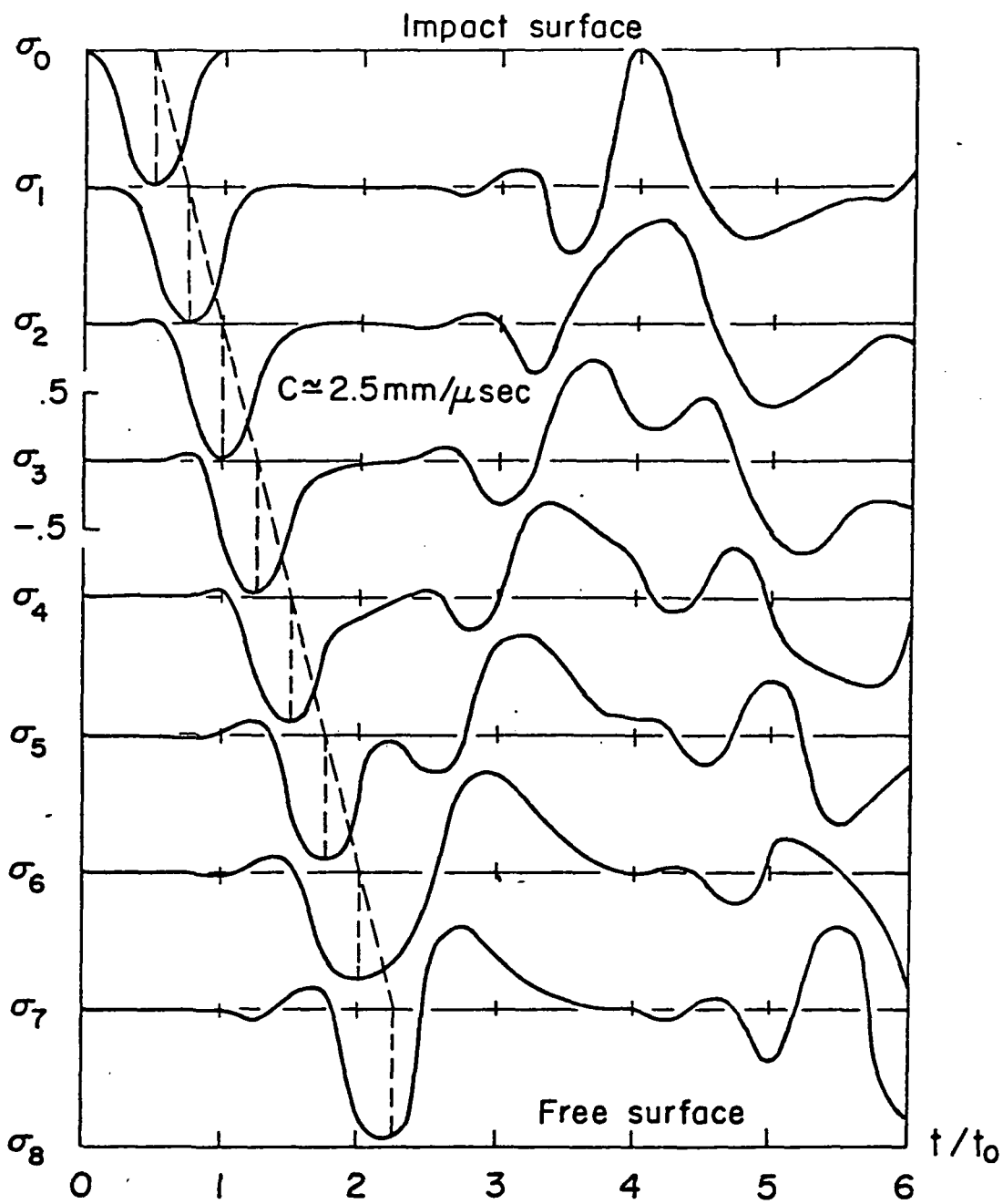


Figure 9 Transverse propagation of normal stress in composite plate; 8-layer Model (55% Graphite Fiber - Epoxy Matrix, $\pm 15^\circ$ Layup; $\Delta = 1 \text{ cm}$, $t_0 = 2 \mu\text{sec}$, $a = 2 \text{ cm}$)

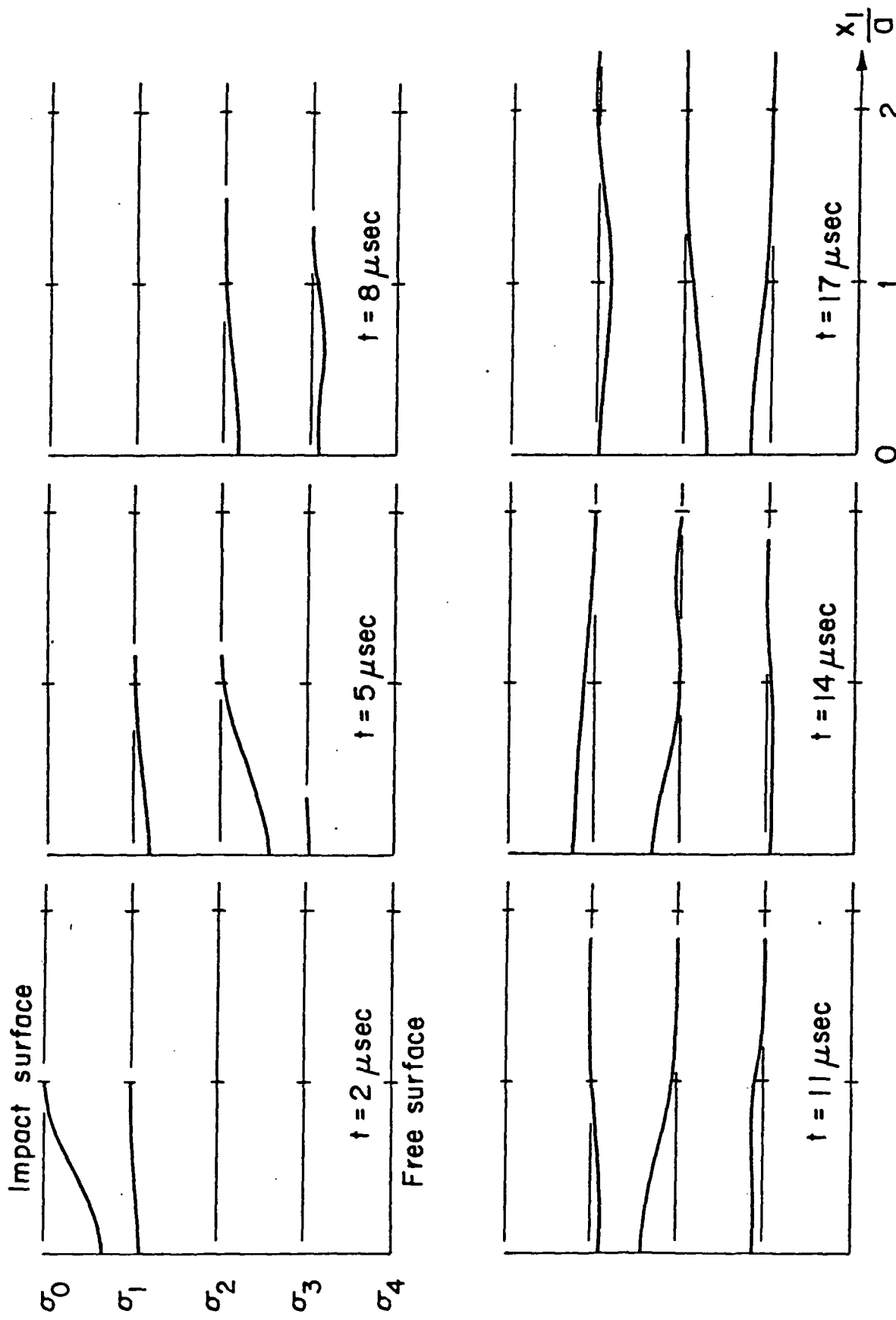


Figure 10. Two Dimensional Propagation of Normal Stress in Isotropic Plate:
4-layer Model ($\lambda = \mu = 1.2 \times 10^7$ psi; $\Delta = 4$ cm, $t_0 = 4 \mu\text{sec}$, $a = 4$ cm)

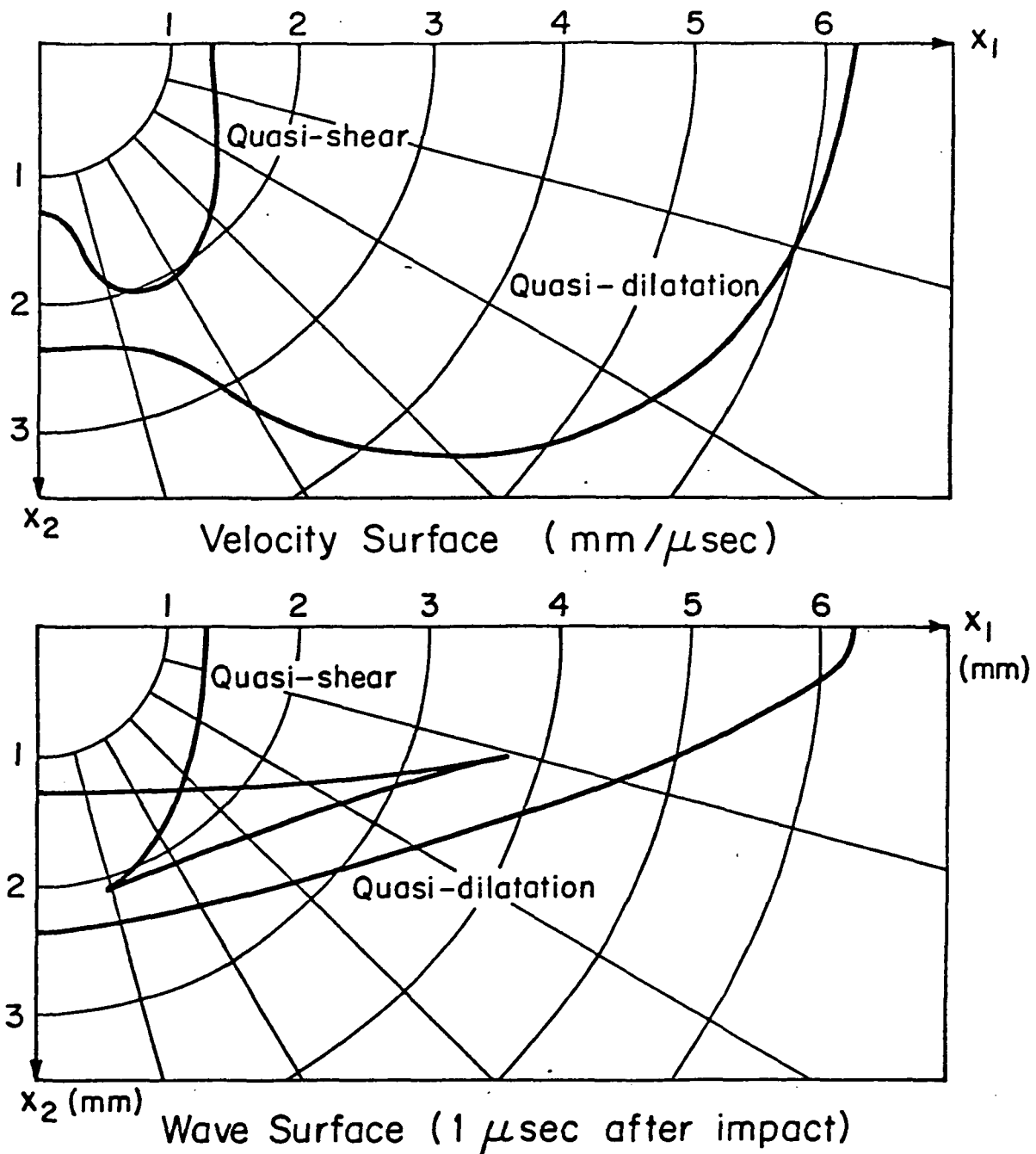


Figure 11. Velocity Surface and Wave Surface of Composite Plate (55% Graphite Fiber-Epoxy Matrix, Layup Angle 45°)

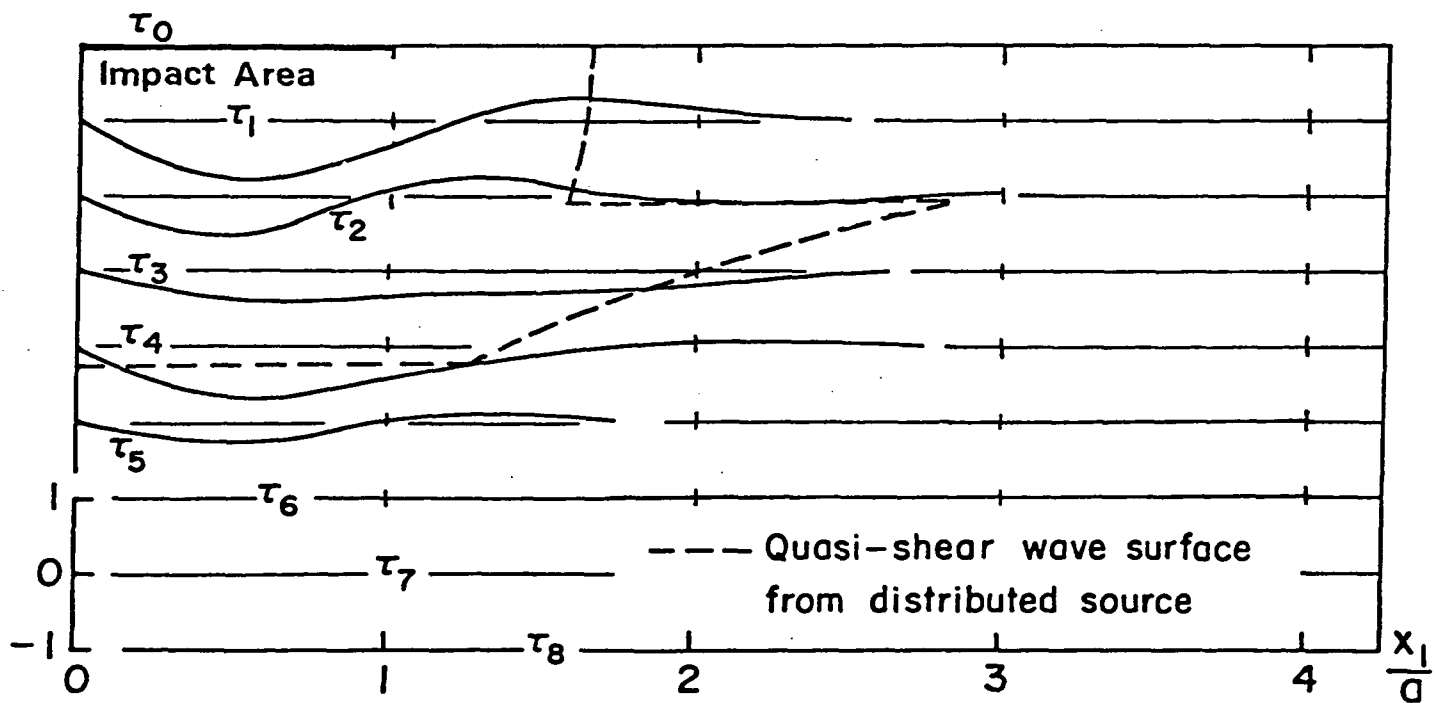
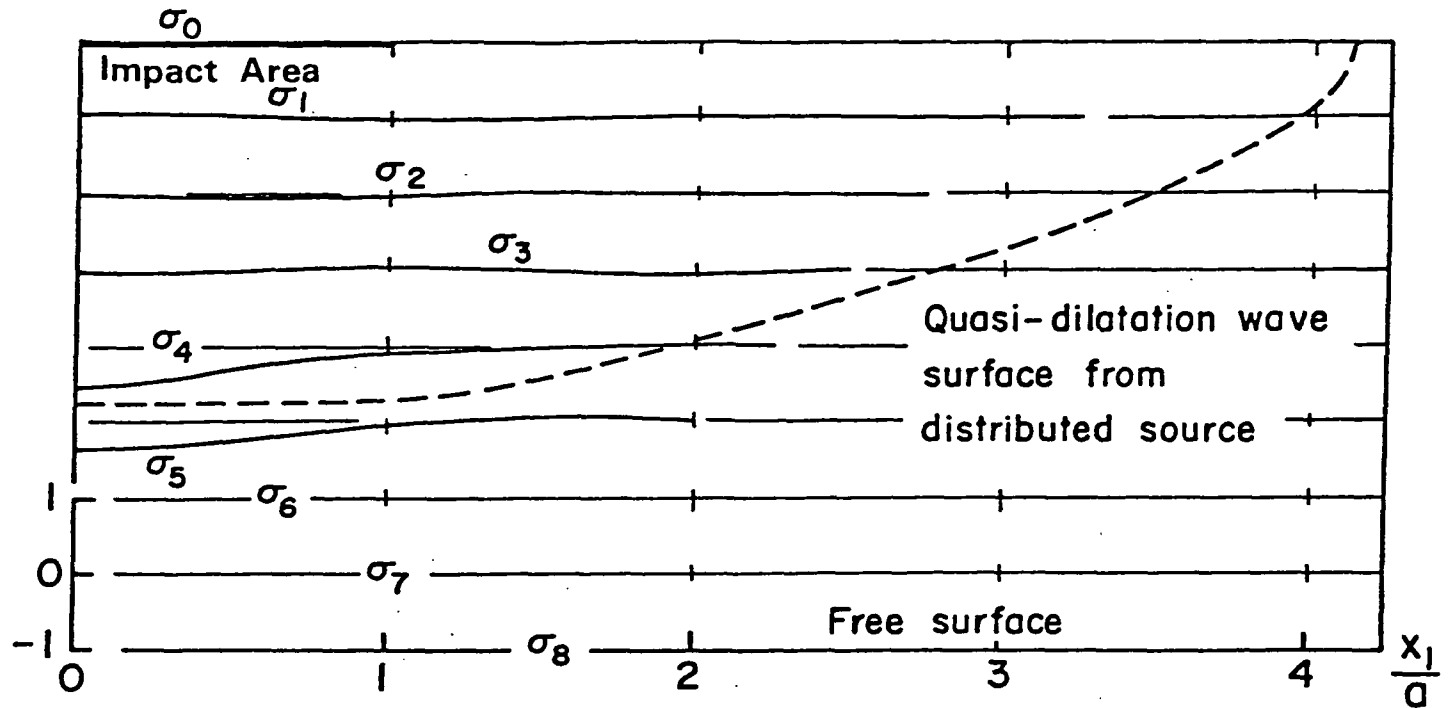


Figure 12a. Wave front $10 \mu\text{sec}$ after impact (without correction factor)
(55% Graphite Fiber-Epoxy Matrix, $\pm 45^\circ$ Layup; $\Delta = 4 \text{ cm}$,
8-layer Model; $t_0 = 4 \mu\text{sec}$, $a = 2 \text{ cm}$)

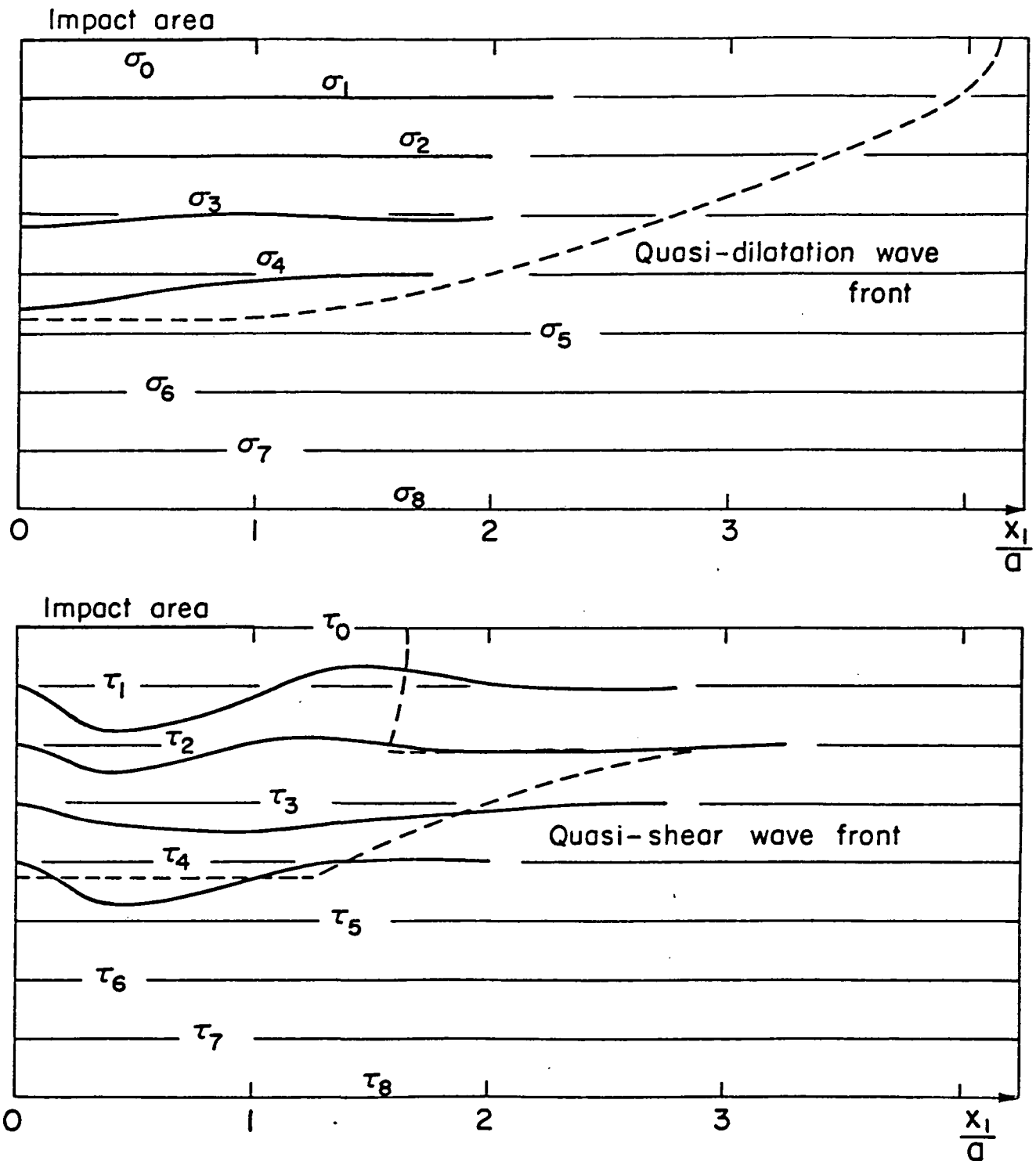


Figure 12b. Wave front 10 μ sec after impact (with correction factor)
(55% Graphite Fiber-Epoxy Matrix, $\pm 45^\circ$ Layup; $\Delta = 4$ cm,
8-layer Model; $t = 4 \mu$ sec, $a = 2$ cm)

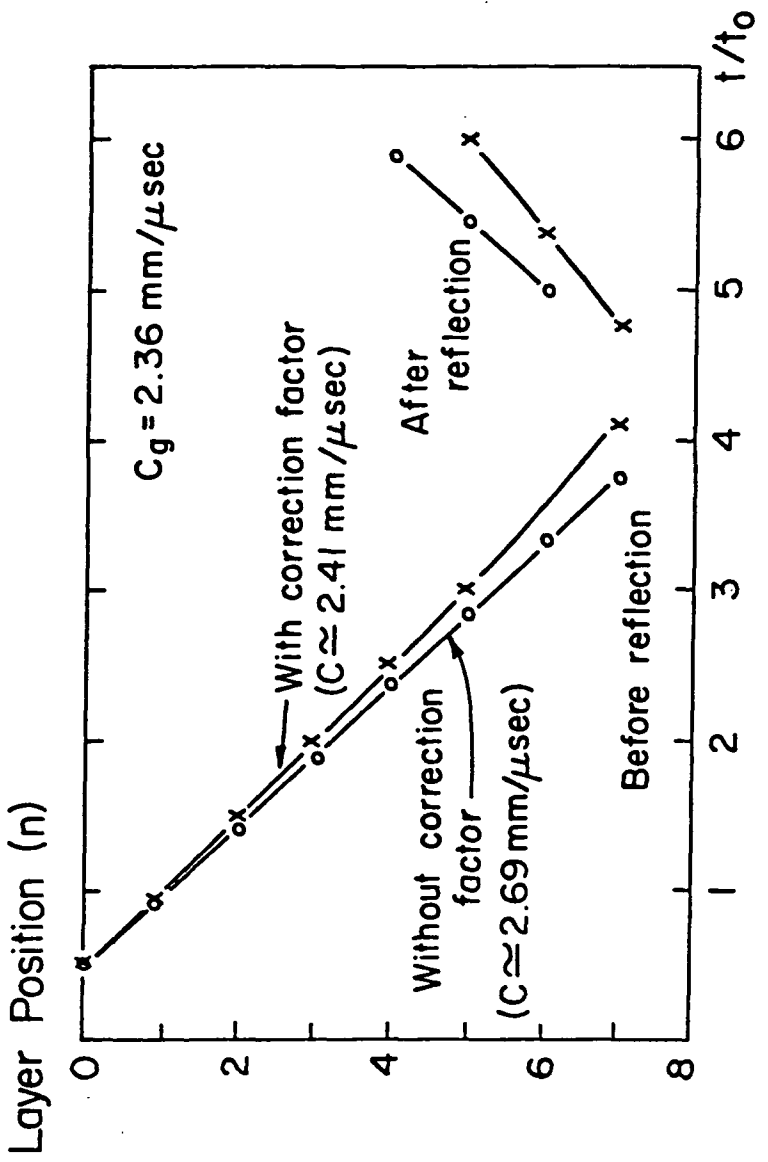


Figure 13 Effect of correction factors on transverse propagation of $\max \sigma_n(x_1 = 0)$; 8-layer Model. (55% Graphite Fiber-Epoxy Matrix, $\pm 45^\circ$ Layup; $\Delta = 4 \text{ cm}$, $t_0 = 4 \mu\text{sec}$, $a = 2 \text{ cm}$)

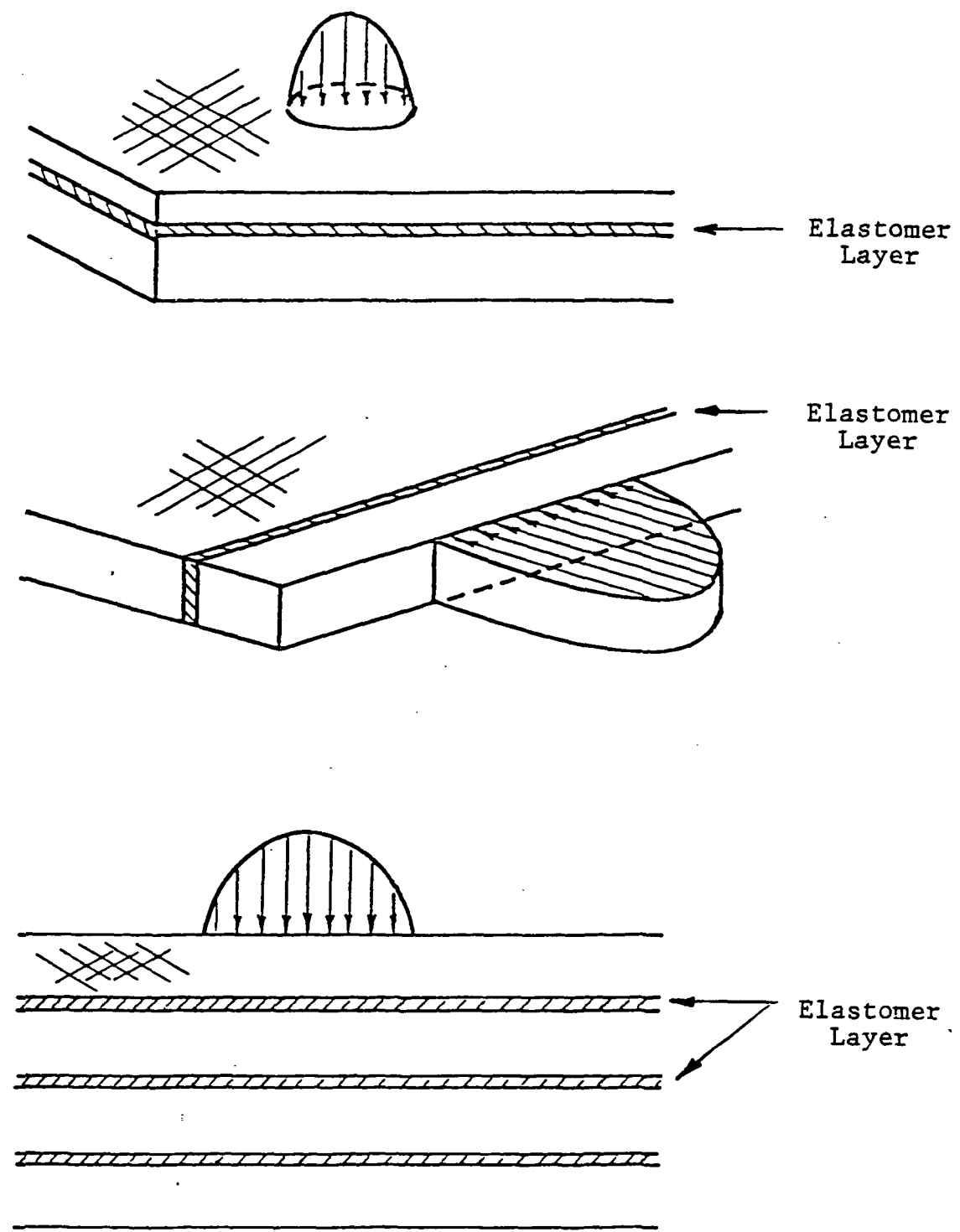


Figure 14. Viscoelastic Impact Energy Absorbing Models

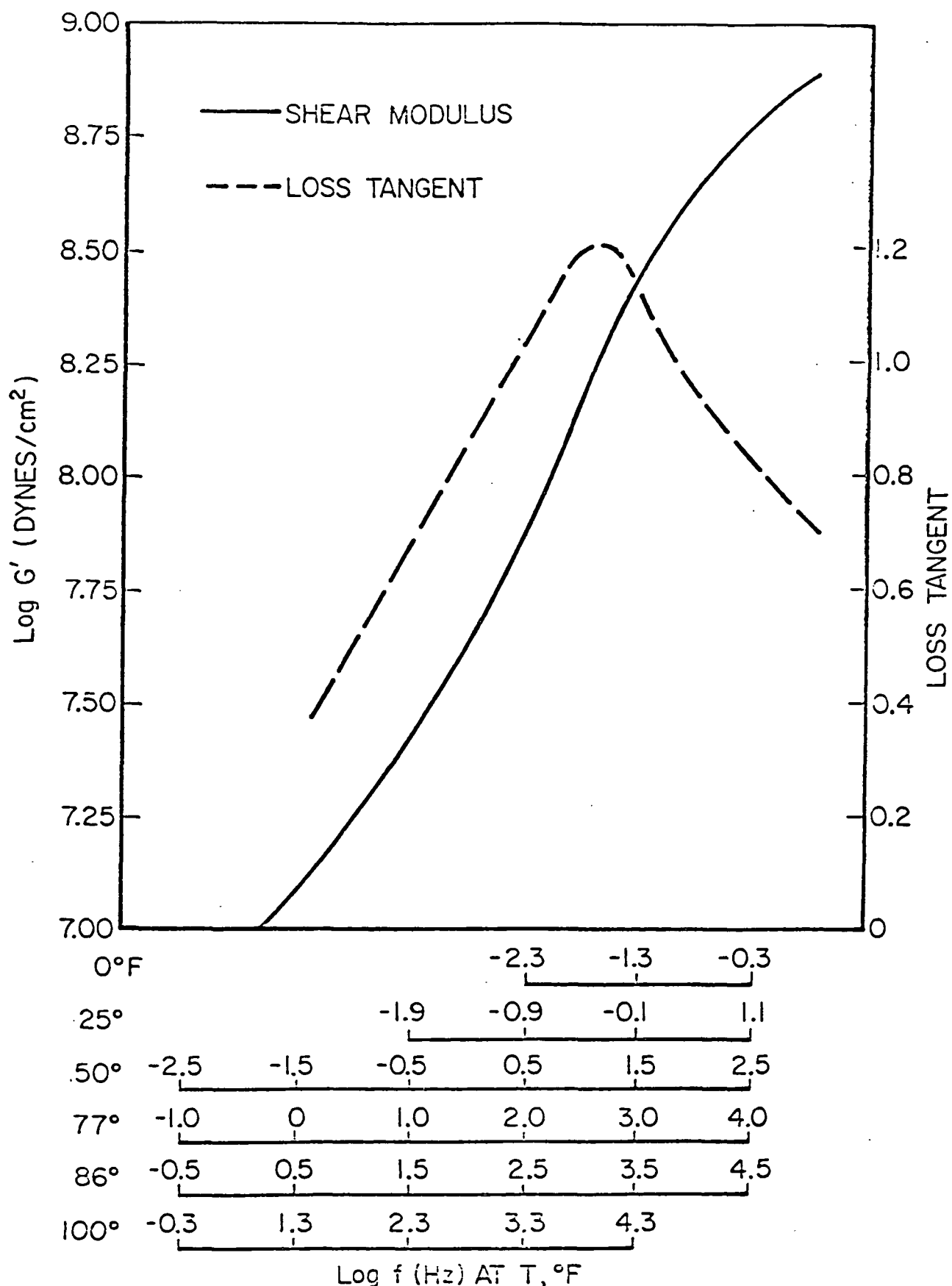


FIGURE 15a SHEAR MODULUS AND LOSS TANGENT AT T °F VS FREQUENCY FOR DUPONT LR3-604

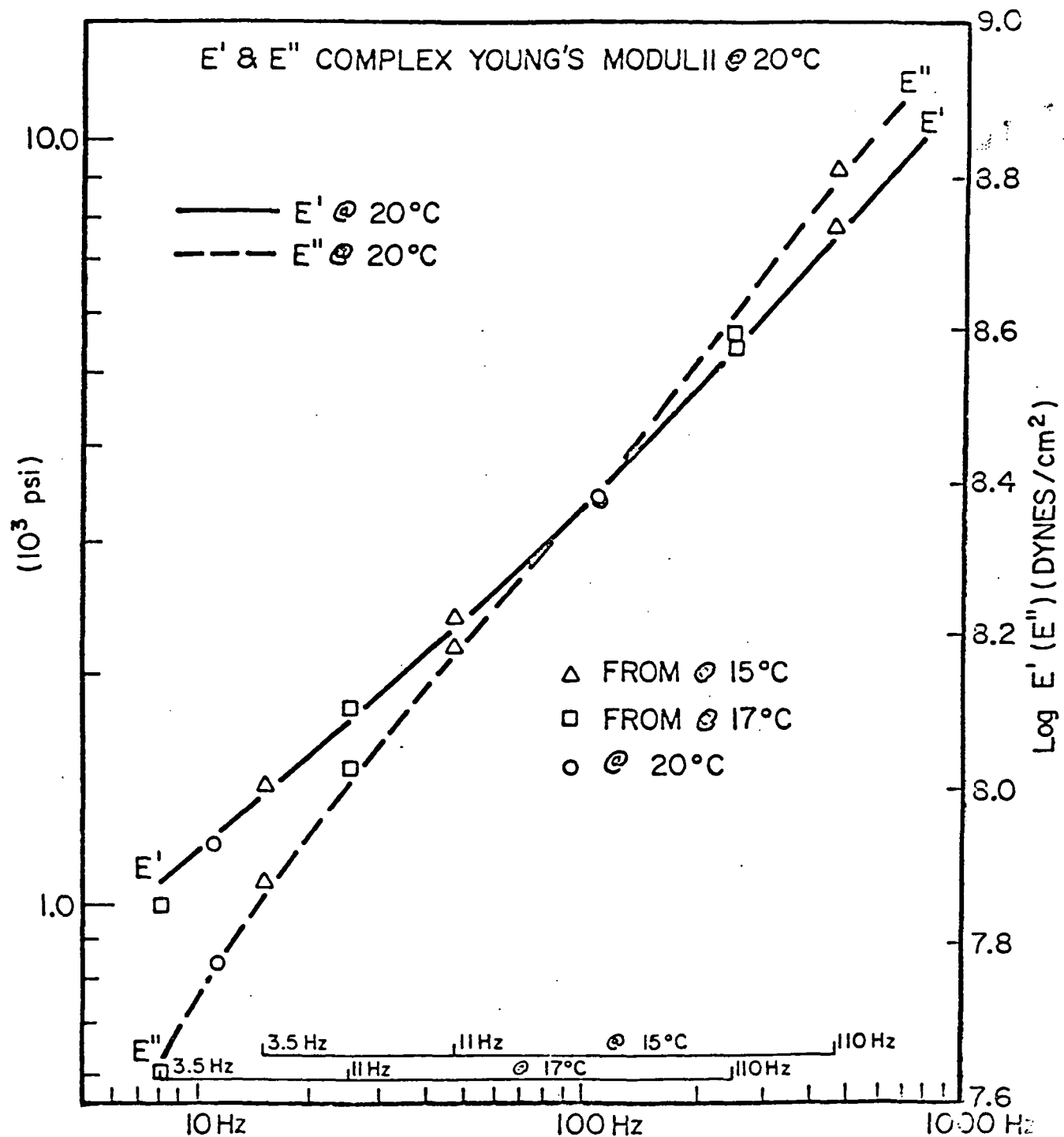


FIGURE 15b. THE COMPLEX YOUNG'S MODULUS OF LR3-604 MEASURED

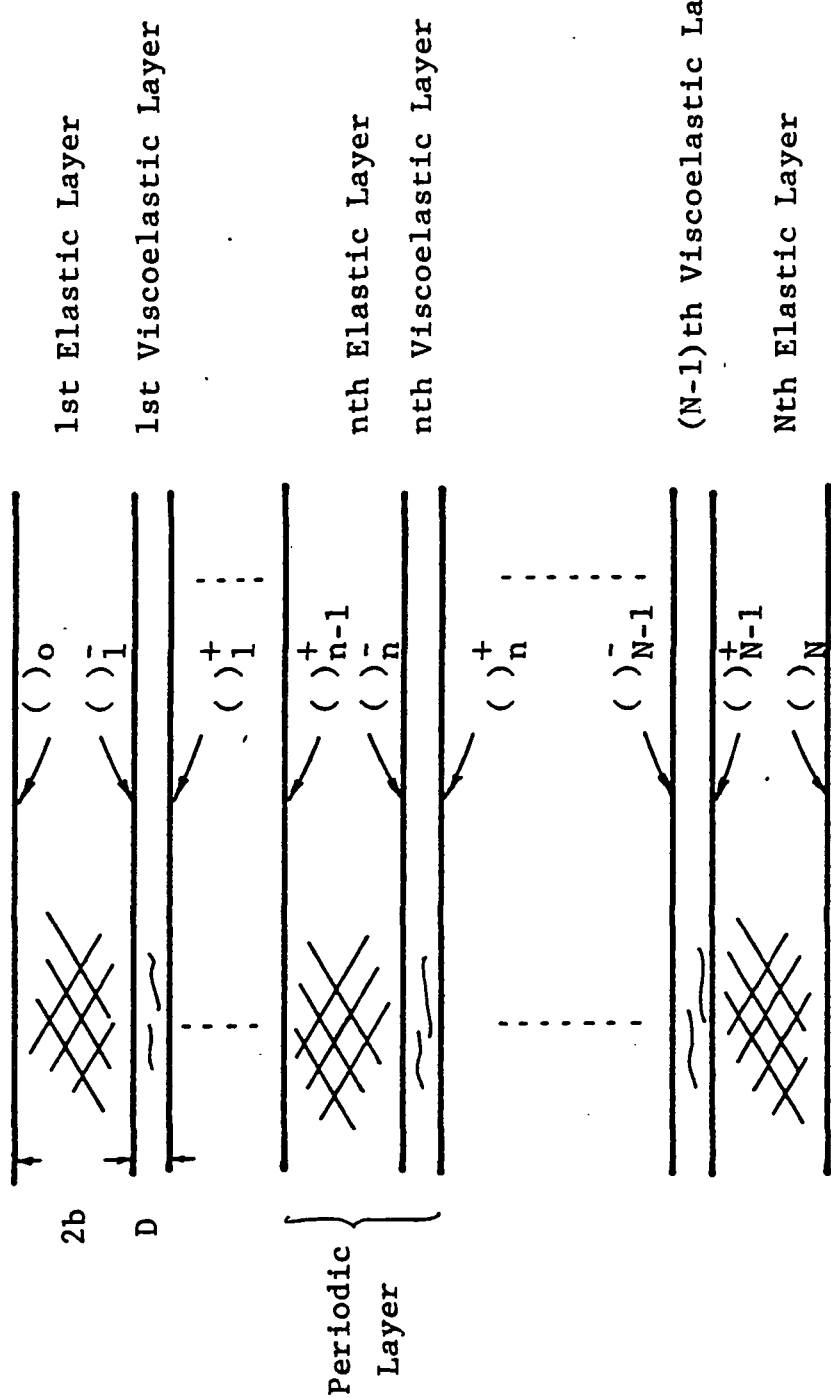


Figure 16. Plate with Viscoelastic Layers

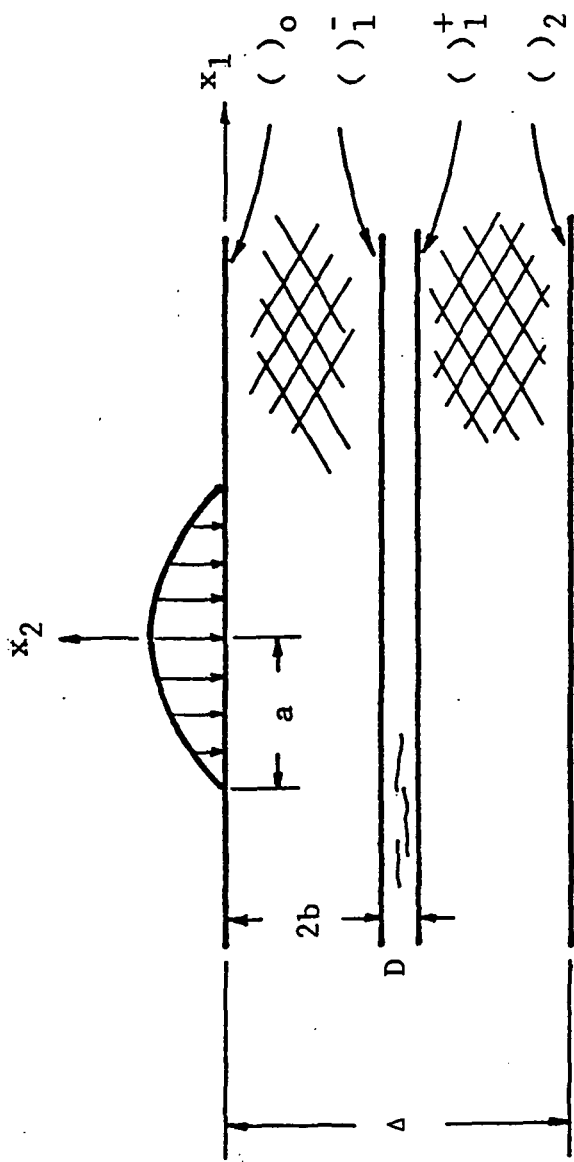


Figure 17. Impact of Plate Made of 2 Elastic Layers
and a Viscoelastic Layer

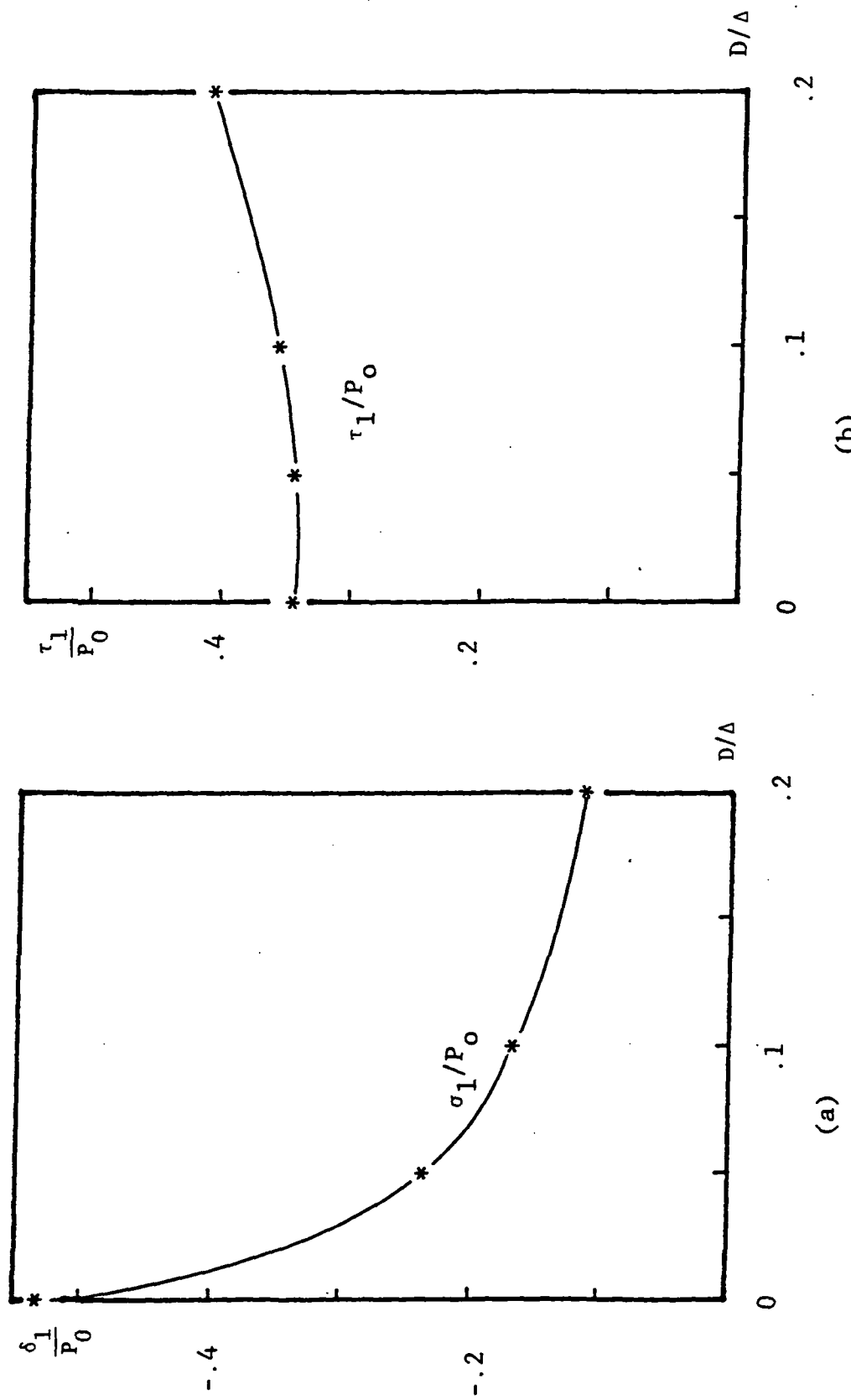


Figure 18. Peak Value of Interlaminar Stress Vs. Elastomer Thickness (two elastic layers and a viscoelastic layer; $\Delta = 1$ cm, $t_0 = 10 \mu\text{sec}$, $a = 4$ cm)
*Calculated values

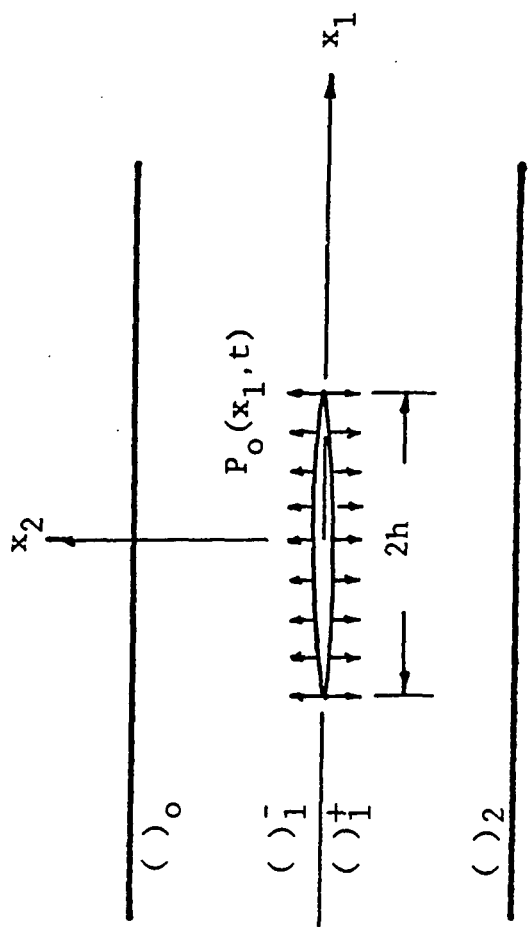
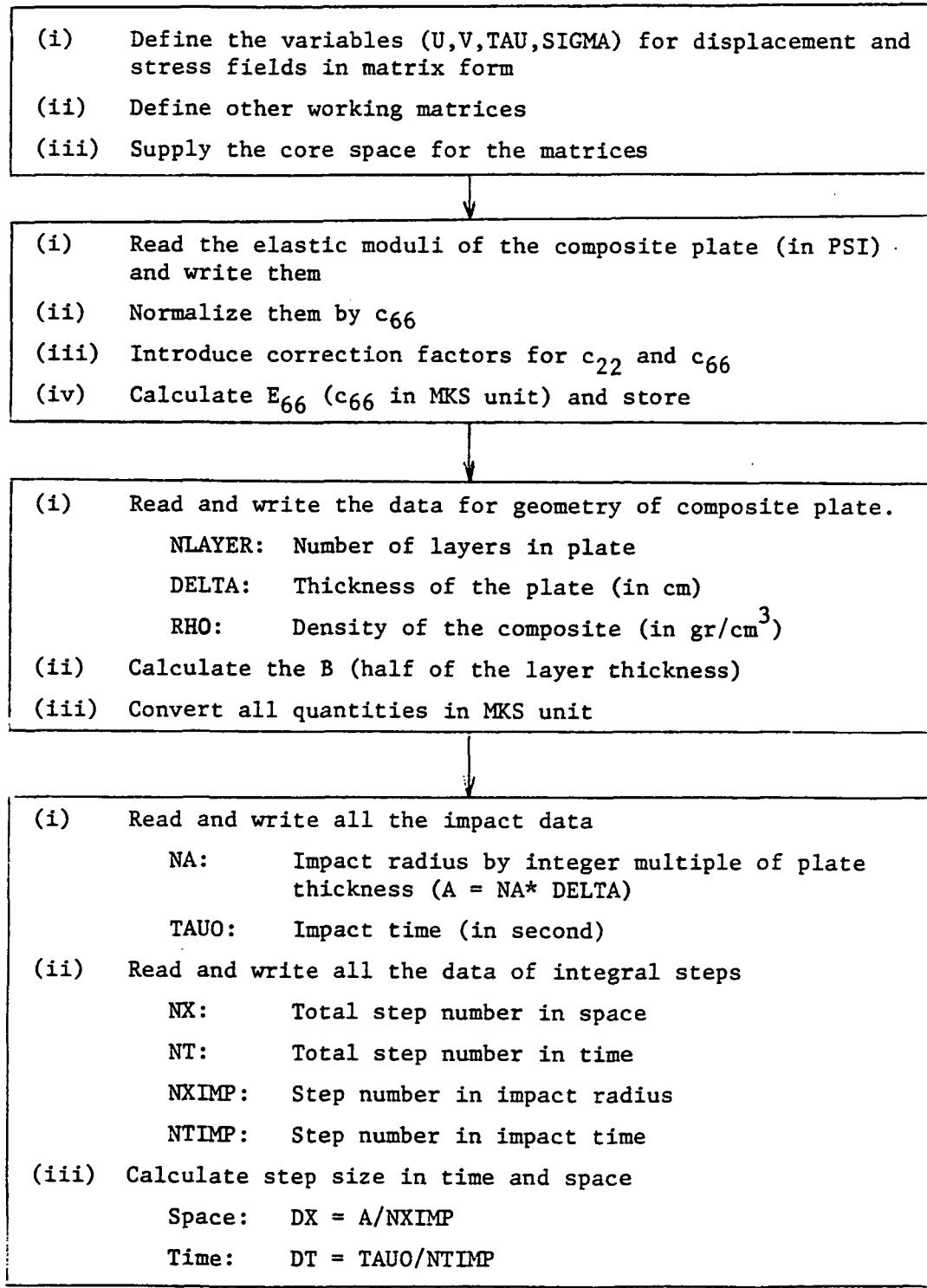


Figure 19. Composite Plate with Crack

APPENDIX A FLOW CHART

In this flow chart and program, $U(I,J)$, $V(I,J)$, $TAU(I,J)$, $SIGMA(I,J)$ and $SIGMA1(I,J)$ represent \hat{U} , \hat{V} , \hat{T} and $\hat{\Sigma}$ in Eq. (II-17,18) and integral transform of σ_{11}





(i) Calculate normalization units

Space: UNITX = DELTA (Thickness of the plate)

Time: UNITT = $A/\sqrt{E_{66}/\rho}$ (Time required for the quasi-shear wave to travel the impact radius)

(ii) Normalized all quantities by UNITT and UNITX

(iii) Calculate integral limits (ω_o and k_o) in Fast Fourier Transform



Calculate $Q_0(I,J)$, $CBX(I,J)$, $CAX(I,J)$, $XIBX(I,J)$, $YIAX(I,J)$ $Y3AX(I,J)$, over a half of the range of integration ($I = 1 \sim NT$, $J = 1, NX/2$).

Q_0 : Impact function given in Eq. (II-22)

CBX , CAX : $\cos\beta$ and $\cos\alpha$ in Eq. (II-16,17) by DPHASE

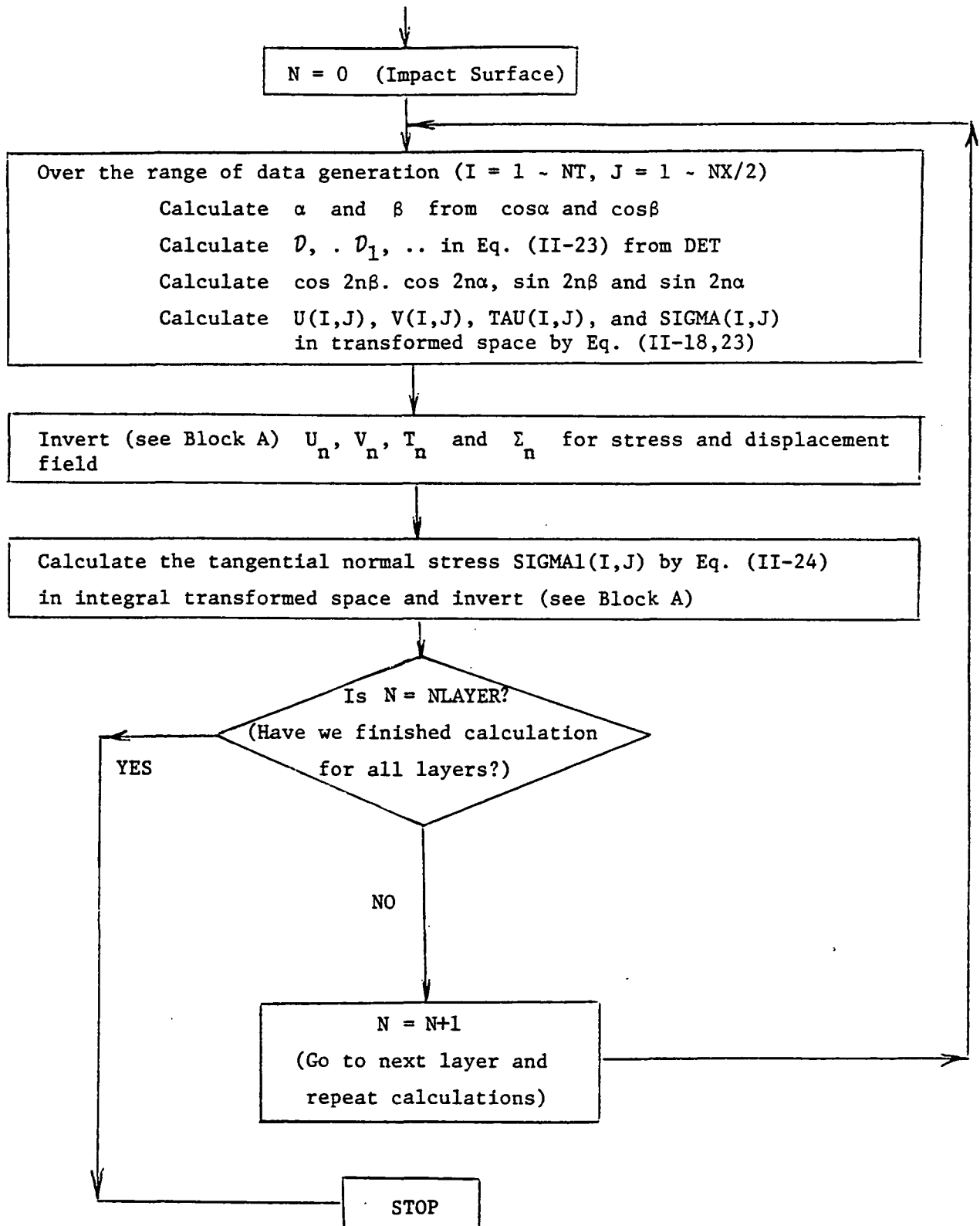
$XIBX$, $X2BX$...: $X_1(\beta)$, $X_2(\beta)$ in Eq. (II-18,19) by DELL

$YIAX$, $Y2AX$...: $Y_1(\alpha)$, $Y_2(\alpha)$ in Eq. (II-18,19) by DELL



Invert (see Block A) and check the impact function σ_o with Q_0





Block A Inversion

- (i) Data $xx(I,J)$ in integral transformed space are generated for a half of the inverse transform range: $I = 1 \sim NT$, $J = 1 \sim NX/2$
- (ii) Generate full data over $J = 1 \sim NX$ by FLIP
 - Symmetric flip: $V(I,J)$, $SIGMA(I,J)$, $SIGMAL(I,J)$, $Q0(I,J)$
 - Antisymmetric flip: $U(I,J)$, $TAU(I,J)$
- (iii) Invert them for displacement and stress fields by FOURT
- (iv) Take care of the coordinate shifts and multiplication factors in FOURT by FACT
- (v) Print out by MAP

APPENDIX B SAMPLE COMPUTER DECK

64	32	8	24	Data Card 4	
2	6.E-06			Data Card 3	
8	1.	1.44		Data Card 2	
15	0.2456E 08	0.4000E 06	0.1170E 07	0.3552E 06	Data Card 1

/GD.SYSIN DD *

PROGRAM IN SOURCE DECK (see Appendix C)

EXEC FORTGOLG

LIMITS REGION=207K,LINES=5K,CLASS=C

JOB CARD

APPENDIX C LISTING OF PROGRAM AND SAMPLE OUTPUT

>1 RELEASE 2.0

MAIN

DATE = 77139

21/11/39

```
C*****
C
C THIS PROGRAM CALCULATES THE TRANSIENT PROPAGATION OF STRESS WAVE
C IN A LAMINATED COMPOSITE PLATE DUE TO A NORMAL IMPACT.
C
C -----
C
C THE PRESENT PROGRAM IS A PART OF THE RESEARCH PROJECT OF
C PROFESSOR FRANCIS C. MOON
C DEPARTMENT OF THEORETICAL AND APPLIED MECHANICS
C CORNELL UNIVERSITY
C AND SUPPORTED BY NASA-LEWIS RESEARCH CENTER.
C
C
C*****
C
C FOLLOWING USER'S GUIDES ARE PROVIDED BY DR. B.S.KIM AND ALL THE EQUATION
C NUMERS CORRESPOND EQUATIONS IN THE ACCOMPANYING TECHNICAL REPORT
C
C -----
C
C 1. DATA TO BE SUPPLIED BY 4 DATA CARDS (IN THE ORDER OF READING)
C
C
C IANGLE: FIBER LAYUP ANGLE IN COMPOSITES
C C11,C12.. : ELASTIC MODULI OF COMPOSITE LAYER(IN PSI)
C
C NLAYER: NUMBER OF THE LAYERS IN THE GIVEN PLATE
C D,DELTA: THICKNESS OF COMPOSITE PLATE(IN CM)
C RHO: MASS DENSITY OF COMPOSITE LAYER(IN GR/CM**3)
C
C NA: RADIUS OF THE IMPACT AS A MULTIPLE OF THE PLATE THICKNESS
C TAU0: IMPACT TIME(IN SECOND)
C
C
C NX: NUMBER OF INTEGRATION STEPS IN SPACE
C NT: NUMBER OF INTEGRATION STEPS IN TIME DOMAIN
C NXIMP: NUMBER OF SPACE STEPS IN IMPACT RADIUS
C NTIMP: NUMBER OF TIME STEPS IN IMPACT TIME
C
C
C -----
C
C
C 2. WITH THE ABOVE DATA FOLLOWING PRIMARY DATA ARE CALCULATED
```

1 RELEASE 2.0

MAIN

DATE = 77139

21/11/39

C B: A HALF OF THE LAYER THICKNESS
C
C K: WAVE NUMBER FOR FOURIER TRANSFORM
C S: LAPLACE TRANSFORM VARIABLE
C
C KO: LIMIT OF INTEGRATION FOR INVERSE FOURIER TRANSFORM FOR X
C OMEGA0: LIMIT OF INTEGRATION FOR INVERSE TRANSFORM IN TIME
C CO: LAPLACE TRANSFORM PARAMETER
C
C
C

C 3. DISPLACEMENT AND STRESS FIELDS ARE CALCULATED IN TRANSFORMED SPACE
C AND BY INVERSIONS THESE BECOME DISPLACEMENTS AND STRESSES.
C THEY ARE GIVEN IN A MATRIX FORM AS XX(I,J) REPRESENTING QUANTITY AT
C ITH TIME STEP AND JTH SPACE STEP IN X
C

C U(I,J): HORIZONTAL DISPLACEMENT
C V(I,J): VERTICAL DISPLACEMENT
C SIGMA(I,J): NORMAL STRESS
C TAU(I,J): SHEAR STRESS
C SIGMA1(I,J): TANGENTIAL NORMAL STRESS
C
C
C

C 4. FOLLOWINGS ARE WORKING MATRICES FOR THIS PROGRAM
C

C DATA(I,J), SUB(I,J): WORKING MATRICES FOR SUBROUTINE FOURT
C Q0(I,J): INTEGRAL TRANSFORM OF IMPACT FUCTION GIVEN IN EQ(II-22)
C
C CAX(I,J), CBX(I,J): COS(ALPHA) AND COS(BETA) IN EQ(II-16)
C X1BX(I,J), Y1AX(I,J),..: X1(BETA), Y1(ALPHA),.. IN EQ(II-18)
C
C

C 5. FOLLOWING SUBROUTINE ARE SUPPLIED IN THE PRESENT PROGLAM
C

C DPHASE: CALCULATES COS(BETA) AND CCS(ALPHA) IN EQ(II-16) WITH GIVEN
C VALUES OF WAVE NUMBER K AND LAPLACE TRANSFORM VARIABLE
C
C DELL: CALCULATES X1(BETA), Y1(ALPHA),.. IN EQ (II-19,20)

1 RELEASE 2.0

MAIN

DATE = 77139

21/11/39

C
C DET: CALCULATE D,D1,.. IN EQ(II-23)
C
C FLIP: THIS PROGRAM GENERATES ONLY A HALF OF THE DATA (X>0) DUE
C TO SYMMETRY AND FLIP THEM TO FIND FULL DATA ALONG X AXIS
C
C MAP: CONTROLLS THE PRINTOUT FORMAT
C
C FACT: TAKES CARES OF THE COORDINATE SHIFT AND MULTIPLICATION FACTORS
C IN FOURIER-LAPLACE DOUBLE INTEGRAL TRANSFORMS
C
C FGURT: IS FAST FOURIER TRANSFORM ROUTINE SUPPLIED BY IBM
C
C*****
C
IMPLICIT REAL*8(K)
COMPLEX DATA(32,64),SUB(32,32),CAX(32,32),CBX(32,32),Q0(32,32)
COMPLEX SIGMA(32,32),SIGMA1(32,32),TAU(32,32)
COMPLEX U(32,32),V(32,32),VX(32,32)
COMPLEX Y1AX(32,32),Y2AX(32,32),Y3AX(32,32)
COMPLEX X1BX(32,32),X2BX(32,32),X3BX(32,32)
DIMENSION NN(2),MM(32)
C
REAL*8 C11,C12,C22,C66,CHAT,E66,V66,PI,P2
REAL*8 DCOS,DSIN,DBLE,DSQRT,DFLOAT,DLOG
REAL*8 DELTA,D,RHO,FN,F,KX(32),B,TAU0,A,DX,DT,UNITT,UNITX
REAL*8 Q,OMEGA0,BL,C0
C
COMPLEX*16 CDEXP,CDLOG,CDSQRT,CDCOS,CDSIN
COMPLEX*16 BETA,ALPHA,CB,CA,SB,SA,C2NB,C2NA,S2NB,S2NA
COMPLEX*16 S,SI,S2,D1,D2,D3,D4
COMPLEX*16 Y1A,Y2A,Y3A,X1B,X2B,X3B
C
COMMON Y1A,Y2A,Y3A,X1B,X2B,X3B,D1,D2,D3,D4,C11,C12,C22,C66,CHAT
EQUIVALENCE (DELTA,D)
EQUIVALENCE (DATA(1,1),SUB(1,1))
C
SI=(0.D 00,1.D 00)
PI=3.1415926536D 00
P2=PI*2.D 00
INDEX=0
INDEX=1
C
WRITE(6,4)
4 FORMAT('1'//////////20X,'*** WAVE PROPAGATION IN COMPOSITE P
1LATE ***')

1 RELEASE 2.0

MAIN

DATE = 77139

21/11/39

```
      WRITE(6,5)
5       FORMAT(22X,'GRAPHITE FIBER(55%)-EPOXY MATRIX COMPOSITE')
C
C***** INPUT DATA FOR ELASTIC PROPERTIES OF COMPOSITE PLATE
C ALL THE DATA ARE SUPPLIED IN PSI UNIT BUT NORMALIZED BY C66
C WHICH IS CONSTANT REGARDLESS THE LAYUP ANGLE
C
C
100    READ (5,101) IANGLE,C11,C12,C22,C66
101    FORMAT(I10,4D15.7)
      CHAT=C11-C12**2/C22
      IF (IANGLE.EQ.100) GO TO 200
      WRITE(6,102) IANGLE,C11,C12,C22,C66
102    FORMAT(// 20X,'LAYUP ANGLE=',I3,3X,'DEGREE'
      $ /20X,'C(1,1)=',D12.5,' PSI',10X,'C(1,2)=',D12.5,' PSI'
      $ /20X,'C(2,2)=',D12.5,' PSI',10X,'C(6,6)=',D12.5,' PSI'//)
      GO TO 201
200    CONTINUE
      WRITE(6,210) C11,C12,C22,C66
210    FORMAT(/20X,' PLATE IS ISOTROPIC WITH POISSON''S RATIO 1/4'
      $ /20X,'C(1,1)=',D12.5,' PSI',10X,'C(1,2)=',D12.5,' PSI'
      $ /20X,'C(2,2)=',D12.5,' PSI',10X,'C(6,6)=',D12.5,' PSI'//)
201    CONTINUE
C
      E66=C66*6892.2D 00
      C11=C11/C66
      C12=C12/C66
      C22=C22/C66
      CHAT=CHAT/C66
      C66=1.D 00
C
C***** WITH CORRECTION FACTOR
C
      C66=PI**2/12.D 00
      C22=C22*C66
C
C
C-----
```

C INPUT DATA FOR GEOMETRY OF COMPOSITE PLATE
C ALL THE DATA ARE FIRST SUPPLIED IN CGS UNIT BUT CONVERTED INTO MKS UNIT

120 READ(5,120) NLAYER,DELTA,RHO
120 FORMAT(I10,2D20.10)

;1 RELEASE 2.0

MAIN

DATE = 77139

21/11/39

```
NL1=NAYER+1
FN=DFLOAT(NAYER)
B=DELTA/FN
WRITE(6,121) DELTA,RHO,NAYER,B
121 FORMAT(20X,'TOTAL THICKNESS OF COMPOSITE PLATE ; DELTA=',F10.5,
$ ' CM'
$ 20X,'DENSITY OF COMPOSITE ; RHO=',F10.5,' GR/CM**3'
$ 20X, 'PLATE IS MADE OF ',I3,3X, 'IDENTICAL LAYERS'
$ 20X,'LAYER THICKNESS ; 2B=',F10.5,' CM'//)
C
DELTA=DELTA/100.D 00
RHO=RHO*1000.D 00
B=B/200.D 00
C
C
C -----
C INPUT DATA FOR IMPACT
C
C
READ(5,60) NA,TAU0
60 FORMAT(I10,D20.10)
READ(5,111) NX,NT,NXIMP,NTIMP
111 FORMAT(4I10)
C
WRITE(6,112) NX,NXIMP,NT,NTIMP
112 FORMAT(20X,'TOTAL SPACE STEPS; NX=',I3,5X,'WITH',I3,2X,'STEPS FOR
$ CONTACT RADIUS'
$ 20X,'TOTAL TIME STEPS ; NT=',I3,5X,'WITH',I3,2X,'STEPS FOR CONTAC
$ T TIME'//)
C
A=DFLOAT(NA)*DELTA
DX=A/DFLOAT(NXIMP)
DT=TAU0/DFLOAT(NTIMP)
C
WRITE(6,61) A,DX,TAU0,DT
61 FORMAT(20X,'CONTACT RADIUS ; A=',D12.5,' M'
$ 20X,'SPACE STEP ; DX=',D12.5,' M'
$ 20X,'CONTACT TIME ; TAU0=',D12.5,' SECOND'
$ 20X,'TIME STEP ; DT=',D12.5,' SECOND'//)
C
C
C -----
C NORMALIZE ALL THE INPUT DATA
C
C
V66=DSQRT(E66/RHO)
```

1 RELEASE 2.0

MAIN

DATE = 77139

21/11/39

```
UNITT=A/V66
UNITX=DELTA
F=D*D*RHO/(E66*UNITT**2)/2.D 00/FN
```

C

```
NX2=NX/2
NN(1)=NT
NN(2)=NX
DX=DX/UNITX
DT=DT/UNITT
K0=PI/DX
OMEGA0=PI/DT
BL=A/D
CO=DLOG(1.D 06*2.D 00*DT)/(3.D 00*DT*DFLOAT(NT))
```

C

C

C

```
*****
```

C

C

```
C CALCULATE THE IMPACT INPUT FUNCTION Q0(I,J) IN EQ(II-22)
C CALCULATE COS(BETA) AND COS(ALPHA) IN EQ(II-16) BY SUBROUTINE DPHASE
C CALCULATE X1(BETA), Y1(ALPHA) ,.. BY SUBROUTINE DELL
```

C

C

```
DO 30 J=1,NX2
K=2.D 00*K0*(DFLOAT(J)-.5)/DFLOAT(NX)-K0
K2=K**2
KX(J)=K
Q=PI**2/DSQRT(P2)*DSIN(K*BL)/K/((K*BL)**2-PI**2)
```

C

```
DO 30 I=1,NT
S=CO+SI*OMEGA0*(1.D 00-(DFLOAT(I)-.5D 00)*2.D 00/DFLOAT(NT))
S2=S**2*F
Q0(I,J)=Q/2./S*(1.D 00-CDEXP(-S*TAU0/UNITT))*(P2*UNITT)**2
$ /((S*TAU0)**2+(P2*UNITT)**2)
```

C

```
CALL DPHASE (K,S2,CB,CA,NLAYER)
CBX(I,J)=CB
CAX(I,J)=CA
```

C

```
CALL DELL(K,S2,CB,CA,SI,NLAYER)
Y1AX(I,J)=Y1A
Y2AX(I,J)=Y2A
Y3AX(I,J)=Y3A
X1BX(I,J)=X1B
X2BX(I,J)=X2B
X3BX(I,J)=X3B
```

C

ORIGINAL PAGE IS
DE POOR QUALITY

51 RELEASE 2.0 MAIN DATE = 77139 21/11/39

30 CONTINUE
C
C
C
C ****=
C
C REPRODUCE THE IMPACT FUNCTION TO CHECK INPUT
C
DO 300 I=1,NT
DO 300 J=1,NX2
300 SUB(I,J)=Q0(I,J)
CALL FLIP(DATA,NX,NX2,NT,+1)
CALL FOURT(DATA,NN,2,-1,1,0)
CALL FACT(DATA,NX,NT,CO,OMEGAO,K0,PI,SI)
WRITE(6,301)
301 FORMAT('1'//////////20X, '*** REPRODUCTION OF IMPACT FUNCTIO
IN ***')
CALL MAP(DATA,NX,NT,NX2,MM,INDEX)
C
C
C
C ****=
C
C
C THIS IS THE MAIN PART OF THE PROGRAM.
C
C CALCULATE D(BETA),DBAR(ALPHA),.. IN EQ(II-19,20) BY SUBROUTINE DET
C NEXT CALCULATE 1,V,.. IN EQ(II-18) IN TRANSFORMED SPACE
C AND FLIP TO FIND FULL DATA AND INVERT THEM BY MEANS OF FOURT.
C REPEAT THIS PROCESS FROM N=0 TO NLAYER
C
DO 11 N=1,NL1
NY=N-1
NYY=NY-1
C
C
C -----
C
C GENERATION OF DATA FOR DISPLACEMENTS AND STRESS IN TRANSFORMED SPACE
C
DO 100 J=1,NX2
DO 100 I=1,NT
CB=CBX(I,J)
CA=CAX(I,J)
X1B=X1BX(I,J)
X2B=X2BX(I,J)
X3B=X3BX(I,J)

1 RELEASE 2.0

MAIN

DATE = 77139

21/11/39

```
Y1A=Y1AX(I,J)
Y2A=Y2AX(I,J)
Y3A=Y3AX(I,J)
```

C

```
SB=CDSQRT(1.D 00-CB**2)
SA=CDSQRT(1.D 00-CA**2)
BETA=CB+SI*SB
ALPHA=CA+SI*SA
BETA=CDLOG(BETA)/SI
ALPHA=CDLOG(ALPHA)/SI
```

C

```
CALL DET(ALPHA,BETA,SI,FN)
C2NB=CDCOS(2.D 00*BETA*DFLOAT(NY))
S2NB=CDSIN(2.D 00*BETA*DFLOAT(NY))
C2NA=CDCOS(2.D 00*ALPHA*DFLCAT(NY))
S2NA=CDSIN(2.D 00*ALPHA*DFLOAT(NY))
```

C

```
U(I,J)=(X1B*(D1*C2NB+SI*D2*S2NB)+Y1A*(D4*C2NA+SI*D3*S2NA))*Q0(I,J)
V(I,J)=(X2B*(D2*C2NB+SI*D1*S2NB)+Y2A*(D3*C2NA+SI*D4*S2NA))*Q0(I,J)
TAU(I,J)=(X3B*(D2*C2NB+SI*D1*S2NB)+(D3*C2NA+SI*D4*S2NA))*Q0(I,J)
SIGMA(I,J)=((D1*C2NB+SI*D2*S2NB)+Y3A*(D4*C2NA+SI*D3*S2NA))*Q0(I,J)
```

100 CONTINUE

C

C

C

C INVERSION AND PRINTOUT OF HORIZONTAL DISPLACEMENT UN(I,J)

C

```
DO 10 I=1,NT
DO 10 J=1,NX2
10 SUB(I,J)=U(I,J)
CALL FLIP(DATA,NX,NX2,NT,-1)
CALL FOURT(DATA,NN,2,-1,1,0)
CALL FACT(DATA,NX,NT,C0,OMEGAO,K0,PI,SI)
WRITE(6,981) NY
981 FORMAT('1'//////////20X,'U',I3)
CALL MAP(DATA,NX,NT,NX2,MM,INDEX)
```

C

C

C

C INVERSION AND PRINTOUT OF VERTICAL DISPLACEMENT VN(I,J)

C

```
DO 20 I=1,NT
DO 20 J=1,NX2
20 SUB(I,J)=V(I,J)
CALL FLIP(DATA,NX,NX2,NT,+1)
CALL FOURT(DATA,NN,2,-1,1,0)
```

>1 RELEASE 2.0 MAIN DATE = 77139 21/11/39

```
CALL FACT(DATA,NX,NT,CO,OMEGAO,KO,PI,SI)
WRITE(6,982) NY
982 FORMAT('1'//////////20X,'V',I3)
CALL MAP(DATA,NX,NT,NX2,MM,INDEX)

C
C
C
C-----
```

C INVERSION AND PRINTOUT OF SHEAR STRESS TAU(I,J)

C

```
DO 35 I=1,NT
DO 35 J=1,NX2
35 SUB(I,J)=TAU(I,J)
CALL FLIP(DATA,NX,NX2,NT,-1)
CALL FOURT(DATA,NN,2,-1,1,0)
CALL FACT(DATA,NX,NT,CO,OMEGAO,KO,PI,SI)
WRITE(6,983) NY
983 FORMAT('1'//////////20X,'TAU',I3)
CALL MAP(DATA,NX,NT,NX2,MM,INDEX)

C
C
C
C-----
```

C INVERSION AND PRINTOUT OF NORMAL STRESS SIGMA(I,J)

C

```
DO 40 I=1,NT
DO 40 J=1,NX2
40 SUB(I,J)=SIGMA(I,J)
CALL FLIP(DATA,NX,NX2,NT,+1)
CALL FOURT(DATA,NN,2,-1,1,0)
CALL FACT(DATA,NX,NT,CO,OMEGAO,KO,PI,SI)
WRITE(6,984) NY
984 FORMAT('1'//////////20X,'SIGMA',I3)
CALL MAP(DATA,NX,NT,NX2,MM,INDEX)

C
C
C
C-----
```

C INVERSION AND PRINTOUT OF TANGENTIAL NORMAL STRESS SIGMA1(I,J)

C

```
IF (NY.EQ.0) GO TO 160
DO 50 I=1,NT
DO 50 J=1,NX2
50 SUB(I,J)=SIGMA1(I,J)+FN*C12*V(I,J)
CALL FLIP(DATA,NX,NX2,NT,+1)
CALL FOURT(DATA,NN,2,-1,1,0)
CALL FACT(DATA,NX,NT,CO,OMEGAO,KO,PI,SI)
WRITE(6,985) NYY
```

G1 RELEASE 2.0 MAIN DATE = 77139 21/11/39

```
985 FORMAT('1'//////////20X,'SIGMA1',I3)
      CALL MAP(DATA,NX,NT,NX2,MM,INDEX)
C
      IF (NY.EQ.NLAYER) GO TO 70
      DO 51 I=1,NT
      DO 51 J=1,NX2
51      SIGMA1(I,J)=-SI*KX(J)*C11*U(I,J)-FN*C12*VX(I,J)
      GO TO 80
C
160      CONTINUE
      DO 161 I=1,NT
      DO 161 J=1,NT
161      SIGMA1(I,J)=-SI*KX(J)*C11*U(I,J)-FN*C12*V(I,J)
      GO TO 80
C
70      CONTINUE
      DO 71 I=1,NT
      DO 71 J=1,NX2
71      SUB(I,J)=-SI*KX(J)*C11*U(I,J)+FN*C12*(V(I,J)-VX(I,J))
      CALL FLIP(DATA,NX,NX2,NT,+1)
      CALL FOURT(DATA,NN,2,-1,1,0)
      CALL FACT(DATA,NX,NT,CO,OMEGAO,KO,PI,SI)
      WRITE(6,985) NY
      CALL MAP(DATA,NX,NT,NX2,MM,INDEX)
      GO TO 90
C
80      CONTINUE
      DO 81 I=1,NT
      DO 81 J=1,NX2
81      VX(I,J)=V(I,J)
C
90      CONTINUE
C
C
11      CONTINUE
C
***** ****
C
C
C
C
      STOP
      END
```

G1 RELEASE 2.0

MAIN

DATE = 77139

21/11/39

```
C
C
C*****THIS SUBROUTINE CALCULATES THE PHASE SHIFT BETA AND ALPHA FROM
C      EQ(II-15,16) OF THE PRESENT REPORT WITH GIVEN VALUES OF
C      WAVE NUMBER K AND LAPLACE TRANSFORM VARIABLE S
C
C      CA=COS(ALPHA)
C      CB=COS(BETA)
C
C*****SUBROUTINE DPHASE(K,S ,CB,CA,NLAYER)
IMPLICIT COMPLEX*16(A,X,Y)
COMPLEX*16 ROOTP,ROOTM,S,CDSQRT,DCMPLX,DCB,DCA
COMPLEX*16 D1,D2,D3,D4
COMPLEX*16 CB,CA
REAL*8 C11,C12,C22,C66,CHAT,N,K2,DFLOAT,DBLE,K
C
COMMON Y1A,Y2A,Y3A,X1B,X2B,X3B,D1,D2,D3,D4,C11,C12,C22,C66,CHAT
ROOTP(AA,AB,AC)=(-AB+CDSQRT(AB**2-4.D 00*AA*AC))/(2.D 00*AA)
ROOTM(AA,AB,AC)=(-AB-CDSQRT(AB**2-4.D 00*AA*AC))/(2.D 00*AA)
C
N=DFLOAT(NLAYER)*2.D 00
K2=K**2
C
C
A1=(K2*C11/N+S)*(K2*C66/N+S)
A2=K2*CHAT/(3.D 00*N)+N*C66+S/3.D 00-C12*C66*K2/(3.D 00*N*C22)
A2=A2*(-C12*K2/(3.D 00*N)+N*C22+S/3.D 00)
A3=N*C22+S/3.D 00-K2*C12*(C66*K2/N+S)/(9.D 00*N**2*C22)+C66*K2/
$ (3.D 00*N)
A3=A3*(C11*K2/N+S)-K2*(C12+C66)**2
A3=A3+(C66*K2/N+S)*(CHAT*K2/(3.D 00*N)+N*C66+S/3.+C12**2*K2/
$ (3.D 00*C22))
C
AA=A1+A2-A3
AB=A3-2.D 00*A2
AC=A2
DCB=ROOTP(AA,AB,AC)
DCA=ROOTM(AA,AB,AC)
C
CB=CDSQRT(DCB)
CA=CDSQRT(DCA)
RETURN
END
```

ORIGINAL PAGE IS
OF POOR QUALITY

G1 RELEASE 2.0

MAIN

DATE = 77139

21/11/39

```
C
C
C***** THIS SUBROUTINE CALCULATES DELTA(BETA), DELTABAR(ALPHA), DELTA1(BETA), ..
C      IN EQ(II-19,20) AND X1(BETA), Y1(ALPHA) IN EQ(II-18,19,20)
C
C      X1B=X1(BETA),    Y1A=Y1(ALPHA)
C      .
C      .
C
C***** SUBROUTINE DELL (K,S,CB,CA,SI,NLAYER)
C      IMPLICIT REAL*8(K),COMPLEX*16(S,X,D,Y)
C      COMPLEX*16 SB,CB,CDSQRT,SA,CA
C      REAL*8 N,DFLOAT
C      REAL*8 C11,C12,C22,C66,CHAT
C
C      COMMON Y1A,Y2A,Y3A,X1B,X2B,X3E,D1,D2,D3,D4,C11,C12,C22,C66,CHAT
C
C      K2=K**2
C      N=DFLOAT(NLAYER)
C
C
S11=S+C11*K2/2.D 00/N
S66=S+C66*K2/2.D 00/N
SA=CDSQRT(1.D 00-CA**2)
SB=CDSQRT(1.D 00-CB**2)
C
C
DELTAB=CB**3*S11*S66+SB**2*CB*(-C66*(C66+C12)*K2
$ +S66*(S/3.D 00+CHAT*K2/6.D 00/N+2.D 00*N*C66))
DEL1B=SI*K*SB**2*CB*(-C66-C12+C12*S66/6.D 00/N/C22)
DEL2B=SI*SB**3*(C12*C66*K2/6.D 00/N/C22-S/3.D 00
$ -CHAT*K2/6.D 00/N-2.D 00*N*C66)-SI*CB**2*SB*S11
DEL3B=CB**2*SB*(C12*K*S11*S66/6.D 00/N/C22-C66*K*S11)
$ +SB**3*(C12*K*(S/3.D 00+CHAT*K2/6.D 00/N+2.D 00*N*C66)
$ -C12**2*C66*K*K2/6.D 00/N/C22)
C
C
DELTAA=SI*CA**2*SA*((C12+C66)*C66*K2-S66*(S/3.D 00+CHAT*K2
$ /6.D 00/N+2.D 00*N*C66+C12**2*K2/6.D 00/N/C22))
$ +SI*SA**3*(S/3.D 00+2.D 00*N*C22)*(C66*C12*K2/6.D 00/N/C22
$ -S/3.D 00-CHAT*K2/6.D 00/N-2.D 00*N*C66)
DEL1A=SA**2*CA*(-K2*C12*S66/6.D 00/6.D 00/N**2/C22+C66*K2/6.D 00/N
$ +S/3.D 00+2.D 00*N*C22)+CA**3*S66
DEL2A=CA**2*SA*K*(C12+C66)
```

G1 RELEASE 2.0

DELL

DATE = 77139

21/11/39

```
$ +SA**3*(K/6.D 00/N*(S/3.D 00+CHAT*K2/6.D 00/N+2.D 00*N*C66)
$ -C66*C12*K**3/36.D 00/C22/N**2)
DEL3A=-SI*CA**3*C12*K*S66+SI*SA**2*CA*(C66*K*(S/3.D 00+2.D 00*N
$ *C22+C66*K2/6.D 00/N)-K/6.D 00/N*S66*(S/3.D 00+CHAT*K2/6.D 00
$ /N+2.D 00*N*C66))
```

C

C

```
X1B==DEL1B/DELTAB
X2B==DEL2B/DELTAB
X3B==DEL3B/DELTAB
Y1A==DEL1A/DELTAA
Y2A==DEL2A/DELTAA
Y3A==DEL3A/DELTAA
```

C

```
RETURN
END
```

G1 RELEASE 2.0

MAIN

DATE = 77139

21/11/39

```
C
C
C***** THIS SUBROUTINE CALCUALTES D,D1,.. IN EQ(II-23) OF THE PRESENT REPORT
C
C***** SUBROUTINE DET(ALPHA,BETA,SI,FN)
IMPLICIT COMPLEX*16(D,X,Y)
COMPLEX*16 ALPHA,BETA
COMPLEX*16 C2NB,C2NA,S2NA,S2NB,CDSQRT,SI
REAL*8 FN
REAL*8 C11,C12,C22,C66,CHAT
C
COMMON Y1A,Y2A,Y3A,X1B,X2B,X3B,D1,D2,D3,D4,C11,C12,C22,C66,CHAT
C
C2NA=CDCOS(2.D 00*ALPHA*FN)
S2NA=CDSIN(2.D 00*ALPHA*FN)
C2NB=CDCOS(2.D 00*BETA*FN)
S2NB=CDSIN(2.D 00*BETA*FN)
C
X=Y3A*X3B*(1.D 00-C2NA*C2NB)
Y=X3B*Y3A*S2NB*C2NA-S2NA*C2NB
C
D=-2.D 00*X+(1.D 00+X3B**2*Y3A**2)*S2NA*S2NB
D1=-(X-S2NA*S2NB)
D2=-SI*Y
D3=SI*Y*X3B
D4=X3B*(X3B*Y3A*S2NB*S2NA+C2NA*C2NB-1.D 00)
C
D1=D1/D
D2=D2/D
D3=D3/D
D4=D4/D
C
RETURN
END
```

G1 RELEASE 2.0

MAIN

DATE = 77139

21/11/39

```
C
C
C*****ALL THE DATA IN THE MAIN PROGRAM ARE GENERATED FOR ONLY HALF OF THE
C      PLATE WHEN X>0. DUE TO SYMMETRY OF THE PROBLEM WE CAN GENERATE
C      THE FULL DATA BY FLIPPING THE HALF OF THE DATA.
C
C
C*****SUBROUTINE FLIP(DATA,NX,NX2,NT,INDEX)
COMPLEX DATA(NT,NX)
DO 10 J=1,NX2
JJ=NX+1-J
DO 10 I=1,NT
DATA(I,JJ)=FLOAT(INDEX)*DATA(I,J)
10 CONTINUE
RETURN
END
```

ORIGINAL PAGE IS
OF POOR QUALITY

G1 RELEASE 2.0

MAIN

DATE = 77139

21/11/39

```
C
C
C*****THIS SUBROUTINE TAKES CARE OF THE COORDINATE SHIFT IN
C LAPLACE AND FOURIER TRANSFORM IN THE PROCESS OF APPLYING
C FAST FOURIER TRANSFORM ALGORITHM
C
C
C*****SUBROUTINE FACT(DATA,NX,NT,C0,W0,K0,PI,SI)
COMPLEX DATA(NT,NX)
COMPLEX*16 CDEXP,SI
REAL*8 DEXP,DSQRT,DFLOAT
REAL*8 C0,W0,PI,K0,FT,FX
FX=DFLOAT(NX)
FT=DFLOAT(NT)
NX2=NX/2
C
DO 10 L=1,NX2
DO 10 M=1,NT
DATA(M,L)=DATA(M,L)*4.D 00*K0*W0/(DSQRT(2.D 00*PI)**3*FT*FX)
$ *DEXP(C0*PI*DFLOAT(M-1)/W0)*CDEXP(SI*PI*(1.D 00-1.D 00/FT)
$ *DFLOAT(L-1))*CDEXP(SI*PI*(1.D 00-1.D 00/FT)*DFLOAT(M-1))
10 CONTINUE
RETURN
END
```

ORIGINAL PAGE IS
OF POOR QUALITY

G1 RELEASE 2.0

MAIN

DATE = 77139

21/11/39

```
C*****
C THIS SUBROUTINE CONTROLS THE FORMAT OF THE PRINTOUT OF THE FINAL RESULTS
C
C      IF INDEX=0: ALL THE NUMERICAL VALUES ARE PRINTED
C                  =1: THE MAXIMUM AND NORMALIZED VALUES ARE PRINTED
C
C*****
C
SUBROUTINE MAP(DATA,NX,NT,NX2,MM,INDEX)
COMPLEX DATA(NT,NX),S
DIMENSION MM(NX2)
IF (INDEX.EQ.1) GO TO 200
DO 44 IQ=1,NT
44  WRITE(6,15) IQ,(DATA(IQ,I),I=1,NX2)
15   FORMAT(I5,2E14.5,2X,2E14.5,2X,2E14.5,2X,2E14.5/
$           3(5X,2E14.5,2X,2E14.5,2X,2E14.5,2X,2E14.5)/
$           4(5X,2E14.5,2X,2E14.5,2X,2E14.5,2X,2E14.5)/)
200  CONTINUE
C*** FIND THE MAXIMUM VALUE
RS= 1.E-3
NT5=NT-5
NX5=NX2-5
DO 114 I=1,NT5
DO 114 J= 1,NX5
S= DATA(I,J)
TP= REAL(S)/RS
IF (ABS(TP).LT.1.) GO TO 114
RS= REAL(S)
114  CONTINUE
WRITE (6,516) RS
516  FORMAT(20X,'***  MAXIMUM VALUE =',E12.5,' ***'//)
DO 119 I=1,NT5
DO 113 J=1,NX5
S= DATA(I,J)
113  MM(J)= REAL(S)/RS*100
WRITE(6,515) (MM(KIM),KIM=1,27)
119  CONTINUE
515  FORMAT(10X,27I3)
RETURN
END
```

1 RELEASE 2.0

FOURT

DATE = 77139

21/11/39

```
SUBROUTINE FOURT(DATA,NN,NDIM,ISIGN,IFORM,WORK)
DIMENSION DATA(1),NN(1),IFACT(32),WORK(1)
TWOPI=6.283185307
IF(NDIM>1)920,1,1
1 NTOT=2
DO 2 IDIM=1,NDIM
IF(NN(IDIM))920,920,2
2 NTOT=NTOT*NN(IDIM)
C
C MAIN LOOP FOR EACH DIMENSION
C
NP1=2
DO 910 IDIM=1,NDIM
N=NN(IDIM)
NP2=NP1*N
IF(N-1)920,900,5
C
C FACTOR N
C
5 M=N
NTWO=NP1
IF=1
IDIV=2
/0 IQUOT=M/IDIV
IREM=M-IDIV*IQUOT
IF(IQUOT-IDIV)50,11,11
// IF(IREM)20,12,20
/2 NTWO=NTWO+NTWO
M=IQUOT
GO TO 10
20 IDIV=3
30 IQUOT=M/IDIV
IREM=M-IDIV*IQUOT
IF(IQUOT-IDIV)60,31,31
31 IF(IREM)40,32,40
32 IFACT(IF)=IDIV
IF=IF+1
M=IQUOT
GO TO 30
40 IDIV=IDIV+2
GO TO 30
50 IF(IREM)60,51,60
51 NTWO=NTWO+NTWO
GO TO 70
60 IFACT(IF)=M
C
C SEPARATE FOUR CASES--
C   1. COMPLEX TRANSFORM OR REAL TRANSFORM FOR THE 4TH, 5TH, ETC.
```

ORIGINAL PAGE IS
IN POOR QUALITY

FFTT000
FFTTO770
FFTTO780
FFTTO790
FFTTO800
FFTTO810
FFTTO820
FFTTO830
FFTTO840
FFTTO850
FFTTO860
FFTTO870
FFTTO880
FFTTO890
FFTTO900
FFTTO910
FFTTO920
FFTTO930
FFTTO940
FFTTO950
FFTTO960
FFTTO970
FFTTO980
FFTTO990
FFTTO1000
FFTTO1010
FFTTO1020
FFTTO1030
FFTTO1040
FFTTO1050
FFTTO1060
FFTTO1070
FFTTO1080
FFTTO1090
FFTTO1100
FFTTO1110
FFTTO1120
FFTTO1130
FFTTO1140
FFTTO1150
FFTTO1160
FFTTO1170
FFTTO1180
FFTTO1190
FFTTO1200
FFTTO1210
FFTTO1220
FFTTO1230

1 RELEASE 2.0

FOURT

DATE = 77139

21/11/39

C DIMENSIONS.
C 2. REAL TRANSFORM FOR THE 2ND OR 3RD DIMENSION. METHOD--
C TRANSFORM HALF THE DATA, SUPPLYING THE CTHER HALF BY CON-
C JUGATE SYMMETRY.
C 3. REAL TRANSFORM FOR THE 1ST DIMENSION, N ODD. METHOD--
C TRANSFORM HALF THE DATA AT EACH STAGE, SUPPLYING THE OTHER
C HALF BY CONJUGATE SYMMETRY.
C 4. REAL TRANSFORM FOR THE 1ST DIMENSION, N EVEN. METHOD--
C TRANSFORM A COMPLEX ARRAY OF LENGTH N/2 WHOSE REAL PARTS
C ARE THE EVEN NUMBERED REAL VALUES AND WHOSE IMAGINARY PARTS
C ARE THE ODD NUMBERED REAL VALUES. SEPARATE AND SUPPLY
C THE SECOND HALF BY CONJUGATE SYMMETRY.
C
70 NON2=NP1*(NP2/NTWO)
 ICASE=1
 IF(IDIM-4)71,90,90
71 IF(IFORM)72,72,90
72 ICASE=2
 IF(IDIM-1)73,73,90
73 ICASE=3
 IF(NTWO-NP1)90,90,74
74 ICASE=4
 NTWO=NTWO/2
 N=N/2
 NP2=NP2/2
 NTOT=NTOT/2
 I=3
 DO 80 J=2,NTOT
 DATA(J)=DATA(I)
80 I=I+2
90 I1RNG=NP1
 IF(ICASE-2)100,95,100
95 I1RNG=NP0*(1+NPREV/2)
C
C SHUFFLE ON THE FACTORS OF TWO IN N. AS THE SHUFFLING
C CAN BE DONE BY SIMPLE INTERCHANGE, NO WORKING ARRAY IS NEEDED
C
100 IF(NTWO-NP1)600,600,110
110 NP2HF=NP2/2
 J=1
 DO 150 I2=1,NP2,NON2
 IF(J-I2)120,130,130
120 I1MAX=I2+NON2-2
 DO 125 I1=I2,I1MAX,2
 DO 125 I3=I1,NTOT,NP2
 J3=J+I3-I2
 TEMPIR=DATA(I3)
 TEMPI=DATA(I3+1)

1 RELEASE 2.0 FOURT DATE = 77139 21/11/39

```
DATA(I3)=DATA(J3)          FFTT172
DATA(I3+1)=DATA(J3+1)       FFTT173
DATA(J3)=TEMPI             FFTT174
125 DATA(J3+1)=TEMPI        FFTT175
130 M=NP2HF                 FFTT176
140 IF(J-M)150,150,145      FFTT177
145 J=J-M                   FFTT178
M=M/2                      FFTT179
IF(M-NON2)150,140,140      FFTT180
150 J=J+M                   FFTT181
C
C MAIN LOOP FOR FACTORS OF TWO. PERFORM FOURIER TRANSFORMS OF FFTT182
C LENGTH FOUR, WITH ONE OF LENGTH TWO IF NEEDED. THE TWIDDLE FACTOR FFTT183
C W=EXP(ISIGN*2*PI*SQRT(-1)*M/(4*MMAX)). CHECK FOR W=ISIGN*SQRT(-1) FFTT184
C AND REPEAT FOR W=ISIGN*SQRT(-1)*CONJUGATE(W). FFTT185
C
NON2T=NON2+NON2            FFTT186
IPAR=NTWO/NP1               FFTT187
310 IF(IPAR-2)350,330,320   FFTT188
320 IPAR=IPAR/4              FFTT189
GO TO 310                  FFTT190
330 DO 340 I1=1,I1RNG,2      FFTT191
DO 340 J3=I1,NON2,NP1       FFTT192
DO 340 K1=J3,NTOT,NON2T     FFTT193
K2=K1+NON2                  FFTT194
TEMPI=DATA(K2)               FFTT195
TEMPI=DATA(K2+1)             FFTT196
DATA(K2)=DATA(K1)-TEMPI     FFTT197
DATA(K2+1)=DATA(K1+1)-TEMPI FFTT198
DATA(K1)=DATA(K1)+TEMPI     FFTT199
340 DATA(K1+1)=DATA(K1+1)+TEMPI FFTT200
350 MMAX=NCN2                FFTT201
360 IF(MMAX-NP2HF)370,600,600 FFTT202
370 LMAX=MAX0(NON2T,MMAX/2)  FFTT203
IF(MMAX-NON2)405,405,380    FFTT204
380 THETA=-TWOPI*FLGAT(NON2)/FLOAT(4*MMAX) FFTT205
IF(ISIGN)400,390,390        FFTT206
390 THETA=-THETA            FFTT207
400 WR=COS(THETA)           FFTT208
WI=SIN(THETA)               FFTT209
WSTPR=-2.*WI*WI             FFTT210
WSTPI=2.*WR*WI              FFTT211
405 DO 570 L=NON2,LMAX,NON2T FFTT212
M=L
IF(MMAX-NON2)420,420,410    FFTT213
410 W2R=WR*WR-WI*WI         FFTT214
W2I=2.*WR*WI                FFTT215
W3R=W2R*WR-W2I*WI          FFTT216
FFTT217
FFTT218
FFTT219
```

ORIGINAL PAGE IS
OF POOR QUALITY

1 RELEASE 2.0	FOURT	DATE = 77139	21/11/39
W3I=W2R*WI+W2I*WR			
420	DO 530 I1=1,I1RNG,2		FFTT220
	DO 530 J3=I1,NON2,NP1		FFTT2210
	KMIN=J3+IPAR*M		FFTT2220
	IF(MMAX-NON2)430,430,440		FFTT2230
430	KMIN=J3		FFTT2240
440	KDIF=IPAR*MMAX		FFTT2250
450	KSTEP=4*KDIF		FFTT2260
	DO 520 K1=KMIN,NTOT,KSTEP		FFTT2270
	K2=K1+KDIF		FFTT2280
	K3=K2+KDIF		FFTT2290
	K4=K3+KDIF		FFTT2300
	IF(MMAX-NON2)460,460,480		FFTT2310
460	U1R=DATA(K1)+DATA(K2)		FFTT2320
	U1I=DATA(K1+1)+DATA(K2+1)		FFTT2330
	U2R=DATA(K3)+DATA(K4)		FFTT2340
	U2I=DATA(K3+1)+DATA(K4+1)		FFTT2350
	U3R=DATA(K1)-DATA(K2)		FFTT2360
	U3I=DATA(K1+1)-DATA(K2+1)		FFTT2370
	IF(ISIGN)470,475,475		FFTT2380
470	U4R=DATA(K3+1)-DATA(K4+1)		FFTT2390
	U4I=DATA(K4)-DATA(K3)		FFTT2400
	GO TO 510		FFTT2410
475	U4R=DATA(K4+1)-DATA(K3+1)		FFTT2420
	U4I=DATA(K3)-DATA(K4)		FFTT2430
	GO TO 510		FFTT2440
480	T2R=W2R*DATA(K2)-W2I*DATA(K2+1)		FFTT2450
	T2I=W2R*DATA(K2+1)+W2I*DATA(K2)		FFTT2460
	T3R=WR*DATA(K3)-WI*DATA(K3+1)		FFTT2470
	T3I=WR*DATA(K3+1)+WI*DATA(K3)		FFTT2480
	T4R=W3R*DATA(K4)-W3I*DATA(K4+1)		FFTT2490
	T4I=W3R*DATA(K4+1)+W3I*DATA(K4)		FFTT2500
	U1R=DATA(K1)+T2R		FFTT2510
	U1I=DATA(K1+1)+T2I		FFTT2520
	U2R=T3R+T4R		FFTT2530
	U2I=T3I+T4I		FFTT2540
	U3R=DATA(K1)-T2R		FFTT2550
	U3I=DATA(K1+1)-T2I		FFTT2560
	IF(ISIGN)490,500,500		FFTT2570
490	U4R=T3I-T4I		FFTT2580
	U4I=T4R-T3R		FFTT2590
	GO TO 510		FFTT2600
500	U4R=T4I-T3I		FFTT2610
	U4I=T3R-T4R		FFTT2620
510	DATA(K1)=U1R+U2R		FFTT2630
	DATA(K1+1)=U1I+U2I		FFTT2640
	DATA(K2)=U3R+U4R		FFTT2650
	DATA(K2+1)=U3I+U4I		FFTT2660
			FFTT2670

1 RELEASE 2.0

FOURT

DATE = 77139

21/11/39

```
DATA(K3)=U1R-U2R          FFTT268
DATA(K3+1)=U1I-U2I          FFTT269
DATA(K4)=U3R-U4R          FFTT270
520 DATA(K4+1)=U3I-U4I          FFTT271
KMIN=4*(KMIN-J3)+J3
KDIF=KSTEP
IF(KDIF-NP2)450,530,530
530 CONTINUE
M=MMAX-M
IF(ISIGN)540,550,550
540 TEMPR=WR
WR=-WI
WI=-TEMPR
GO TO 560
550 TEMPR=WR
WR=WI
WI=TEMPR
560 IF(M-LMAX)565,565,410
565 TEMPR=WR
WR=WR*WSTPR-WI*WSTPI+WR
570 WI=WI*WSTPR+TEMPR*WSTPI+WI
IPAR=3-IPAR
MMAX=MMAX+MMAX
GO TO 360
C
C MAIN LOOP FOR FACTORS NOT EQUAL TO TWO. APPLY THE TWIDDLE FACTOR
C W=EXP(ISIGN*2*PI*SQRT(-1)*(J2-1)*(J1-J2)/(NP2*IFP1)), THEN
C PERFORM A FOURIER TRANSFORM OF LENGTH IFACT(IF), MAKING USE OF
C CONJUGATE SYMMETRIES.
C
600 IF(NTWC-NP2)605,700,700
605 IFP1=NON2
IF=1
NP1HF=NP1/2
610 IFP2=IFP1/IFACT(IF)
J1RNG=NP2
IF(ICASE-3)612,611,612
611 J1RNG=(NP2+IFP1)/2
J2STP=NP2/IFACT(IF)
J1RG2=(J2STP+IFP2)/2
612 J2MIN=1+IFP2
IF(IFP1-NP2)615,640,640
615 DO 635 J2=J2MIN,IFP1,IFP2
THETA=-TWOPI*FLOAT(J2-1)/FLOAT(NP2)
IF(ISIGN)625,620,620
620 THETA=-THETA
SINTH=SIN(THETA/2.)
625 WSTPR=-2.*SINTH*SINTH
FFTT273
FFTT274
FFTT275
FFTT276
FFTT277
FFTT278
FFTT279
FFTT280
FFTT281
FFTT282
FFTT283
FFTT284
FFTT285
FFTT286
FFTT287
FFTT288
FFTT289
FFTT290
FFTT291
FFTT292
FFTT293
FFTT294
FFTT295
FFTT296
FFTT297
FFTT298
FFTT299
FFTT300
FFTT301
FFTT302
FFTT303
FFTT304
FFTT305
FFTT306
FFTT307
FFTT308
FFTT309
FFTT310
FFTT311
FFTT312
FFTT313
FFTT314
FFTT315
```

ORIGINAL PAGE IS
OF POOR QUALITY

1 RELEASE 2.0

FOURT

DATE = 77139

21/11/39

```
WSTPI=SIN(THETA)          FFTT3160
WR=WSTPR+1.               FFTT3170
WI=WSTPI                 FFTT3180
J1MIN=J2+IFP1             FFTT3190
DO 635 J1=J1MIN,J1RNG,IFP1 FFTT3200
I1MAX=J1+I1RNG-2          FFTT3210
DO 630 I1=J1,I1MAX,2      FFTT3220
DO 630 I3=I1,NTOT,NP2     FFTT3230
J3MAX=I3+IFP2-NP1         FFTT3240
DO 630 J3=I3,J3MAX,NP1    FFTT3250
TEMPR=DATA(J3)            FFTT3260
DATA(J3)=DATA(J3)*WR-DATA(J3+1)*WI   FFTT3270
630 DATA(J3+1)=TEMPR*WI+DATA(J3+1)*WR FFTT3280
TEMPR=WR                  FFTT3290
WR=WR*WSTPR-WI*WSTPI+WR   FFTT3300
635 WI=TEMPR*WSTPI+WI*WSTPR+WI       FFTT3310
640 THETA=-TWOPI/FLOAT(IFACT(IF))   FFTT3320
IF(ISIGN)650,645,645        FFTT3330
645 THETA=-THETA            FFTT3340
650 SINH=SIN(THETA/2.)       FFTT3350
WSTPR=-2.*SINTH*SINTH     FFTT3360
WSTPI=SIN(THETA)           FFTT3370
KSTEP=2*N/IFACT(IF)       FFTT3380
KRANG=KSTEP*(IFACT(IF)/2)+1 FFTT3390
DO 698 I1=1,I1RNG,2        FFTT3400
DO 698 I3=I1,NTOT,NP2      FFTT3410
DO 690 KMIN=1,KRANG,KSTEP  FFTT3420
J1MAX=I3+J1RNG-IFP1        FFTT3430
DO 680 J1=I3,J1MAX,IFP1    FFTT3440
J3MAX=J1+IFP2-NP1          FFTT3450
DO 680 J3=J1,J3MAX,NP1    FFTT3460
J2MAX=J3+IFP1-IFP2         FFTT3470
K=KMIN+(J3-J1+(J1-I3)/IFACT(IF))/NP1HF FFTT3480
IF(KMIN-1)655,655,665      FFTT3490
655 SUMR=0.                 FFTT3500
SUMI=0.                     FFTT3510
DO 660 J2=J3,J2MAX,IFP2    FFTT3520
SUMR=SUMR+DATA(J2)          FFTT3530
660 SUMI=SUMI+DATA(J2+1)    FFTT3540
WORK(K)=SUMR                FFTT3550
WORK(K+1)=SUMI              FFTT3560
GO TO 680                  FFTT3570
665 KCONJ=K+2*(N-KMIN+1)    FFTT3580
J2=J2MAX                   FFTT3590
SUMR=DATA(J2)               FFTT3600
SUMI=DATA(J2+1)             FFTT3610
OLDSR=0.                    FFTT3620
OLDSI=0.                    FFTT3630
```

1 RELEASE 2.0

FOURT

DATE = 77139

21/11/39

```
J2=J2-IFP2          FFTT364
670  TEMPR=SUMR      FFTT365
     TEMPI=SUMI      FFTT366
     SUMR=TWOZR*SUMR-OLDSR+DATA(J2)  FFTT367
     SUMI=TWOZR*SUMI-OLDSI+DATA(J2+1)  FFTT368
     OLDSR=TEMPR      FFTT369
     OLDSI=TEMPI      FFTT370
     J2=J2-IFP2      FFTT371
     IF(J2-J3)675,675,670      FFTT372
675  TEMPR=WR*SUMR-OLDSR+DATA(J2)  FFTT373
     TEMPI=WI*SUMI      FFTT374
     WORK(K)=TEMPR-TEMPI      FFTT375
     WORK(KCONJ)=TEMPR+TEMPI      FFTT376
     TEMPR=WR*SUMI-OLDSI+DATA(J2+1)  FFTT377
     TEMPI=WI*SUMR      FFTT378
     WORK(K+1)=TEMPR+TEMPI      FFTT379
     WORK(KCONJ+1)=TEMPR-TEMPI      FFTT380
680  CONTINUE        FFTT381
     IF(KMIN-1)685,685,686      FFTT382
685  WR=WSTPR+1.      FFTT383
     WI=WSTPI      FFTT384
     GO TO 690      FFTT385
686  TEMPR=WR      FFTT386
     WR=WR*WSTPR-WI*WSTPI+WR      FFTT387
     WI=TEMPR*WSTPI+WI*WSTPR+WI      FFTT388
690  TWOZR=WR+WR      FFTT389
     IF(ICASE-3)692,691,692      FFTT390
691  IF(IFP1-NP2)695,692,692      FFTT391
692  K=1      FFTT392
     I2MAX=I3+NP2-NP1      FFTT393
     DO 693 I2=I3,I2MAX,NP1      FFTT394
     DATA(I2)=WORK(K)      FFTT395
     DATA(I2+1)=WORK(K+1)      FFTT396
693  K=K+2      FFTT397
     GO TO 698      FFTT398
C
C   COMPLETE A REAL TRANSFORM IN THE 1ST DIMENSION, N ODD, BY CON-
C   JUGATE SYMMETRIES AT EACH STAGE.      FFTT399
C
695  J3MAX=I3+IFP2-NP1      FFTT400
     DO 697 J3=I3,J3MAX,NP1      FFTT401
     J2MAX=J3+NP2-J2STP      FFTT402
     DO 697 J2=J3,J2MAX,J2STP      FFTT403
     J1MAX=J2+J1RG2-IFP2      FFTT404
     J1CNJ=J3+J2MAX+J2STP-J2      FFTT405
     DO 697 J1=J2,J1MAX,IFP2      FFTT406
     K=1+J1-I3      FFTT407
     DATA(J1)=WORK(K)      FFTT408
     FFTT409
     FFTT410
     FFTT411
```

ORIGINAL PAGE IS
OF POOR QUALITY

1 RELEASE 2.0 FOURT

DATE = 77139

21/11/39

```
DATA(J1+1)=WORK(K+1)          FFTT4120
IF(J1-J2)697,697,696          FFTT4130
696 DATA(J1CNJ)=WORK(K)        FFTT4140
      DATA(J1CNJ+1)=-WORK(K+1)  FFTT4150
697 J1CNJ=J1CNJ-IFP2          FFTT4160
698 CONTINUE                   FFTT4170
      IF=IF+1                   FFTT4180
      IFP1=IFP2                 FFTT4190
      IF(IFP1-NP1)700,700,610   FFTT4200
C
C      COMPLETE A REAL TRANSFORM IN THE 1ST DIMENSION, N EVEN, BY CON-
C      JUGATE SYMMETRIES.
C
700 GO TO (900,800,900,701),ICASE
701 NHALF=N
      N=N+N
      THETA=-TWOPI/FLOAT(N)
      IF(ISIGN)703,702,702
702 THETA=-THETA
703 SINTH=SIN(THETA/2.)
      WSTPR=-2.*SINTH*SINTH
      WSTPI=SIN(THETA)
      WR=WSTPR+1.
      WI=WSTPI
      IMIN=3
      JMIN=2*NHALF-1
      GO TO 725
710 J=JMIN
      DO 720 I=IMIN,NTOT,NP2
      SUMR=(DATA(I)+DATA(J))/2.
      SUMI=(DATA(I+1)+DATA(J+1))/2.
      DIFR=(DATA(I)-DATA(J))/2.
      DIFI=(DATA(I+1)-DATA(J+1))/2.
      TEMPR=WR*SUMI+WI*DIFR
      TEMPI=WI*SUMI-WR*DIFR
      DATA(I)=SUMR+TEMP
      DATA(I+1)=DIFI+TEMPI
      DATA(J)=SUMR-TEMP
      DATA(J+1)=-DIFI+TEMPI
720 J=J+NP2
      IMIN=IMIN+2
      JMIN=JMIN-2
      TEMPR=WR
      WR=WR*WSTPR-WI*WSTPI+WR
      WI=TEMP*WSTPI+WI*WSTPR+WI
725 IF(IMIN-JMIN)710,730,740
730 IF(ISIGN)731,740,740
731 DO 735 I=IMIN,NTOT,NP2
      FFTT4210
      FFTT4220
      FFTT4230
      FFTT4240
      FFTT4250
      FFTT4260
      FFTT4270
      FFTT4280
      FFTT4290
      FFTT4300
      FFTT4310
      FFTT4320
      FFTT4330
      FFTT4340
      FFTT4350
      FFTT4360
      FFTT4370
      FFTT4380
      FFTT4390
      FFTT4400
      FFTT4410
      FFTT4420
      FFTT4430
      FFTT4440
      FFTT4450
      FFTT4460
      FFTT4470
      FFTT4480
      FFTT4490
      FFTT4500
      FFTT4510
      FFTT4520
      FFTT4530
      FFTT4540
      FFTT4550
      FFTT4560
      FFTT4570
      FFTT4580
      FFTT4590
```

1 RELEASE 2.0

FOURT

DATE = 77139

21/11/39

735	DATA(I+1)=-DATA(I+1)	FFTT460C
740	NP2=NP2+NP2	FFTT461C
	NTOT=NTOT+NTOT	FFTT462C
	J=NTOT+1	FFTT463C
	I MAX=NTOT/2+1	FFTT464C
745	I MIN=I MAX-2*NHALF	FFTT465C
	I=IMIN	FFTT466C
	GO TO 755	FFTT467C
750	DATA(J)=DATA(I)	FFTT468C
	DATA(J+1)=-DATA(I+1)	FFTT469C
755	I=I+2	FFTT470C
	J=J-2	FFTT471C
	IF(I-I MAX)750,760,760	FFTT472C
760	DATA(J)=DATA(IMIN)-DATA(IMIN+1)	FFTT473C
	DATA(J+1)=0.	FFTT474C
	IF(I-J)770,780,780	FFTT475C
765	DATA(J)=DATA(I)	FFTT476C
	DATA(J+1)=DATA(I+1)	FFTT477C
770	I=I-2	FFTT478C
	J=J-2	FFTT479C
	IF(I-IMIN)775,775,765	FFTT480C
775	DATA(J)=DATA(IMIN)+DATA(IMIN+1)	FFTT481C
	DATA(J+1)=0.	FFTT482C
	I MAX=IMIN	FFTT483C
	GO TO 745	FFTT484C
780	DATA(1)=DATA(1)+DATA(2)	FFTT485C
	DATA(2)=0.	FFTT486C
	GO TO 900	FFTT487C
C	COMPLETE A REAL TRANSFORM FOR THE 2ND OR 3RD DIMENSION BY	FFTT488C
C	CONJUGATE SYMMETRIES.	FFTT489C
C		FFTT490C
800	IF(I1RNG-NP1)805,900,900	FFTT491C
805	DO 860 I3=1,NTOT,NP2	FFTT492C
	I2MAX=I3+NP2-NP1	FFTT493C
	DO 860 I2=I3,I2MAX,NP1	FFTT494C
	IMIN=I2+I1RNG	FFTT495C
	I MAX=I2+NP1-2	FFTT496C
	J MAX=2*I3+NP1-IMIN	FFTT497C
	IF(I2-I3)820,820,810	FFTT498C
810	J MAX=J MAX+NP2	FFTT499C
820	IF(IDIM-2)850,850,830	FFTT500C
830	J=J MAX+NPO	FFTT501C
	DO 840 I=IMIN,I MAX,2	FFTT502C
	DATA(I)=DATA(J)	FFTT503C
	DATA(I+1)=-DATA(J+1)	FFTT504C
840	J=J-2	FFTT505C
850	J=J MAX	FFTT506C
		FFTT507C

ORIGINAL PAGE IS
OF POOR QUALITY

1 RELEASE 2.0

FOURT

DATE = 77139

21/11/39

```
DO 860 I=IMIN,IMAX,NPO  
DATA(I)=DATA(J)  
DATA(I+1)=-DATA(J+1)  
860 J=J-NPO  
C  
C      END OF LOOP ON EACH DIMENSION  
C  
900 NPO=NP1  
NP1=NP2  
910 NPREV=N  
920 RETURN  
END
```

FFTT5080
FFTT5090
FFTT5100
FFTT5110
FFTT5120
FFTT5130
FFTT5140
FFTT5150
FFTT5160
FFTT5170
FFTT5180
FFTT5190

*** WAVE PROPAGATION IN COMPOSITE PLATE ***
GRAPHITE FIBER (55%)-EPOXY MATRIX COMPOSITE

LAYUP ANGLE= 15 DEGREE
C(1,1)= 0.24560D+08 PSI
C(2,2)= 0.11700D+07 PSI

TOTAL THICKNESS OF COMPOSITE PLATE : DELTA= 1.00000 CM
DENSITY OF COMPOSITE ; RHO= 1.44000 GR/CM**3
PLATE IS MADE OF 8 IDENTICAL LAYERS
LAYER THICKNESS ; 2B= 0.12500 CM

TOTAL SPACE STEPS ; NX= 64 WITH 8 STEPS FOR CONTACT RADIUS
TOTAL TIME STEPS ; NT= 32 WITH 24 STEPS FOR CONTACT TIME

CONTACT RADIUS ; A= 0.20000D-01 M
SPACE STEP ; DX= 0.25000D-02 M
CONTACT TIME ; TAU0= 0.60000D-05 SECOND
TIME STEP ; DT= 0.25000D-06 SECOND

ORIGINAL PAGE IS
OF POOR QUALITY

*** REPRODUCTION OF IMPACT FUNCTION ***
*** MAXIMUM VALUE = -0.10003E+01 ***

SIGMA 1 MAXIMUM VALUE = -0.100067E+01 ***

ORIGINAL PAGE E
FOR QUALITY

SIGMA 3 MAXIMUM VALUE = -0.96697E+00 ***

SIGMA 5 MAXIMUM VALUE = -0.98567E+00 ***

ORIGINAL PAGE IS
OF POOR QUALITY

SIGMA 7 MAXIMUM VALUE =-0.53190E+00 ***

U 4 *** MAXIMUM VALUE = 3.86667E-02 ***

V 4 MAXIMUM VALUE = 0.18217E+00 *****

SIGMA 4 MAXIMUM VALUE = -0.94195E+0 ***

SIGMA1⁴
*** MAXIMUM VALUE =-0.34042E+00 ***

2	2	2	2	2	2	2	1	1	1	1	1	1	1	1	1	1	1	1	1	1	0
2	2	2	2	2	2	2	2	2	2	2	2	2	2	2	2	2	2	2	2	2	-1
2	2	2	2	2	2	2	3	3	3	3	3	3	3	3	3	3	3	3	3	-1	
2	1	1	1	2	2	2	2	2	2	2	2	2	2	2	2	2	2	2	2	-1	
1	1	1	1	1	1	1	2	2	2	2	2	2	2	2	2	2	2	2	2	1	
0	0	0	0	0	0	0	0	1	1	1	1	1	1	1	1	1	1	1	1	0	
0	0	0	0	0	0	0	0	0	0	1	1	1	1	1	1	1	1	1	1	0	
2	2	2	2	1	0	0	0	0	0	0	0	1	1	1	1	1	1	1	1	1	
11	11	9	6	3	0	-1	-2	-1	0	0	1	1	1	1	1	1	1	1	1	0	
26	25	21	16	9	3	0	-3	-2	0	0	0	1	1	1	1	1	1	1	1	1	
44	42	36	28	19	10	2	-2	-3	-2	0	0	1	1	1	1	1	1	1	1	1	
62	60	53	43	31	19	9	2	-1	-3	-3	-2	-1	0	0	1	1	1	1	1	1	
79	76	69	58	45	32	19	10	3	0	-2	-2	-1	0	0	1	1	1	1	1	1	
91	89	82	72	59	46	32	21	12	5	1	-1	-2	-2	-1	0	1	1	1	1	1	
98	96	91	82	72	59	46	34	23	15	8	3	0	-1	-1	0	1	1	1	1	1	
100	98	95	88	80	70	59	48	37	27	18	10	4	1	0	-1	0	0	1	1	1	
95	95	93	89	85	78	70	61	51	40	30	20	12	6	2	0	0	1	2	2	1	
85	85	85	85	84	81	77	71	62	53	42	32	22	14	8	4	1	0	1	2	2	
70	71	73	75	78	79	79	76	71	64	54	44	34	25	17	10	6	3	2	1	1	
53	54	57	62	67	72	76	77	75	71	64	56	46	37	27	19	13	8	5	3	2	
34	36	40	46	53	61	67	72	74	74	71	65	57	48	39	30	22	15	10	5	2	
18	19	24	30	38	47	55	63	69	72	73	70	66	59	51	42	32	24	16	10	5	
3	5	8	14	22	31	41	50	59	66	71	72	71	67	60	52	42	33	23	15	8	
-9	-8	-5	0	6	15	25	36	46	56	64	69	71	70	66	60	51	41	31	21	13	
-24	-23	-20	-15	-8	0	10	21	32	44	54	62	67	70	68	64	57	48	38	29	20	